

Lawrence Berkeley National Laboratory

LBL Publications

Title

THE HYDROGENOLYSIS OF CYCLOPROPANE ON PLATINUM STEPPED SINGLE CRYSTALS AT ATMOSPHERIC PRESSURE

Permalink

<https://escholarship.org/uc/item/1xn3t3f6>

Author

Kahn, Daniel R.

Publication Date

1973-09-01

THE HYDROGENOLYSIS OF CYCLOPROPANE ON
PLATINUM STEPPED SINGLE CRYSTALS AT
ATMOSPHERIC PRESSURE

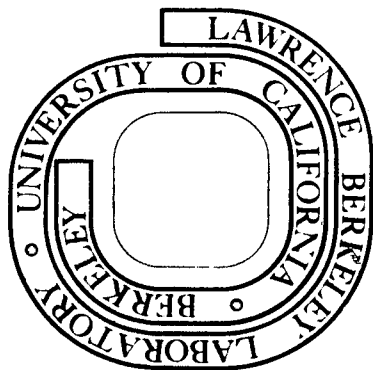
Daniel R. Kahn
(Ph.D. thesis)

September 1973

Prepared for the U. S. Atomic Energy Commission
under Contract W-7405-ENG-48

For Reference

Not to be taken from this room



DISCLAIMER

This document was prepared as an account of work sponsored by the United States Government. While this document is believed to contain correct information, neither the United States Government nor any agency thereof, nor the Regents of the University of California, nor any of their employees, makes any warranty, express or implied, or assumes any legal responsibility for the accuracy, completeness, or usefulness of any information, apparatus, product, or process disclosed, or represents that its use would not infringe privately owned rights. Reference herein to any specific commercial product, process, or service by its trade name, trademark, manufacturer, or otherwise, does not necessarily constitute or imply its endorsement, recommendation, or favoring by the United States Government or any agency thereof, or the Regents of the University of California. The views and opinions of authors expressed herein do not necessarily state or reflect those of the United States Government or any agency thereof or the Regents of the University of California.

THE HYDROGENOLYSIS OF CYCLOPROPANE ON PLATINUM
STEPPED SINGLE CRYSTALS AT ATMOSPHERIC PRESSURE

Table of Contents

ABSTRACT vii

ACKNOWLEDGMENTS ix

LIST OF TABLES x

LIST OF FIGURES xii

CHAPTER I. INTRODUCTION AND BACKGROUND

 A. Studies of Metal Catalysts on an Atomic Scale 1

 B. Studies of the Effect of Metal Crystallite Size
 on Specific Activity and Selectivity in
 Heterogeneous Catalysts 4

 C. Research Objectives Employing Oriented Platinum
 Single Crystals as Heterogeneous Catalysts 9

CHAPTER II. EXPERIMENTAL APPARATUS 11

CHAPTER III. EXPERIMENTAL RESULTS

 A. Introduction 18

 B. Preliminary Experiments on the Pt(S)-[7(111)×(111)]
 Single Crystal 19

 C. The Hydrogenolysis of Cyclopropane on the
 Pt(S)-[6(111)×(100)] Single Crystal

 1. Introduction 23

 2. Blank Runs (with Tantalum Support Only) 27

 3. Reproducibility of Experimental Runs 28

 4. Activation Energy on the Unpoisoned Catalyst 33

 5. Activation Energy on the Partially Deactivated Catalyst 41

 6. Reaction Rate Order with Respect to Cyclopropane 43

 7. Activation Energy for the Poisoning Process 52

8. Catalyst Activity following Minimal Hydrogen Pretreatment	58
9. Catalyst Activity Without Oxygen Pretreatment	61
10. Summary and Conclusions	63
CHAPTER IV. DISCUSSION OF RESULTS	66
APPENDICES	
A. Design of the Experimental Apparatus	73
1. Over-all Reactor Design Requirements	73
2. Initial Calculations for the Design of the High Pressure Reactor	74
3. Criterion for Importance of External Mass Transfer	80
4. Design of the UHV-High Pressure Reactor System	83
5. Construction of the High Pressure Flow Loop and Gas Manifold Assembly	94
B. Preparation of Platinum Single Crystals	98
C. Purity of Materials	104
1. Gases	104
2. Calcium Impurity in the Platinum Single Crystals	104
3. Sulfur Impurity in the Tantalum Electrodes	106
D. Volume Calibrations for the High Pressure Flow Loop	109
E. Analytical System: Calibration of the Gas Chromatograph for the Cyclopropane Hydrogenolysis Reaction	113
F. Experimental Data for the Preliminary Runs on the Pt(S)-[7(111)×(111)] Single Crystal	120
G. Experimental Procedure for a Standard Run During the Cyclopropane Hydrogenolysis on the Pt(S)-[6(111)×(100)] Single Crystal	134
H. Analysis of Hydrogen Pretreatment	136

I. Experimental Data for the Cyclopropane Hydrogenolysis on the Pt(S)-[6(111)×(100)] Single Crystal	140
J. Summary of Calculations for Obtaining Dimensionless Data Plots in Figure III-10.	155
LITERATURE CITED	161

THE HYDROGENOLYSIS OF CYCLOPROPANE ON PLATINUM
STEPPED SINGLE CRYSTALS AT ATMOSPHERIC PRESSURE

Daniel R. Kahn

Inorganic Materials Research Division, Lawrence Berkeley Laboratory and
Department of Chemical Engineering; University of California
Berkeley, California

ABSTRACT

A review of the current literature in surface chemistry and heterogeneous catalysis has revealed that there is a gap between chemisorption and surface reaction studies performed in ultra-high vacuum (10^{-4} to 10^{-9} torr) on single crystal surfaces and those carried out at 1 atmosphere on highly dispersed supported catalysts. Although the low pressure work is of fundamental importance to catalysis, a direct correspondence between these studies and more conventional catalytic experiments is obscured by a number of factors, not the least of which is the enormous difference in total pressure--some 10^7 to 10^{12} orders of magnitude. Hence there is a need to measure the activity of single crystal surfaces at high and low pressure. Furthermore, it has been shown that single crystal surfaces would serve as ideal models for highly dispersed supported metal catalysts.

An apparatus was therefore constructed to study catalytic reactions on one or more platinum single crystals in situ both at 1 atmosphere total pressure and in ultra-high vacuum. The main feature of the design is a novel movable bellows-cup mechanism by which the catalyst can be encased in a small volume for the high pressure experiments. A gas chromatographic sampling technique is employed to monitor the formation of products in the high pressure system.

Using this apparatus, the cyclopropane hydrogenolysis has been investigated at 1 atm pressure on a platinum stepped single crystal (Pt(S)-[6(111)×(100)]) having a total surface area of 0.76 cm². Initial specific reaction rates were reproducible to about 10%, and to within a factor of two were identical to published values for this reaction on highly dispersed supported platinum catalysts. The activation energy for the unpoisoned catalyst was found to be 12.2 kcal/mole, while that for the partially deactivated catalyst was 10.5 kcal/mole. The order of the reaction with respect to cyclopropane was determined to be 0.8 ± 0.2. The conditions of hydrogen pretreatment were found to be important factors in determining the initial shape of the reaction rate curve.

This work has shown that it is possible to measure rates of reaction on a single platinum crystal having a surface area of 1 cm² at atmospheric pressure using a thermal conductivity detector of a gas chromatograph. Studies of this type appear to be well suited to discover the relationship between the morphology of the catalyst surface and its heterogeneous catalytic activity.

ACKNOWLEDGMENTS

As I complete my graduate work at U. C. Berkeley, I must in retrospect acknowledge the great number of people who assisted me in attaining the Ph.D. degree.

First, I am especially grateful to my research directors, Professors Eugene E. Petersen and Gabor A. Somorjai. Gene's remarkable mechanical ability, his method of approaching problems, and above all, his friendship and confidence in me will never be forgotten. Gabor's limitless energy and enthusiasm for the project, and his ability to perceive a problem were always sources of inspiration to me.

I wish to thank my friends and colleagues, Louis Hegedus, Farhang Shadman, Julian Landau, Alan Benke, and Richard Herz for their technical advice and suggestions throughout the course of this work. For boosting my morale during the low points I will always be indebted to John Krochta, Cathy Hester, and Gil Roque.

The design and construction of the apparatus would not have been possible without the expert advice and skill of the craftsmen at the College of Chemistry Machine Shop: Slim Bohac, Carl Baugh, Carl Gaskins, and Bob Waite. I am grateful to Emery Kozak for the time, patience, and many helpful suggestions that he provided me during the design period.

I would like to thank Gloria Pelatowski for preparing the line drawings, and Doug Krietz who aided in the preparation of thesis mats and slides. Special thanks are in order to Mrs. Shirley Ashley and the secretarial staff at IMRD for cheerfully typing the final manuscript.

The author gratefully acknowledges financial support of this work in the form of grants from the National Science Foundation, the U. S. Atomic Energy Commission, and the U. S. Department of the Army.

LIST OF TABLES

<u>Table</u>	<u>Page</u>
I-1. Relationship between degree of dispersion and metal crystallite size.	6
I-2. Survey of structure-sensitivity studies.	7
III-1. Summary of catalytic runs on the Pt(s)-[7(111)x(111)] single crystal surface.	20
III-2. Summary of catalytic runs on the Pt(s)-[6(111)x(100)] single crystal surface.	25
III-3. Rates of the cyclopropane hydrogenolysis reaction on the Pt(s)-[6(111)x(100)] single crystal surface.	26
III-4. Summary of initial rate data for the determination of E^* for the cyclopropane hydrogenolysis on the Pt(s)-[6(111)x(100)] single crystal.	36
III-5A. Physical characteristics of the platinum catalyst pellet used by Hegedus. ^{50,51}	38
III-5B. Initial rate data for the cyclopropane hydrogenolysis using the catalyst pellet of Hegedus. ^{50,51}	38
III-6. Comparison of initial specific rate data for the cyclopropane hydrogenolysis on platinum catalysts.	40
III-7. Summary of rate data during the latter half of Run 14 -- Calculation of E_p^* .	44
III-8. Calculation of reaction order with respect to cyclopropane.	49
III-9. Summary of calculations for activation energy of the poisoning process. $t_p = B \exp(-E_{pp}^*/RT)$.	54
A-1. Rate data from Hegedus ^{50,51} for the hydrogenolysis of cyclopropane on a platinum/alumina catalyst.	77

<u>Table</u>	<u>Page</u>
B-1. Typical mass spectrographic analysis of "MARZ" grade platinum. ³²	99
B-2. Platinum single crystal surface area.	102
D-1. Summary of high pressure reactor system volumes.	112
E-1. Summary of operating conditions for the analytical system.	115
E-2. Summary of G. C. calibrations for the cyclopropane hydrogenolysis reaction.	116
E-3. Component G. C. peak sensitivities at various pressures.	117

LIST OF FIGURES

<u>Figure</u>	<u>Page</u>
II-1. Schematic of flow loop for high pressure (1 atm) catalysis on single crystal platinum surfaces	12
II-2. Schematic representation of platinum stepped surfaces. (A) Pt(s)-[7(111)×(111)] surface, consisting of a terrace geometry of (111) orientation 7 atoms wide and a step geometry of (111) orientation	15
(B) Pt(s)-[6(111)×(100)] surface, having a terrace geometry of (111) orientation 6 atoms wide and a step geometry of (100) orientation	15
III-1. Run 10A. Cyclopropane hydrogenolysis on the Pt(s)-[6(111)×(100)] surface	30
III-2. Runs 12A and 12B. Cyclopropane hydrogenolysis on the Pt(s)-[6(111)×(100)] surface	32
III-3. Data of Run 15 for the cyclopropane hydrogenolysis	34
III-4. Data of Run 16 for the cyclopropane hydrogenolysis	35
III-5. Activation energy for the hydrogenolysis of cyclopropane based upon initial reaction rates on the Pt(s)-[6(111)×(100)] single crystal ($A_s = 0.76 \text{ cm}^2$). $P_{CP}^0 = 135 \text{ torr}$. $P_{H_2}^0 = 675 \text{ torr}$	37
III-6. Run 14. Hydrogenolysis of cyclopropane on the Pt(s)-[6(111)×(100)] surface: Temperature stepping experiment	42

<u>Figure</u>	<u>Page</u>
III-7. Run 14. Activation energy for the cyclopropane hydrogenolysis on the partially deactivated catalyst . . .	45
III-8. Run 17. Cyclopropane hydrogenolysis on the Pt(s)-[6(111)×(100)] surface. $P_{CP}^O = 200$ torr. $P_{H_2}^O = 675$ torr	46
III-9. Determination of reaction order with respect to cyclopropane	51
III-10A. Non-dimensionalized reaction rate data for the cyclopropane hydrogenolysis on the Pt(s)-[6(111)×(100)] single crystal	53
III-10B. Non-dimensionalized reaction rate versus time.	56
III-11. Activation energy for the poisoning process during the cyclopropane hydrogenolysis on the Pt(s)-[6(111)×(100)] surface	57
III-12. Effect of varying hydrogen pretreatment conditions	59
A-1. Overall view of equipment for UHV and high pressure studies, including reactors, mass spectrometer, gas chromatograph, and associated electronics	84
A-2. Close-up of the UHV-high pressure reactor assembly	85
A-3. Close-up of the UHV-high pressure reactor fabricated for the present studies. Flanges visible include, from left to right, those for a nude ion gauge, an Auger electron gun assembly (not shown), a viewing port, and the "bellows-cup" assembly	86
A-4a. Top view of UHV-high pressure with bellows-cup assembly withdrawn to expose catalyst single crystal to UHV	89

<u>Figure</u>	<u>Page</u>
A-4b. Top view of UHV-high pressure reactor with bellows-cup assembly extended to encase catalyst single crystal in a small volume for high pressure studies	90
A-5a. Close-up of the reactor flange, detailing the gold O-ring seated in the reactor flange wall, the tantalum electrodes, and the Pt/Pt-10% Rh thermocouple wires . .	92
A-5b. Close-up of reactor flange, with reactor cup seated on the gold O-ring to form high pressure reactor . . .	93
A-6. Schematic representation of the high pressure flow loop and gas manifold assembly	96
D-1. Schematic of high pressure flow loop and gas manifold assembly: key to identification of reactor system volumes.	110

CHAPTER I

INTRODUCTION AND BACKGROUND

Almost 50 years have elapsed since H. S. Taylor first introduced the concept of surface heterogeneity to describe the catalytic activity of metal solids.^{1,2} Since then the term "active sites" or "active centers" has become well known to refer to the location of a catalytic event on a solid surface. The fact remains that although "active centers" are frequently discussed in heterogeneous catalytic reactions, their nature is very poorly understood. Part of the reason lies in the fact that several basic unknowns in the catalytic process remain to be explored in a systematic manner. These include the physical and chemical state of the metallic surface during reaction, and the exact nature of the metal-adsorbate and adsorbate-adsorbate surface interactions. As new sophisticated techniques become available for studying chemical reaction processes on metal surfaces, the field of catalysis will continue to develop into a more fundamental science.

A. Studies of Metal Catalysts on an Atomic Scale

Two new tools for studying the surface of a solid on an atomic scale have become commercially available during the last 7-8 years. One technique is low energy electron diffraction (LEED), whereby one can determine the structure of well-defined clean surfaces, the possible rearrangement of these surfaces in the presence of adsorbed gases, and the structure of adsorbed gases relative to the metal substrate.³ Using Auger electron spectroscopy (AES), it is possible to obtain a quantitative estimate of the composition of surface species down to 1% of a monolayer, thereby gaining valuable information about impurities at the surface. It should

be noted here that practically all this work is done in ultrahigh vacuum (10^{-4} to 10^{-11} torr) due to the nature of the techniques and the equipment used in the analyses. These methods are of particular importance to catalytic chemists because of the obvious value that such information has in the interpretation of chemical reactions on catalytic surfaces. The reader is referred to recent reviews⁴⁻⁷ for detailed descriptions of these techniques and their various applications.

Using the methods described above there has been increasing interest in studying well-defined catalyst surfaces, notably oriented single crystals of known initial chemical purity. Somorjai and coworkers have measured surface structure, composition, and some rates of reaction on platinum single crystals at low pressure.⁸⁻¹¹ Both low Miller Index and high Miller Index crystal faces of platinum have been examined. The latter have been shown to consist of low index (111) and (100) terraces of constant width, linked by steps of monatomic height, and to exhibit remarkable thermal stability.⁸ One particular reaction which has been studied extensively is the dehydrocyclization of n-heptane to form toluene.¹⁰ This was investigated between 100°C and 400°C at pressures in the 10^{-4} torr range on single crystals having surface areas of less than 1 cm^2 . A mass spectrometric technique was used to monitor the formation of product. The initial rate of toluene formation on the high index or stepped surface was found to be approximately an order of magnitude greater than initial rates on low index surfaces.

The chemisorption properties of stepped platinum surfaces have been shown to be very different from those of low index platinum surfaces.⁹ Two striking examples which are of particular importance to catalysis are

those involving hydrogen and oxygen. Both chemisorb readily at relatively low temperatures on stepped surfaces but do not chemisorb easily on low index faces. Furthermore, it has been shown that the dissociation of these diatomic molecules takes place at the atomic steps on the high index surfaces.

In a molecular beam study of H₂/D₂ exchange on low and high Miller Index platinum single crystal surfaces, Bernasek, Siekhaus, and Somorjai¹² showed that the exchange reaction took place readily on a high index (997) platinum single crystal surface, whereas no detectable HD could be measured using a low index (111) platinum surface. The difference in reactivity was ascribed to the unique properties of the stepped surface. It should be pointed out that the H₂/D₂ exchange is known to be a moderately fast reaction on oriented thin films as well as on polycrystalline supported catalysts. Yet the molecular beam configuration is sensitive enough to detect differences in activity that would otherwise be indistinguishable using other analytical techniques.

A direct correspondence between the above chemisorption and surface reaction studies and those carried out in more conventional systems is obscured by a number of factors. Of particular significance is the enormously reduced pressure under which LEED, AES, or mass spectrometric experiments are conducted. Typically, catalytic reaction rates are measured at reactant partial pressures on the order of one atmosphere whereas LEED measurements, for example, are made at 10⁻⁶ to 10⁻¹⁰ torr-- a pressure some 10⁹ to 10¹³ smaller than ordinarily used in catalytic studies. It is possible that at higher pressures larger surface coverages may give rise to "on top" structure that does not form in ultrahigh vacuum.¹³ Hence, chemisorption and surface reaction studies carried out at 1 atm may not be directly correlated with UHV studies. It would seem

logical therefore to study catalytic reactions at high pressures (1 atm or higher) on well-oriented single crystal surfaces. In this manner the results of UHV and high pressure reaction studies could be compared on the same catalyst and under similar reaction conditions, the only difference being the total system pressure.

Before outlining the goals of the present study, and in order to gain a better insight into the justification for the work carried out in this thesis, it is first necessary to review relevant literature involving highly dispersed supported metal catalysts.

B. Studies of the Effect of Metal Crystallite Size
on Specific Activity and Selectivity in
Heterogeneous Catalysts

Work has continued with traditional heterogeneous catalysts in an effort to characterize the nature of "active centers." Recent studies have employed highly dispersed metals supported on inert carriers to investigate fully the geometrical factor in catalysis. Typically, experiments are performed at 1 atm in batch or flow reactors, where the reactants and products are analyzed via gas chromatography. In addition to measuring initial reaction rates, orders of reaction with respect to particular reactants, and activation energies, more emphasis is now being placed on characterizing the catalyst more fully, as to details of preparation, surface area of metal exposed (dispersion), average metal particle size, and the distribution of particle size, in order to make a rational interpretation of catalytic activity. Several excellent reviews of techniques for characterizing highly dispersed catalysts have appeared in the current literature.¹⁴⁻¹⁶ Ideally, a supported catalyst being used in fundamental

research should be characterized by a combination of gas chemisorption, X-ray diffraction, and electron microscopy measurements.

It has been only in the last 6-7 years that more detailed consideration has been given to the possible effects of the state of the metal dispersion on the carrier on catalytic activity. Table I-1 shows the approximate relationship between dispersion and metal crystallite size, where the degree of dispersion of the metal is defined as the ratio of the number of surface metal atoms to the total number of metal atoms.

One would expect the surface heterogeneity to change with crystallite size and possibly have an effect on specific activity for a given reaction or on selectivity in a system of competitive reactions. Indeed a number of investigators have found relationships of this type which has led to classifying reactions into two main groups.¹⁷ The terms "facile" and "structure-insensitive" have been used to describe types of reactions where specific activity is independent of the mode of preparation of the catalyst or the catalyst metal particle size. Hence each surface site is about as effective catalytically as its neighbor. On the other hand, those reactions in which the specific activity or selectivity is a function of metal particle size or mode of catalyst preparation have been termed "demanding" or "structure-sensitive." Table I-2 summarizes a number of reactions which belong to each particular classification.

One of the interesting aspects of the "structure-sensitive" studies has been that the effect is only prevalent in the 15-50Å dia particle size range. The question arises as to the unique properties that metal crystallites of this size range possess. To gain a more fundamental understanding of this phenomenon, a number of models of small crystallites

Table I - 1. Relationship between degree of dispersion and metal crystallite size¹⁵

Dispersion range	Approximate crystallite size
< 0.3	Low dispersion values; metal composed of relatively large crystallites (50-500Å range) with most of the metal atoms occupying internal positions.
0.4 - 0.7	Small crystallites with average diameter of approximately 20-50Å.
0.7 - 1	Dispersion values approaching unity mean that all metal atoms are exposed, and in the limit, approach a completely atomized condition.

Table I - 2. Survey of structure-sensitivity studies

"Structure-insensitive" reactions	"Structure-sensitive" reactions
(a) Benzene hydrogenation -Dorling and Moss ²² Pt/SiO ₂	(a) Ethane hydrogenolysis -Sinfelt et al. 25, 26 Ni/SiO ₂ -Al ₂ O ₃ , Rh/SiO ₂
(b) Dehydrogenation of cyclo- hexane Hydrogenation of cyclopentane H ₂ /D ₂ exchange -Poltorak and Boronin ¹⁹ Pt/SiO ₂	(b) Neopentane hydrogenolysis and isomerization -Boudart et al. 27 Pt/Al ₂ O ₃ , Pt/SiO ₂ , Pt
(c) Cyclopropane hydrogenolysis -Boudart et al. 23 Pt/Al ₂ O ₃ , Pt/SiO ₂ , Pt	(c) Hydrogenolysis of methyl- cyclopentane -Corroleur et al. 28 Pt/Al ₂ O ₃ , Pt/SiO ₂
(d) Ethylene hydrogenation -Dorling, Eastlake, and Moss ²⁴ Pt/SiO ₂	(d) Hydrogenation of 1,2- and 1,3-butadiene -Oliver and Wells ²⁹ Ni/Al ₂ O ₃ , Ni/SiO ₂ , Ni
	(e) Hydrogenation of benzene -Coenen et al. 30 Ni/SiO ₂

has been developed.¹⁸⁻²¹ In brief, small crystallites have been modeled as imperfect cubo-octahedra (fcc metals). It has been assumed that even in the smallest crystallites, metal atoms occupy crystallographic positions. Furthermore, crystallites are shaped so that their free energy is a minimum. This means maximizing the number of bonds between atoms, including surface atoms, and results in particles of roughly spherical shape. The models have shown that in the 15-50Å dia particle range, there is a high fraction of surface atoms in edge, step, and corner positions. In particular, for step sites, the fraction of surface atoms in steps is approximately 0.3 for 15Å dia particles, and decreases an order of magnitude for 50Å dia particles.

It is clear why catalysts of low dispersion do not exhibit surface structure sensitivity. Most of the crystallites are very large and are comprised mainly of regularly packed low index crystal planes. In the very highly dispersed range, the lattice and structural considerations are unimportant due to the very low coordination numbers. It is only in the intermediate range (15-50Å) where there is a rapid change in the coordination number of the surface atoms and where such surface features as steps and edges become important.

Based on these studies of small metal crystallites it would appear that single crystal surfaces would be ideal models for highly dispersed supported metal catalysts. Single crystals containing low index surfaces as well as those exhibiting ordered atomic steps could be independently studied, thereby making it possible to investigate directly the influence of surface morphology on heterogeneous catalytic activity and selectivity.

C. Research Objectives Employing Oriented Platinum Single Crystals as Heterogeneous Catalysts

A survey of the current literature in surface chemistry and heterogeneous catalysis has revealed that there is a gap between chemisorption and surface reaction studies performed in ultrahigh vacuum on single crystal surfaces and those carried out at 1 atm on highly dispersed supported catalysts. Furthermore, studies of small metal crystallites have indicated that single crystal surfaces would serve as ideal models for highly dispersed supported metal catalysts.

The work embodied in this thesis arose out of the need to bridge the gap between these two fundamental areas of catalytic research. The overall objective was to measure reaction rates on well-defined single crystal surfaces both at high pressure (1 atm) and in ultrahigh vacuum (10^4 to 10^8 torr) within the same apparatus. The high pressure measurements would involve the use of gas chromatographic detection while a mass spectrometric technique could be employed in the low pressure measurements. Platinum was chosen as the catalyst to be investigated because of its obvious importance in many industrial processes. Studying various types of reactions on both low index and stepped platinum single crystal surfaces would enable a relationship between surface morphology and catalytic activity to be developed. Furthermore, it was hoped that these results would also show how adsorbed surface structures as determined previously by LEED measurements were related to catalytic activity.

The work presented in succeeding chapters of this thesis is the initial experimental effort towards achieving these extensive goals. Chapter II and Appendices A-E describe the design, construction, and

operation of the experimental apparatus. Results and discussion of high pressure kinetic studies for the hydrogenolysis of cyclopropane on a platinum stepped single crystal surface are presented in Chapters III and IV.

CHAPTER II

EXPERIMENTAL APPARATUS*

The apparatus was constructed to perform catalytic experiments on one or more platinum single crystals both in ultra-high vacuum (UHV) and at 1 atmosphere total pressure without physically altering the position of or severing connections made to the catalyst crystal(s). A schematic of the UHV assembly and the flow loop for the high pressure catalytic measurements is shown in Figure II-1.

The UHV system consists of two 12-inch i.d. multi-flanged S.S. chambers separated by a viton-sealed gate valve. The lower UHV chamber contains a 200 liter/sec ion pump and titanium sublimation pump capable of reducing the pressure in the total assembly to 5×10^{-10} torr. The upper chamber consists of a high pressure reactor within the UHV reactor. The main feature of the design is a movable bellows-cup mechanism by which the stationary catalyst can be encased in a small volume for the high pressure experiments. Flanges in the upper chamber are provided for:

- (a) Monitoring the pressure in the UHV reactor by means of a nude ion gauge;
- (b) Measuring the UHV gas phase composition by a quadrupole mass spectrometer (Granville-Phillips Spectra Scan 750 Residual Gas Analyzer);
- (c) Determining the composition of the catalyst crystal surface down to 1% of a monolayer via the technique of Auger electron spectroscopy;

* For a more complete description of the design and operation of the experimental apparatus and for additional details related to subject matter discussed in this chapter, the reader is referred to Appendices A through H.

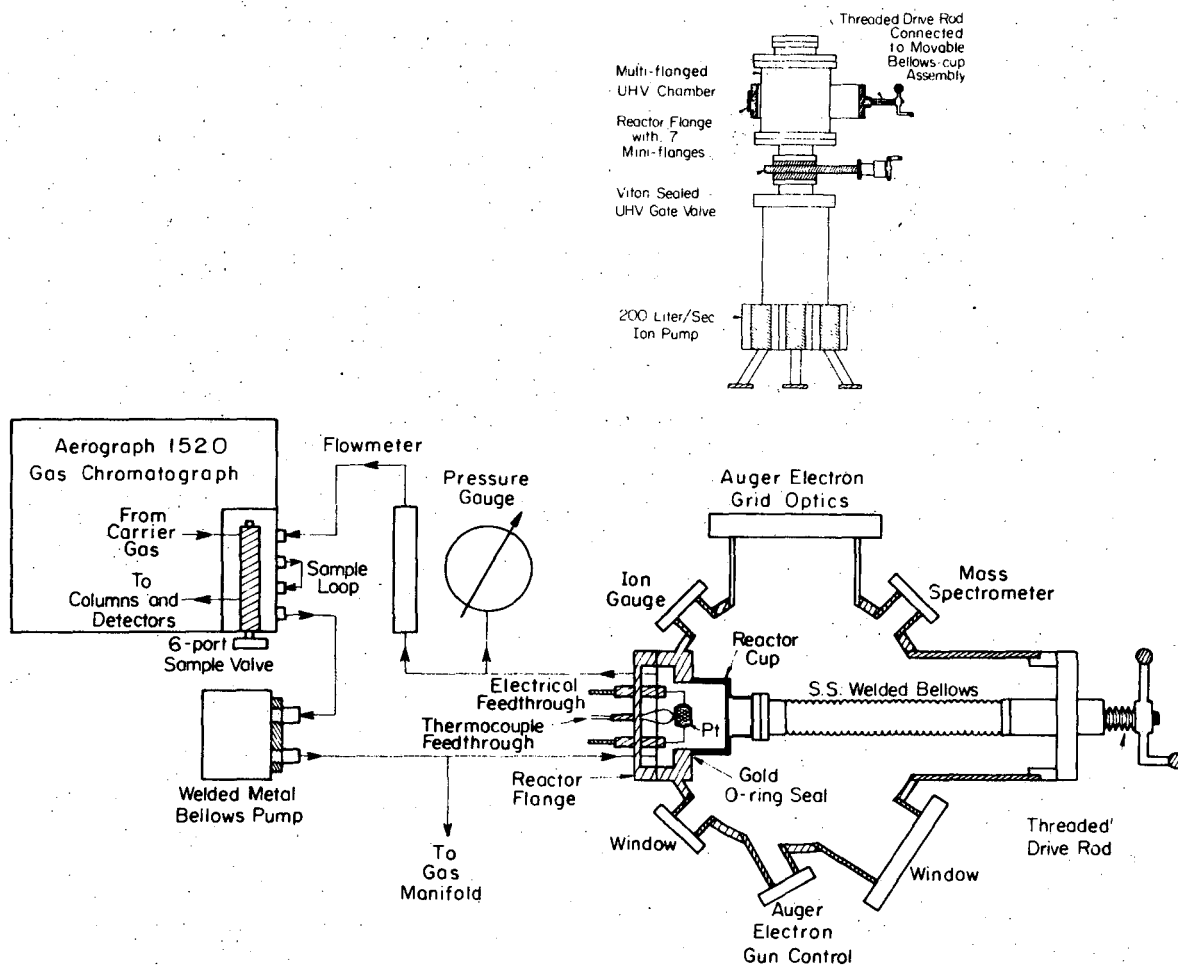


Figure II-1. SCHEMATIC OF FLOW LOOP FOR HIGH PRESSURE (1 ATM) CATALYSIS ON SINGLE CRYSTAL PLATINUM SURFACES

XBL 734-5969A

- (d) Housing the movable S.S. welded bellows-reactor cup assembly; and
- (e) Supporting and heating the catalyst via suitable electrical feed-throughs and serving as one half of the high pressure reactor volume.

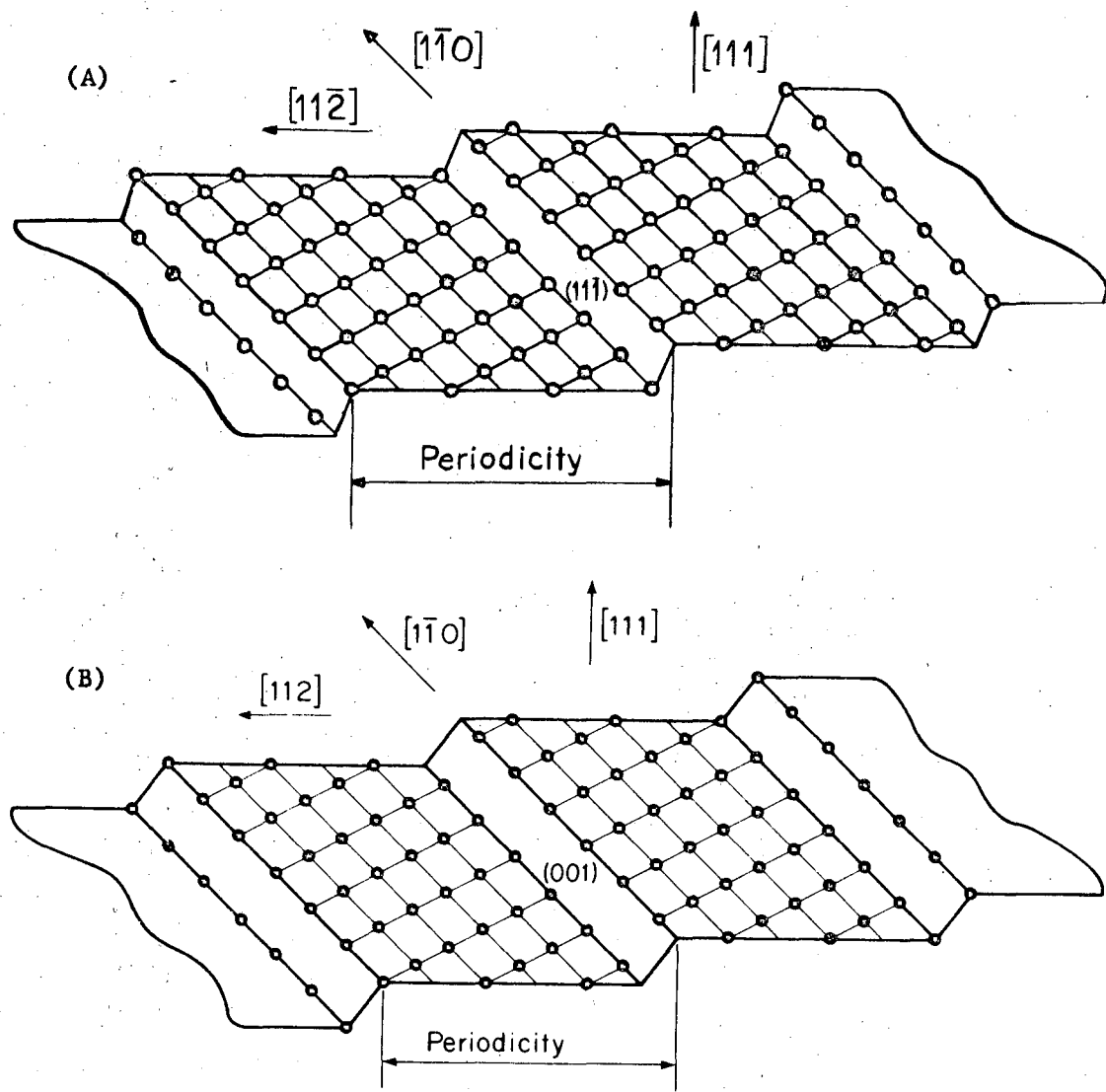
The high pressure reactor volume is isolated from the UHV system by a gold O-ring between two knife edges, one on the reactor cup and the other in the reactor flange. As many as 20 cup closures have been obtained using a single gold O-ring. With a pressure of 1000 torr inside the reactor cup the pressure in the UHV chamber can be maintained at 1×10^{-8} torr, resulting in a negligible loss of reactants or products from the high pressure reactor during the course of a typical catalytic experiment.

The platinum crystal shown in the schematic is supported by means of 0.070-inch dia. tantalum electrodes, which in turn are connected via electrical feedthroughs to a d.c. regulated power supply capable of heating the platinum crystal to 1000°C. A Pt/Pt-10%Rh thermocouple is spot-welded to the edge of the platinum crystal, enabling the crystal temperature to be monitored to within $\pm 0.1^\circ\text{C}$.

The high pressure flow loop (G.C. loop) is fabricated from 1/4-inch o.d. S.S. tubing and consists of a 0-1500 torr Heise gauge measuring absolute pressure to ± 0.25 torr, a 0-5000 scc/min Fischer-Porter flowmeter, and an MB-10 S.S. welded bellows pump (Metal Bellows Corp.) providing a maximum flow rate of 2800 scc/min of air under zero pressure drop. Composition of the gas mixture is measured by routing the flow through a sample valve of a gas chromatograph. The volumes of the reactor cup, G. C. loop, and sample volume are 571 cm^3 , 189 cm^3 , and 0.78 cm^3 , respectively.

The high pressure system can be modeled as a continuously-stirred batch recycle reactor operated under differential reaction conditions (less than 0.1% conversion per pass). Calculations have shown that external mass transport resistances are negligible and need not be considered in the analysis of the kinetic data (Appendix A).

The platinum used in this study was purchased in the form of 1/4-inch dia. single crystal rods grown by electron-beam zone refining (99.99% minimum purity).³² The platinum stepped surfaces were generated by cutting the platinum crystal at small angles from low index planes. The resulting high Miller Index surfaces have been shown to consist of terraces of constant width linked by steps of monatomic height.^{8,33} A schematic representation of the two stepped surfaces used in this study is shown in Figure II-2. Each surface was first X-ray oriented by a back reflection Laue technique to within $\pm 0.5^\circ$. The Pt(S)-[7(111) \times (111)] surface was obtained by sparkmachining at 8.5° from the (111) face towards the (110) plane and had a total surface area of 0.80 cm^2 . The Pt(S)-[6(111) \times (100)] surface was cut at 9.5° from the (111) face towards the (100) plane and had a total surface area of 0.76 cm^2 . A LEED analysis confirmed the orientation of these stepped surfaces.³⁴ The circumferential area of each thin elliptical crystal disc represented approximately 15% of the total surface area and was presumed to be polycrystalline in orientation. After cutting, the crystals were mechanically polished by a series of abrasives, the final polish being 1/4 micron Al_2O_3 powder. They were subsequently etched in hot 50% aqua regia for 10 minutes prior to use.



XBL 738-1084

Figure II-2. Schematic representation of platinum stepped surfaces.
 (A) Pt(S)-[7(111)×(111)] surface, consisting of a terrace geometry of (111) orientation 7 atoms wide and a step geometry of (111) orientation.
 (B) Pt(S)-[6(111)×(100)] surface, having a terrace geometry of (111) orientation 6 atoms wide and a step geometry of (100) orientation.

The 0.070-inch dia. tantalum electrodes used to support the catalyst crystal were triply zone refined (99.999% minimum purity) and etched in an 80% solution of nitric and hydrofluoric acids for 10 minutes.

The cyclopropane was obtained from Matheson and contained less than 0.4% impurities. Propylene accounted for approximately 70% of this impurity. The gas was passed through a bed of activated MgClO_4 to remove traces of water.

Hydrogen was obtained from the Lawrence Berkeley Laboratory and had a minimum purity of 99.99%, the major impurity being oxygen. This was also passed through activated MgClO_4 prior to introduction into the gas chromatograph or reactor flow loop.

In what will be termed a "standard run," the platinum single crystal is first pretreated in 1×10^{-6} torr oxygen at 900-925°C for 2 hours with the reactor cup open. This is sufficient to remove carbonaceous residues from the crystal surface based upon previous LEED-AES measurements.^{35,36} The oxygen is then pumped out of the UHV system for an additional hour, while maintaining the crystal temperature above 900°C, to remove adsorbed oxygen especially at the platinum step sites. The crystal is then cooled rapidly to 300°C, at which time the reactor cup is closed and hydrogen admitted to a total pressure of 780 torr. The platinum crystal is maintained in 1 atm of stagnant hydrogen at 75°C for a period of 2 hours. These conditions are more than sufficient to fully saturate the platinum bulk with hydrogen atoms based upon the solubility and diffusivity data of Ebisuzaki et al.³⁷ During the reduction period a cyclopropane-hydrogen mixture is prepared in the

G.C. loop, such that when expanded into the total reactor volume ($V_R + V_{GC} = 760 \text{ cm}^3$), the initial partial pressures of cyclopropane and hydrogen are 135 torr and 675 torr, respectively. Pre-reaction chromatograms of the mixture in the G.C. loop are taken to determine the initial composition of the reactant mixture. At the conclusion of the reduction period with the bellows circulation pump on, the valves separating the reactor and G.C. loop volumes are opened, thereby routing the flow directly past the catalyst crystal and commencing the catalytic run.

The reaction gases were monitored periodically by means of a 6-port sample valve housed in a Varian Aerograph 1520 gas chromatograph containing dual thermal conductivity detectors. Hydrogen was chosen as a carrier gas to maximize the sensitivity of the thermal conductivity detector and to avoid the anomalous behavior of He/H₂ mixtures reported by Purcell and Ettore.³⁸ The components (propane, propylene, and cyclopropane) were separated at 35°C using a carrier gas flow of 30 ml/min in a 20 ft × 1/8-in. S.S. column packed with 30% bis, 2-methoxy ethyl adipate on 60/80 mesh A/W Chromosorb P. The output from the detectors was recorded on a Honeywell Electronik 15 strip chart recorder. The chromatographic peaks were integrated by the triangulation method. Calibration curves for each hydrocarbon component developed in a range of typical operating conditions were used to convert peak areas to hydrocarbon concentrations (Appendix E).

CHAPTER III

EXPERIMENTAL RESULTS

A. Introduction

Prior to commencing the first catalytic experiment, there were no data available to suggest how reactive a particular single crystal surface might be at 1 atm total pressure. In addition, the relative reactivity of the blank stainless steel chamber was an unknown quantity. If the total initial rate for a particular reaction on a platinum crystal would be too low, there existed the very real possibility that a build-up of carbonaceous surface residues might well obscure a kinetic analysis. Fortunately this was not the case for the cyclopropane hydrogenolysis and propylene hydrogenation reactions. Initial experiments showed that the apparatus described in the preceding chapter was capable of monitoring at 1 atm total pressure the rate of a catalytic reaction on a platinum single crystal having a surface area of only 1 cm².

Preliminary experiments on the Pt(S)-[7(111)×(111)] single crystal surface to determine order of magnitude reactivities for several different types of reactions are described in Section B. These include the hydrogenolysis of cyclopropane, the hydrogenation of propylene, the dehydrocyclization of n-heptane, and the hydrogenolysis and isomerization of neopentane.

Section C presents the results of a more detailed investigation of the cyclopropane/hydrogen reaction on the Pt(S)-[6(111)×(100)] surface. Included in the kinetic analysis are activation energies for the unpoisoned catalyst, the partially deactivated catalyst, and the poisoning

Table III - 1. Summary of catalytic runs on the Pt(s) - [7(111)X(111)] single crystal surface

Run #	H ₂ pretreatment conditions			Reaction conditions				Comments and notes
	(T _c) _{avg} (°C)	P _{H₂} (torr)	Time (min)	P _{H₂} ^o (torr)	P _{HC} ^o		(T _c) _{avg} (°C)	
					(torr)	Hydrocarbon		
1	No pretreatment			654	≈ 18	Cyclopropane	22°C initially 66°C > 30 min	No reaction initially at room temperature; very small C ₃ H ₈ signal after 100 min @ 66°C.
2A	74	172	9.4	668	135.0	ibid	74.2	H ₂ pretreatment only 9.4 min prior to introduction of CP/H ₂ mixture; 4 t _r ≈ 68 min.
3	78	500	60	545	135.0	ibid	111.5	Since P _T ^o < 760 torr, air peak increased very gradually as experiment progressed.
4A	74	765	68	668	135.0	ibid	81.5	Procedure for runs was identical; yet (R _o) _{4B} / (R _o) _{4A} ≈ 3. Very fast initial rate (≈ factor of 10 greater than initial rate of CP hydrogenolysis); significant heating of crystal due to ΔH _{rxn} ; 99% conversion @ t = 118 min.
4B	76	765	68	668	135.0	ibid	88.3	
5B	75	765	69	668	135.0	Propylene	90.4	
6B	330	105 (+695 N ₂)	62	79.0 713.0 N ₂	7.9	N-heptane	342	No measurable toluene observed at 2 hours of reaction time.
7B	313	766	60	668	135.0	Neopentane	315	No products observable during 1 hours of operation, at which time crystal spot-weld breaks, ending run.
8A	76	765	68	664	135.0	Cyclopropane	82.5	Blank run without Pt crystal; after 200 min elapsed time, only 90% of the 0.2% propylene impurity in the CP reacted.
8B	77	765	68	664	135.0	Propylene	82.0	Blank run without Pt crystal; 5.4% conversion @ t = 118 min. Also, (R _o) _{8B} / (R _o) _{5B} = 0.054.

of three. It is believed that a calcium impurity in the platinum crystal and sulfur contamination from the tantalum support rods were responsible for this variation.[†]

Several different types of reactions were investigated next instead of continuing the cyclopropane hydrogenolysis experiments on a contaminated crystal. It was felt that any reaction measured in these experiments would set a lower limit on what could be obtained in future experiments using platinum and tantalum which had been cleaned of impurities.

The hydrogenation of propylene is a very fast reaction and has been widely studied on platinum catalysts. The very rapid disappearance of the propylene impurity was noted in the cyclopropane experiments. Similar to the cyclopropane hydrogenolysis it has been classified as an example of a "facile" reaction.¹⁷

In Run 5B a 135 torr propylene/668 torr H₂ mixture was reacted at an initial temperature of approximately 90°C. The initial rate obtained was about a factor of 60 higher than the corresponding initial rate for the cyclopropane hydrogenolysis reaction in Run 4B. After 118 minutes of elapsed reaction time, practically 99% conversion was attained. A blank run of the propylene-hydrogen reaction (Run 8B) was subsequently made. It was found that after this same time period only 5.4% of the initial 135 torr propylene had been converted

[†] Details regarding the nature of these impurities are discussed in Appendix C.

to propane. It was concluded that between 35°C and 90°C the hydrogenation of propylene was a suitable reaction for further studies on single crystal platinum surfaces.

Two other reactions, considered to be of the "demanding" type,¹⁷ were also tried as possible candidates for future study. These were the dehydrocyclization of n-heptane to form toluene (Run 6B) and the hydrogenolysis and isomerization of neopentane to form isobutane and isopentane, respectively (Run 7B). The former reaction has been studied extensively on single crystal platinum surfaces at low pressures (10^{-4} - 10^{-6} torr) by Somorjai and coworkers.¹⁰

In Run 6B the initial partial pressure of n-heptane charged to the reactor (7.9 torr) was limited by its vapor pressure at room temperature and by the filling procedure employed. At a crystal temperature of 315°C, no products of reaction were detected after 120 minutes of elapsed reaction time. Several reasons can be postulated for this apparent lack of reactivity. The most obvious one is that at these conditions the specific rate of the n-heptane dehydrocyclization was too small to be measured by a thermal conductivity detector. Secondly, the calcium and sulfur impurities heretofore mentioned may well have changed the platinum stepped surface structure, thereby rendering it inactive. Somorjai and coworkers¹⁰ have reported the large variation in activity between high and low index crystal planes of platinum for this reaction at low pressure.

Finally, the reaction of neopentane with hydrogen was attempted. Boudart²⁷ has reported that this reaction is also of the "demanding" type and postulated that it preferentially would occur on Pt(111) sites. It appeared that the use of low index and stepped platinum crystals of (111) and (100) orientation would provide an excellent opportunity to check this hypothesis. In Run 7B, a 135 torr neopentane/664 torr H₂ reaction mixture was circulated past the catalyst crystal maintained at approximately 315°C. Absolutely no products of reaction were observed during the first 60 minutes of operation. Apparently the same reasons given for the lack of reactivity of the n-heptane reaction also apply to this case.

In summary, it was found that the initial rates of reaction for the hydrogenolysis of cyclopropane and the hydrogenation of propylene could easily be measured on a single platinum stepped crystal using a thermal conductivity detector of a gas chromatograph. Low specific reactivity and/or impurity poisoning of the platinum crystal were attributed to the lack of activity for both the n-heptane dehydrocyclization and neopentane isomerization and hydrogenolysis reactions.

C. The Hydrogenolysis of Cyclopropane on the
Pt(S)-[6(111)×(100)] Single Crystal

1. Introduction

The preliminary studies have shown that the hydrogenolysis of cyclopropane was a promising reaction from an experimental standpoint.

The reaction did not involve the complication of side products, the rate of production of propane was easy to follow on a single crystal, and there were sufficient data in the literature to which a comparison of the single crystal data could be made.

Accordingly a more extensive analysis of the cyclopropane hydrogenolysis reaction was initiated. A new calcium-free (by AES standards) platinum stepped crystal having a (111) terrace orientation and a (100) step was cut, polished, and etched, and mounted on triply zone refined etched tantalum electrodes. (See Appendix B for details.)

A series of experiments on this Pt(S)-[6(111)×(100)] single crystal were then commenced to determine a number of important kinetic parameters. These included the activation energy of the main reaction, the activation energy of the poisoning process, and the order of the main reaction with respect to cyclopropane. Reproducibility of the data and the reactivity of the blank system also were determined. Finally, the effects of varying standard oxygen and hydrogen pretreatment procedures on the catalytic activity of the platinum crystal were examined.

A summary of the conditions at which each of the catalytic runs was performed is given in Table III-2. Table III-3 presents the results of these experiments in terms of the initial reaction rate, and at 200 minutes of elapsed time the point rate of reaction and % conversion. Important details relating to the procedure for each run together with tabulated summaries of data can be found in Appendices G and I, respectively.

Table III - 2. Summary of catalytic runs on the Pt(s) - [6(111)X(100)] single crystal surface

Run #	Hydrogen pretreatment conditions			Reaction conditions				Notes and comments
	(T _c) _{avg} (°C)	P _{H₂} (torr)	Time (min)	(T _c) _{avg} (°C)	P _{HC} (torr)	HC	P _{H₂} (torr)	
9A	75	780	120	75.0	135.0	cyclo-C ₃ H ₆	675.0	Blank run without Pt crystal; no CP reactivity; only approx. 45% of 0.22% propylene impurity reacted.
9B	76	780	120	73.9	134.0	C ₃ H ₆	675.0	Blank run without Pt crystal; propylene hydrogenation.
10A	77	780	128	73.6	135.0	cyclo-C ₃ H ₆	675.0	Standard run [†] (T _c = 73.6°C).
11	204 306	780 106	140 64	306.6	8.0	C ₇ H ₁₆	80.0 H ₂ 712.0 N ₂	} Absolutely no toluene formed after 115 min.
12A	75	781	120	74.4	135.0	cyclo-C ₃ H ₆	675.0	
12B	76	780	120	77.7	135.0	cyclo-C ₃ H ₆	675.0	No O ₂ cleaning in UHV; soak in H ₂ overnight; flush, pretreat in H ₂ as in 12A, react.
13	69	50	110 sec.	73.1	135.0	cyclo-C ₃ H ₆	675.0	Minimal H ₂ pretreatment via leak valve.
14	75	780	122		135.0	cyclo-C ₃ H ₆	675.0	Temperature stepping sequence: 38.3, 57.0, 37.3, 74.4, 35.9, 90.5, 35.2, 122.9, 35.9, 95.7, 35.0, 72.8°C.
15	75	780	120	100.2	135.0	cyclo-C ₃ H ₆	675.0	Increase T _c for E* measurement.
16	76	780	120	132.2	135.0	cyclo-C ₃ H ₆	675.0	Increase T _c for E* measurement.
17	77	780	125	78.7	200.0	cyclo-C ₃ H ₆	675.0	Increase CP conc. to find reaction order.

[†]The procedure for a "standard run" is presented in Appendix G.

Table III-3. Rates of the cyclopropane hydrogenolysis reaction on the Pt(s) - [6(111) × (100)] single crystal surface*

Run #	Initial partial pressure of cyclopropane P _{CP} ^o (torr)	Avg. initial crystal temp. T _c ^o (°C)	Initial Reaction Rate**			Conditions at 200 minutes of elapsed reaction time				
			$\left(\frac{\text{moles C}_3\text{H}_8}{\text{min}}\right)$	$\left(\frac{\dagger \text{moles C}_3\text{H}_8}{\text{min} \cdot \text{cm}^2 \text{Pt}}\right)$	$\left(\frac{\text{molecules C}_3\text{H}_8}{\text{min} \cdot \text{cm}^2 \text{Pt}}\right)$	Crystal temp. T _c ^o (°C)	Reaction rate		Initial conversion rate	Initial conversion rate
			$\left(\frac{\text{moles C}_3\text{H}_8}{\text{min}}\right)$	$\left(\frac{\dagger \text{moles C}_3\text{H}_8}{\text{min} \cdot \text{cm}^2 \text{Pt}}\right)$	$\left(\frac{\text{molecules C}_3\text{H}_8}{\text{min} \cdot \text{cm}^2 \text{Pt}}\right)$		$\left(\frac{\text{moles C}_3\text{H}_8}{\text{min}}\right)$	$\left(\frac{\text{moles C}_3\text{H}_8}{\text{min} \cdot \text{cm}^2 \text{Pt}}\right)$	%	%
10A	135.0	73.6	1.49 × 10 ⁻⁶	1.96 × 10 ⁻⁶	1.18 × 10 ¹⁸	74.9	9.7 × 10 ⁻⁸	1.3 × 10 ⁻⁷	6.5	1.7
12A	135.0	74.4	1.33 × 10 ⁻⁶	1.76 × 10 ⁻⁶	1.06 × 10 ¹⁸	78.0	1.62 × 10 ⁻⁷	2.12 × 10 ⁻⁷	12.1	1.7
12B	135.0	77.7	1.22 × 10 ⁻⁷	1.60 × 10 ⁻⁷	9.64 × 10 ¹⁶	(300 - 400 minute reaction period)				
13	135.0	72.4	1.8 × 10 ⁻⁷	2.3 × 10 ⁻⁷	1.4 × 10 ¹⁷	69.8	1.1 × 10 ⁻⁷	1.4 × 10 ⁻⁷	---	1.3
		72.8	1.7 × 10 ⁻⁶	2.2 × 10 ⁻⁶	1.3 × 10 ¹⁸					
14	135.0	Temperature stepping sequence				72.8	1.1 × 10 ⁻⁷	1.4 × 10 ⁻⁷	---	0.85
15	135.0	100.2	4.55 × 10 ⁻⁶	5.98 × 10 ⁻⁶	3.60 × 10 ¹⁸	97.1	2.44 × 10 ⁻⁷	3.20 × 10 ⁻⁷	5.4	3.7
16	135.0	132.2	1.94 × 10 ⁻⁵	2.55 × 10 ⁻⁵	1.54 × 10 ¹⁹	133.8	2.99 × 10 ⁻⁷	3.93 × 10 ⁻⁷	1.5	9.0
17	200.0	78.7	2.47 × 10 ⁻⁶	3.25 × 10 ⁻⁶	1.96 × 10 ¹⁸	78.4	2.44 × 10 ⁻⁷	3.20 × 10 ⁻⁷	9.8	2.1

*The stepped crystal was cleaned for 13 hrs. @ 1 × 10⁻⁶ torr O₂, 903-913°C, prior to use in Run 10A.

**The 0.2% propylene impurity in the cyclopropane which reacted rapidly to propane has been subtracted from the rate data given in this table.

†This quantity is based on the total platinum area exposed, or 0.76 cm², of which 13% represents an edge area of undetermined orientation.

2. Blank Runs (with Tantalum Support Only)

Blank runs were made to determine the activity of the stainless steel reactor, the tantalum electrodes, and the platinum thermocouple wires. If the activity is small it could be subtracted from the results of subsequent catalytic runs.

In Run 9A, following the standard oxygen and hydrogen pretreatment, the reactor was filled to 810 torr with a 5/1 mixture of hydrogen/cyclopropane. At 75°C there was no detectable propane formed during the first 55 minutes of elapsed reaction time. Thereafter a very small propane peak was noticed in the gas chromatograms which increased slightly by the end of the 200-minute run. However, the propane peak formed never exceeded the size of the propylene impurity peak. In summary, at 75°C there was no detectable reaction of cyclopropane to propane in the reactor system without the platinum crystal. The propane which was formed could be attributed completely by mass balance to the reaction of the propylene impurity contained in the cyclopropane. Approximately 45% of the initial 0.22 volume % propylene in the cyclopropane reacted to form propane, corresponding to 4.4×10^{-6} moles of propane.

Following this experiment a second run (9B), identical in every respect to that of Run 9A, was carried out except that propylene was used as the reactant instead of cyclopropane. The reactivity measured was substantial. The initial rate of the propylene hydrogenation at 74°C amounted to 4.93×10^{-6} moles C_3H_8 /min-cm² Pt. At 200 minutes elapsed reaction time the rate was 2.44×10^{-6} moles C_3H_8 /min-cm² Pt, corresponding to 9.2% conversion of the initial propylene reactant.

During the normal 120-minute, high temperature oxygen pretreatment in the course of all the runs presented in this study, it was observed that approximately the last 0.5 cm of each of the two 0.010-inch platinum thermocouple wires leading up to the junction was red hot, or above 700°C. This would indicate that these small cylindrical surface areas may have been cleaned of carbonaceous residues and could well be active catalysts. The total surface area of the cleaned platinum thermocouple wire would amount to approximately 0.08 cm², or 10% of the area of the platinum crystal used in Run 5B. Recall that in this run using a Pt(S)-[7(111)×(111)] crystal having a surface area of 0.80 cm², greater than 99% conversion of the 135 torr propylene was achieved in 200 minutes. The fact that 9.2% of the propylene did react in Run 9B after 200 minutes on a Platinum surface that was 9.1% (0.08 cm²/0.80 + 0.08 cm²) of that available in Run 5B suggests that these small segments of the platinum thermocouple wires were indeed responsible for the activity.

No experiments were performed without the platinum thermocouple wires in the system.

3. Reproducibility of Experimental Runs

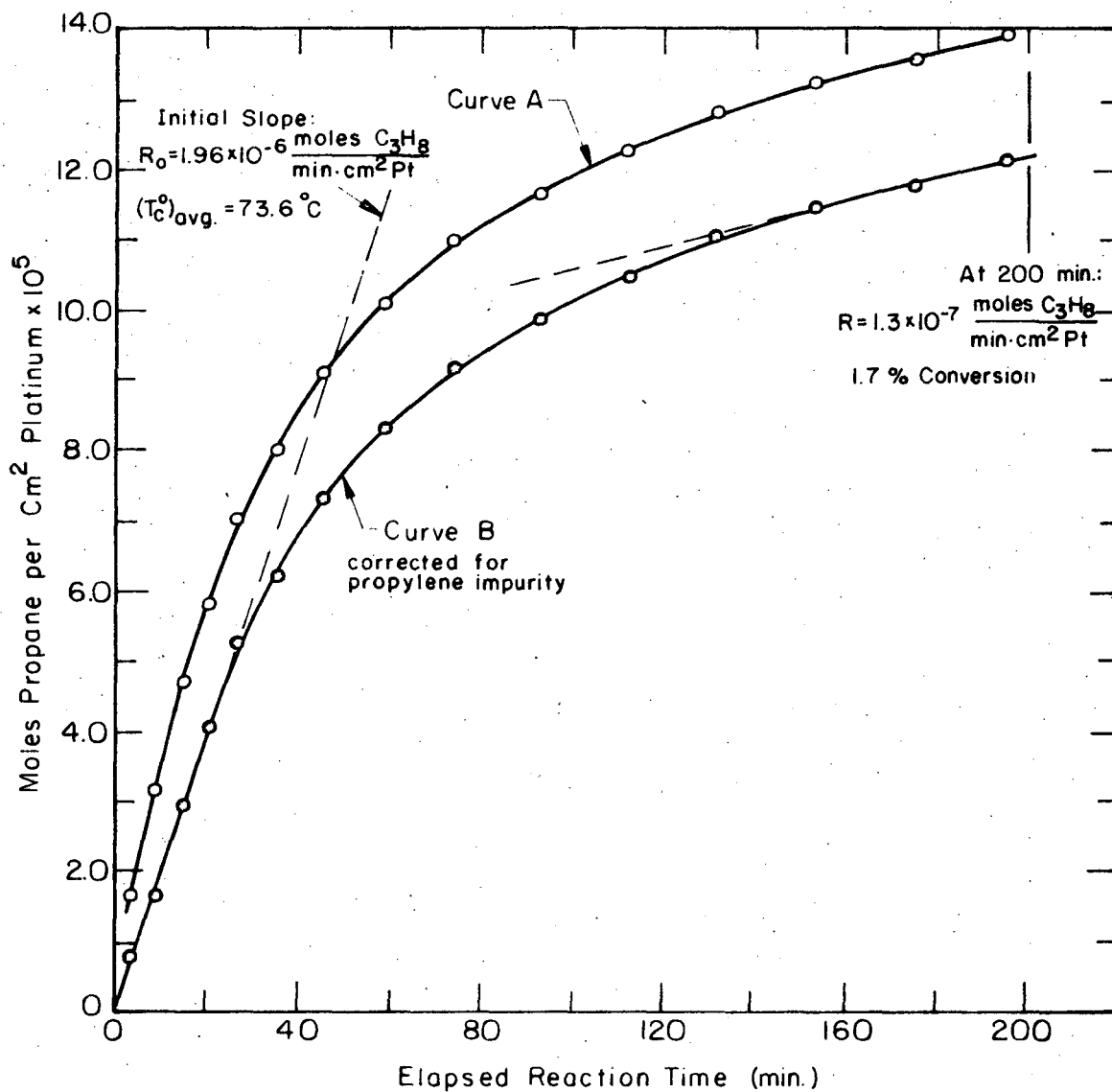
Two experimental runs (10A and 12A) were carried out under identical conditions to determine the reproducibility of the data. The procedure used in these runs was exactly the same as in Run 9A; with the exception that now the platinum single crystal had been inserted into the system.[†]

[†]Details relating to the preparation of the single crystal prior to Run 10A are presented in Appendix B.

Figure III-1 presents a plot of the data for Run 10A in the form of total moles of propane formed per square centimeter of platinum surface as a function of elapsed reaction time.^{††} The upper curve (A) represents the data calculated from the gas chromatograms without correcting for the propylene impurity. Analysis of the third reaction chromatogram (third data point at approximately 15 minutes) revealed that there was no detectable propylene remaining in the system. The amount of the initial propylene impurity could be estimated by three methods: (1) Using the absolute propylene peak area from pre-reaction chromatograms; (2) Using the relative % propylene in pre-reaction chromatograms together with the measured initial cyclopropane concentration; or (3) Extrapolating back to zero time the first three to four data points after no detectable propylene remained in the system. An average of these values was normally taken to be the initial propylene concentration.

The lower curve (B) of Fig. III-1 represents the data with the propylene contribution to the propane concentration subtracted out. In most subsequent presentations of data only the corrected figures as exemplified by curve B will be shown. The initial rate of the cyclopropane hydrogenolysis and the rate and conversion at 200 minutes of elapsed reaction time are provided in both Fig. III-1 and Table III-3. It should be noted that the data points generally follow a smooth curve, indicating that the experimental techniques employed were good and that

^{††} Appendix I provides tabular summaries of all raw and calculated data for each run presented in this section. The G. C. calibration curves for cyclopropane, propane, and propylene can be found in Appendix E.



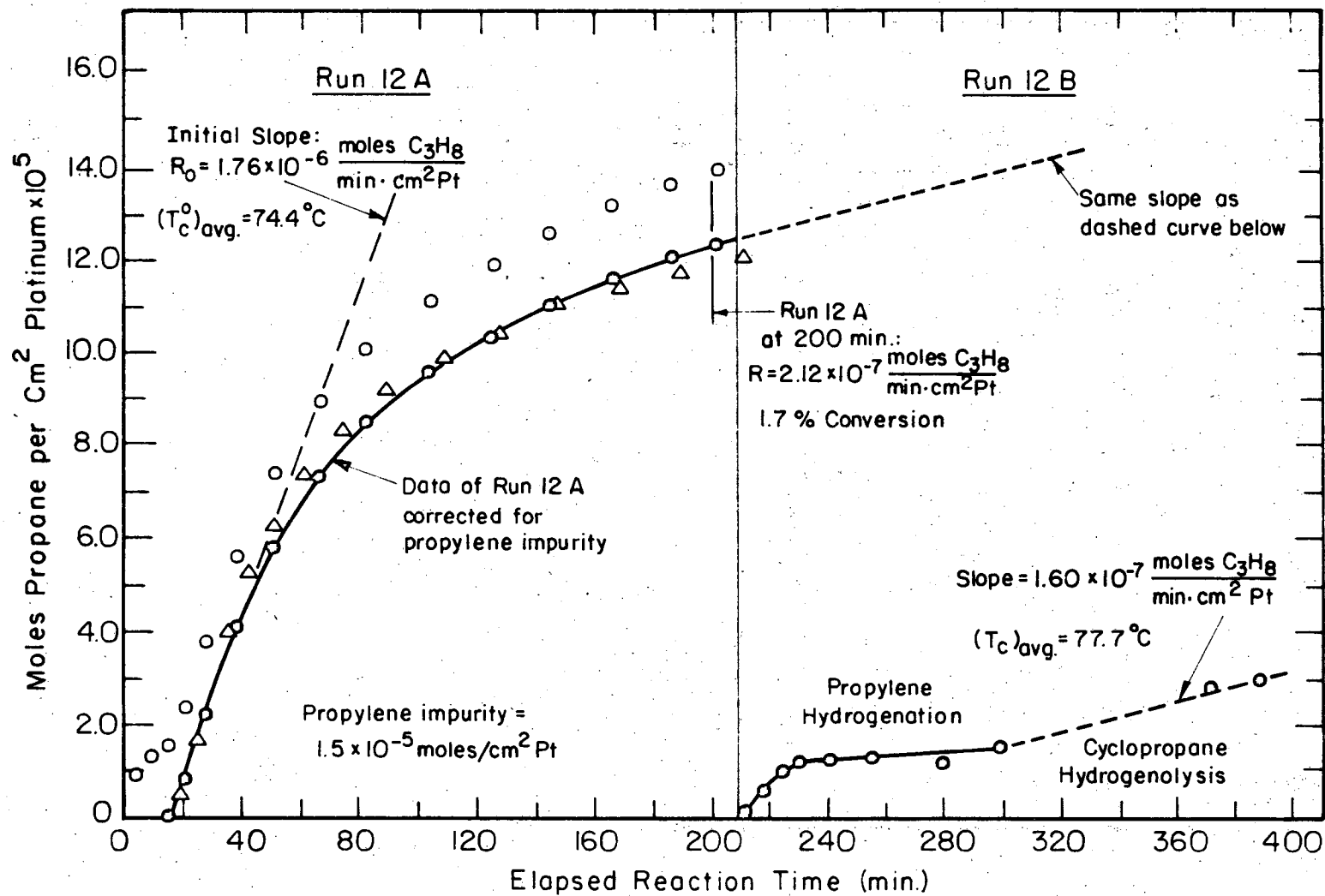
XBL 738-1639

Figure III-1. Run 10A. Cyclopropane hydrogenolysis on the Pt(S)-[6(111)×(100)] surface. $P_{CP}^{\circ} = 135$ torr. $P_{H_2}^{\circ} = 675$ torr.

the calculation of chromatographic peak areas by the triangulation method was consistent.

Run 12A was then made to check whether the data obtained in Run 10A could be reproduced under the same experimental conditions. The only important difference between the two runs was that in Run 10A the initial reaction temperature was 73.6°C while that in Run 12A was 74.4°C. Figure III-2 and Table III-3 summarize the pertinent reaction rate data. Note that on subtracting the propylene contribution from the raw calculated data in Figure III-2 there appears to be a delay time of approximately 15 minutes, after which the cyclopropane hydrogenolysis reaction begins to take place. The reason for this anomaly is one of procedural error. The reactor bypass valve had been inadvertently left open for the first 50 minutes of the run, in effect causing the initial partial pressure of cyclopropane in the reactor cup to have been lower than that in the recirculation loop for a short, but indeterminable, period of time. Apparently 15 minutes was sufficient for this mixing process to occur and provide a reasonably uniform concentration of cyclopropane and propane in the total reactor volume. This is substantiated by the smooth rate of rise of propane measured in the sample loop after 15 minutes of elapsed reaction time.

To make a valid comparison between Runs 10A and 12A the corrected data of Run 10A has been plotted in Figure III-2 with a time shift of 15.0 minutes. The curves are remarkably similar in shape. The initial rates differ by approximately 10% while the conversion at 20.0 minutes of elapsed reaction time is identical in both cases (1.7%). Considering the sources of error in these experiments, the agreement is quite good,



XBL 738-1640

Figure III-2. Runs 12A and 12B. Cyclopropane hydrogenolysis on the Pt(S)-[6(111)×(100)] surface. Open circles: data of Run 12A uncorrected for propylene impurity. Open triangles: data of Run 10A with 15-minute time shift.

leading to the conclusion that the data are probably reproducible to about 10%.

A further discussion of Figure III-2 as it relates to Run 12B will be presented in a later section of this chapter.

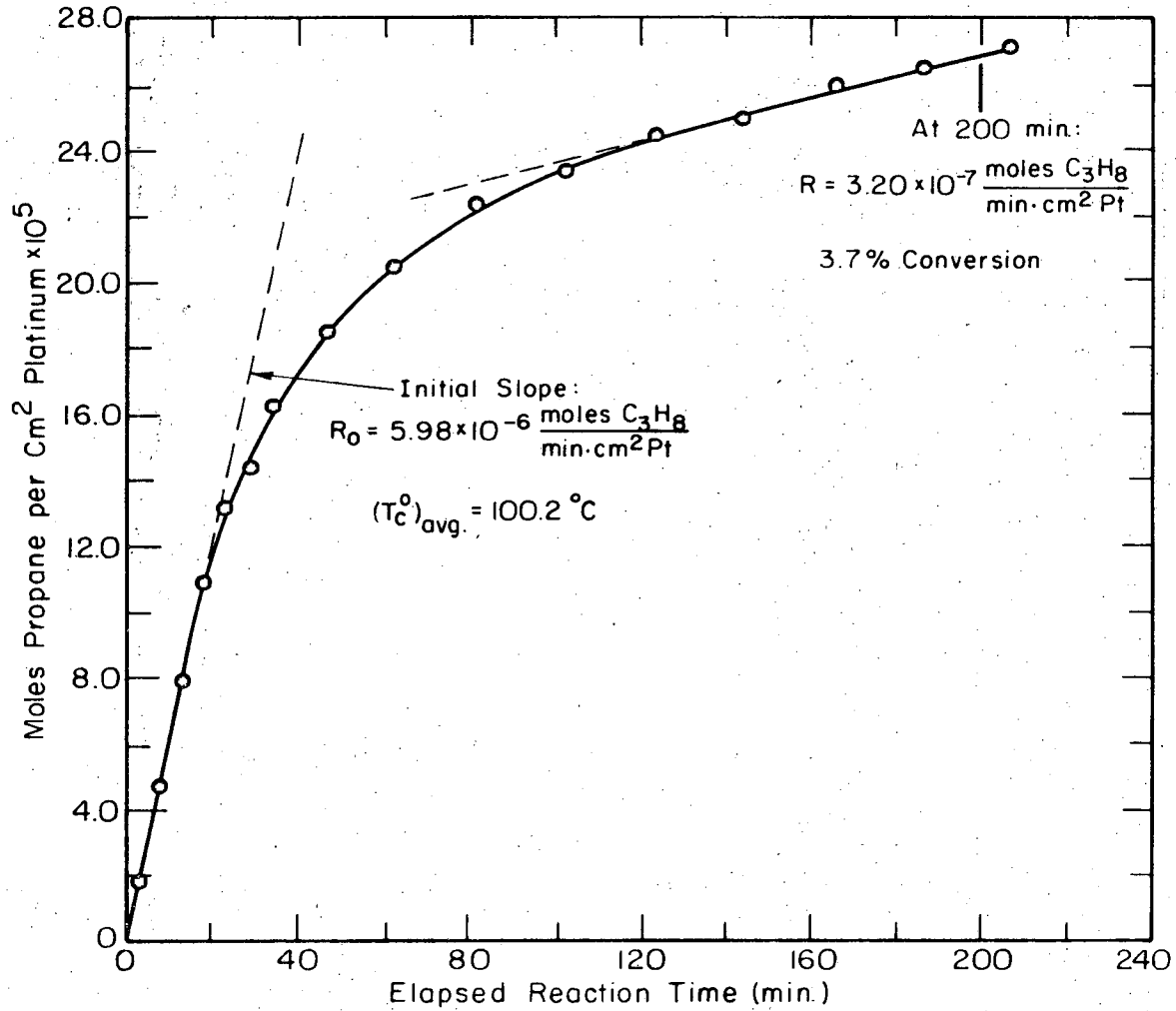
4. Activation Energy on the Unpoisoned Catalyst

Additional rate measurements at several higher temperatures provided a basis for calculating a value of the activation energy for the main reaction. In Run 15 (Figures III-3) the average initial crystal temperature was maintained at 100.2°C, while for Run 16 (Figure III-4) this temperature was 132.2°C.

The initial rate and temperature data for Runs 10A, 12A, 15, and 16 are summarized in Table III-4. An Arrhenius plot of these points was constructed in Figure III-5 and the best straight line drawn through the data. The activation energy of the cyclopropane hydrogenolysis reaction calculated from this plot was $E^* = 12.2 \pm 1.0$ kcal/mole. Values of the activation energy reported in the literature for the hydrogenolysis of cyclopropane on platinum catalysts range from 8.0 to 12.2 kcal/mole.³⁹⁻⁵⁰

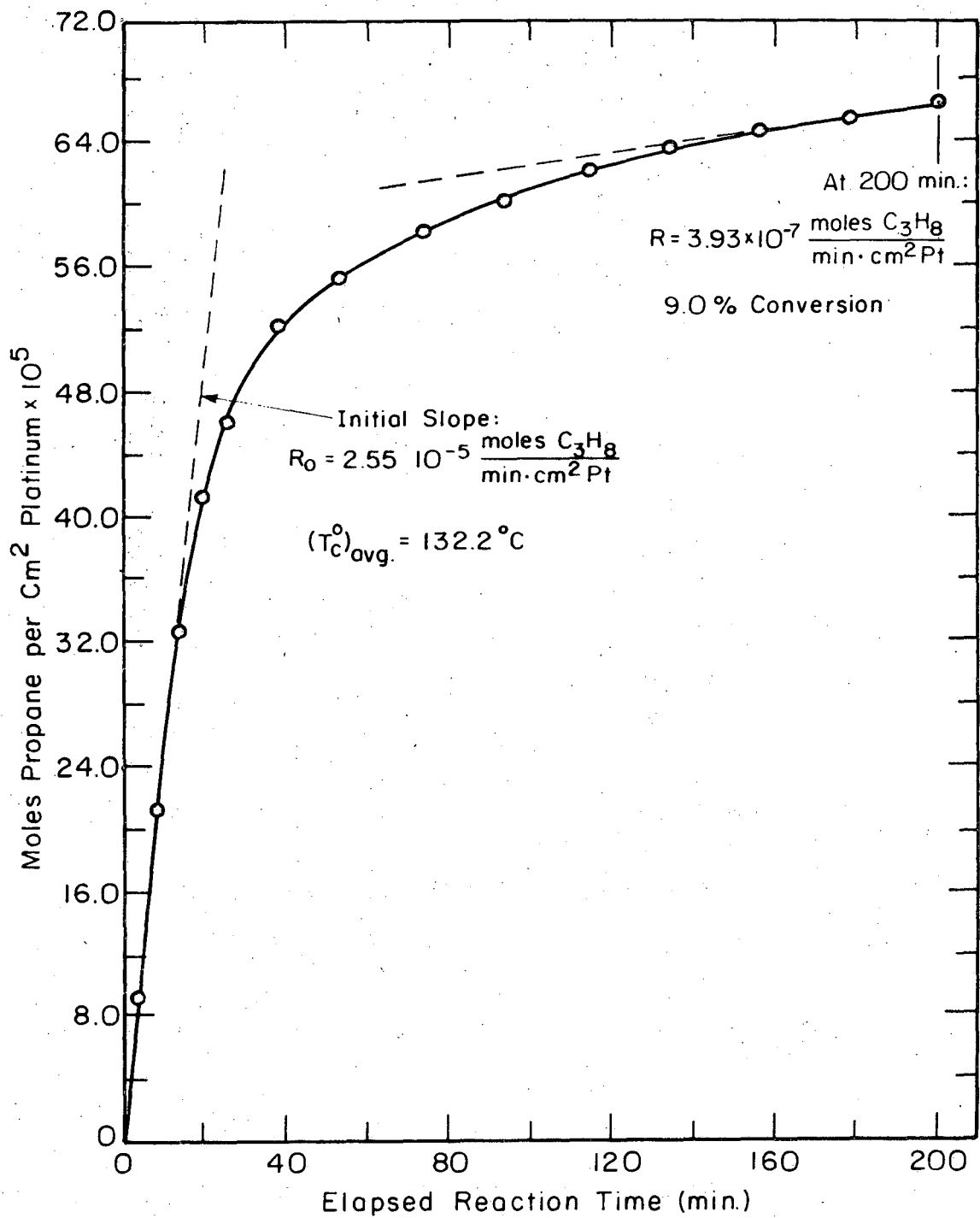
Having obtained a value of E^* , it was possible to compare the initial specific rates of reaction on the stepped single crystal surface with specific rates reported on polycrystalline supported platinum catalysts.

Hegedus^{50,51} carried out a series of cyclopropane hydrogenolysis experiments on single pellets of Pt/Al₂O₃. The physical characteristics of one typical pellet and kinetic reaction rate data obtained on this catalyst are given in Tables III-5A and III-5B. Using this information and assuming 100% dispersion of the platinum, the rate of the cyclopropane hydrogenolysis at 75°C and 135 for CP was calculated and is



XBL 738-1641

Figure III-3. Data of Run 15 for the cyclopropane hydrogenolysis.

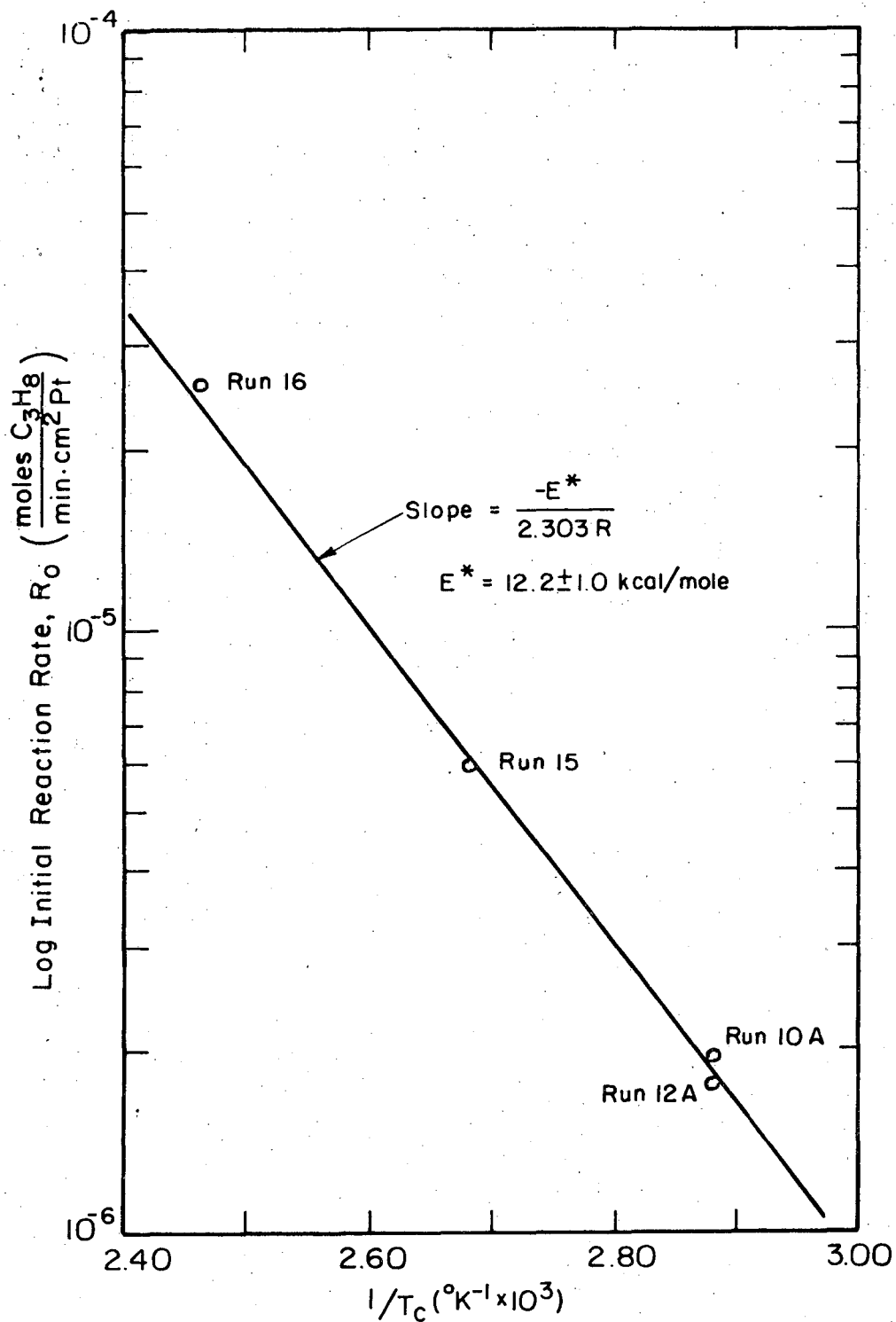


XBL 738-1642

Figure III-4. Data of Run 16 for the cyclopropane hydrogenolysis.

Table III - 4. Summary of the initial rate data for the determination of E^* for the cyclopropane hydrogenolysis on the Pt(s) - [6(111) X (100)] single crystal

Run #	Initial partial pressure of cyclopropane P_{CP}° (torr)	Crystal temperature averaged over initial rate measurement		$\frac{1}{T_c}$ ($^{\circ}K^{-1} \times 10^3$)	Initial reaction rate R_0 $\left(\frac{\text{moles } C_3H_8}{\text{min} \cdot \text{cm}^2 \text{Pt}} \right)$
		T_c ($^{\circ}C$)	T_c ($^{\circ}K$)		
10A	135.0	73.5	346.7	2.88	1.96×10^{-6}
12A	135.0	74.4	347.6	2.88	1.76×10^{-6}
15	135.0	100.2	373.4	2.68	5.98×10^{-6}
16	135.0	132.2	405.4	2.46	2.55×10^{-5}



XBL 738-1643

Figure III-5. Activation energy for the hydrogenolysis of cyclopropane based upon initial reaction rates on the Pt(S)-[6(111)×(100)] single crystal ($A_s = 0.76 \text{ cm}^2$). $P_{cp}^\circ = 135 \text{ torr}$. $P_{H_2}^\circ = 675 \text{ torr}$.

Table III - 5A. Physical characteristics of the platinum catalyst pellet used by Hegedus^{50, 51}

-
- 0.25 wt % Pt on $\eta\text{-Al}_2\text{O}_3$ diluted with $\eta\text{-Al}_2\text{O}_3$ to 0.04 wt % Pt
 - $\eta\text{-Al}_2\text{O}_3$ surface area = $230 \text{ m}^2/\text{gram}$
 - Weight of pellet = 0.295 grams
 - Pellet density = 1.14 grams/cm^3
-

Table III - 5B. Initial rate data for the cyclopropane hydrogenolysis using the catalyst pellet of Hegedus^{50, 51}

-
- Catalyst calcined in 3% O_2 in N_2 @ $400\text{-}410^\circ\text{C}$ for 2 hrs.
 - Catalyst reduced in H_2 @ 300°C for 10 hrs.
 - $C_{\text{H}_2}^\circ = 41.4 \times 10^{-6} \frac{\text{moles}}{\text{cm}^3}$ ($P_{\text{H}_2}^\circ = 900 \text{ torr}$)
 - $C_{\text{CP}}^\circ = 3.45 \times 10^{-6} \frac{\text{moles}}{\text{cm}^3}$ ($P_{\text{CP}}^\circ = 75.0 \text{ torr}$)
 - $T_{\text{rxn}} = 75^\circ\text{C}$
 - $(k a)_i = 2.61 \text{ sec}^{-1}$
 - Reaction found to be first order in cyclopropane concentration.
-

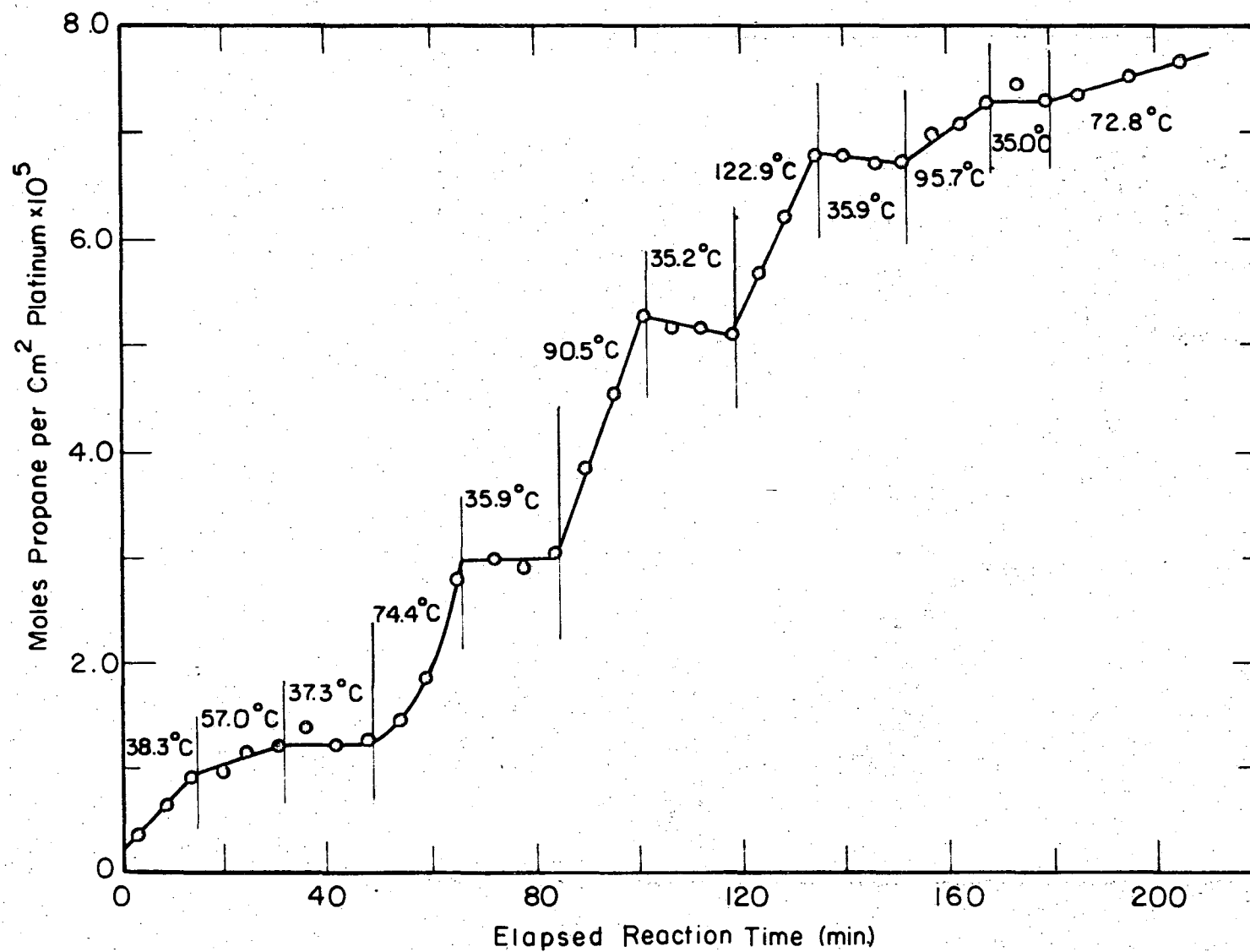
presented in Table III-6. A more realistic value for the platinum dispersion, say 50%, would result in a specific rate ($820 \frac{\text{molecules C}_3\text{H}_8}{\text{min. Pt site}}$) which is nearly the same as the average of the four rates in Runs 10A, 12A, 15, and 16 ($812 \frac{\text{molecules C}_3\text{H}_8}{\text{min. Pt site}}$).

Boudart and coworkers²³ have studied the cyclopropane-hydrogen reaction over a number of highly dispersed $\eta\text{-Al}_2\text{O}_3$ and $\gamma\text{-Al}_2\text{O}_3$ supported platinum catalysts. A turnover number ($\frac{\text{molecules converted}}{\text{min. catalyst site}}$) of $N = 9.8$ was reported for a series of these highly dispersed catalysts at 0°C and 10 torr initial cyclopropane partial pressure. The specific rates calculated from this data are given in Table III-6, based upon the kinetic parameters of Dougharty⁴⁵ and assuming a platinum site density of 1.12×10^{15} atoms/cm². To within a factor of two, the initial rate data of Boudart and that of the present study are identical.

It can be concluded from comparisons of initial rate data appearing in the literature for the cyclopropane hydrogenolysis reaction that the stepped platinum single crystal used in this study behaves very much like a highly dispersed supported platinum catalyst.

Table III-6. Comparison of initial specific rate data for the cyclopropane hydrogenolysis on platinum catalysts

Data source	Type of catalyst	Calculated specific reaction Rate @ $P_{CP}^{\circ} = 135$ torr and $T = 75^{\circ}C$		Comments
		$\left(\frac{\text{moles } C_3H_8}{\text{min} \cdot \text{cm}^2 \text{Pt}}\right)$	$\left(\frac{\text{molecules } C_3H_8}{\text{min} \cdot \text{Pt site}}\right)$	
Present study	Run 10A	2.1×10^{-6}		-- Rate on Pt(s) - [6(111) \times (100)] single crystal based on $E^* = 12.2$ kcal/mole. * Value based upon 87% (111) orientation and 13% polycrystalline orientation.
	Run 12A	1.8×10^{-6}		
	Run 15	1.8×10^{-6}		
	Run 16	2.1×10^{-6}		
	Average	1.95×10^{-6}	* 812	
Hegedus ^{50, 51} See Table III-5	0.04 Wt% Pt on η - Al_2O_3	7.7×10^{-7} based on 100% Pt dispersion	* 410	* Based upon avg. Pt site density of 1.12×10^{15} atoms/Pt site. This value would be nearly equal to average of above values if dispersion was approximately 50%.
Boudart et al. ²³ and Dougharty ⁴⁵	0.3% and 2.0% Pt on η - Al_2O_3 ; 0.3% and 0.6% Pt on γ - Al_2O_3	8.9×10^{-7}	480	-- $\eta_{CP} = 0.2$, $E^* = 8.5$ kcal/mole.
		2.5×10^{-6}	1340	-- $\eta_{CP} = 0.6$, $E^* = 8.5$ kcal/mole. (Dougharty reports $E^* = 8-9$ kcal/mole and $n = 0.2$ to 0.6)



XBL738-1644

Figure III-6. Run 14. Hydrogenolysis of cyclopropane on the Pt(S)-[6(111) x (100)] surface: Temperature stepping experiment. (Note: the data has not been corrected for the propylene impurity.)

structure or amount of carbonaceous residues on the surface of the platinum crystal, the latter three rate periods shown in Figure III-6 were used to determine E_p^* . The calculations are summarized in Table III-7 and in the Arrhenius plot of Figure III-7. The activation energy of the cyclopropane hydrogenolysis reaction on the partially deactivated platinum single crystal was found to be $E_p^* = 10.5$ kcal/mole.

6. Reaction Rate Order with Respect to Cyclopropane

An experimental run at a higher initial partial pressure of cyclopropane was made to provide a basis for calculating the order of the reaction with respect to cyclopropane. In Run 17 the partial pressure of cyclopropane was increased to 200 torr while maintaining the hydrogen partial pressure constant at 675 torr. Table III-3 and Figure III-8 summarize the results of this experiment, where the initial reaction temperature was maintained at 78.7°C.

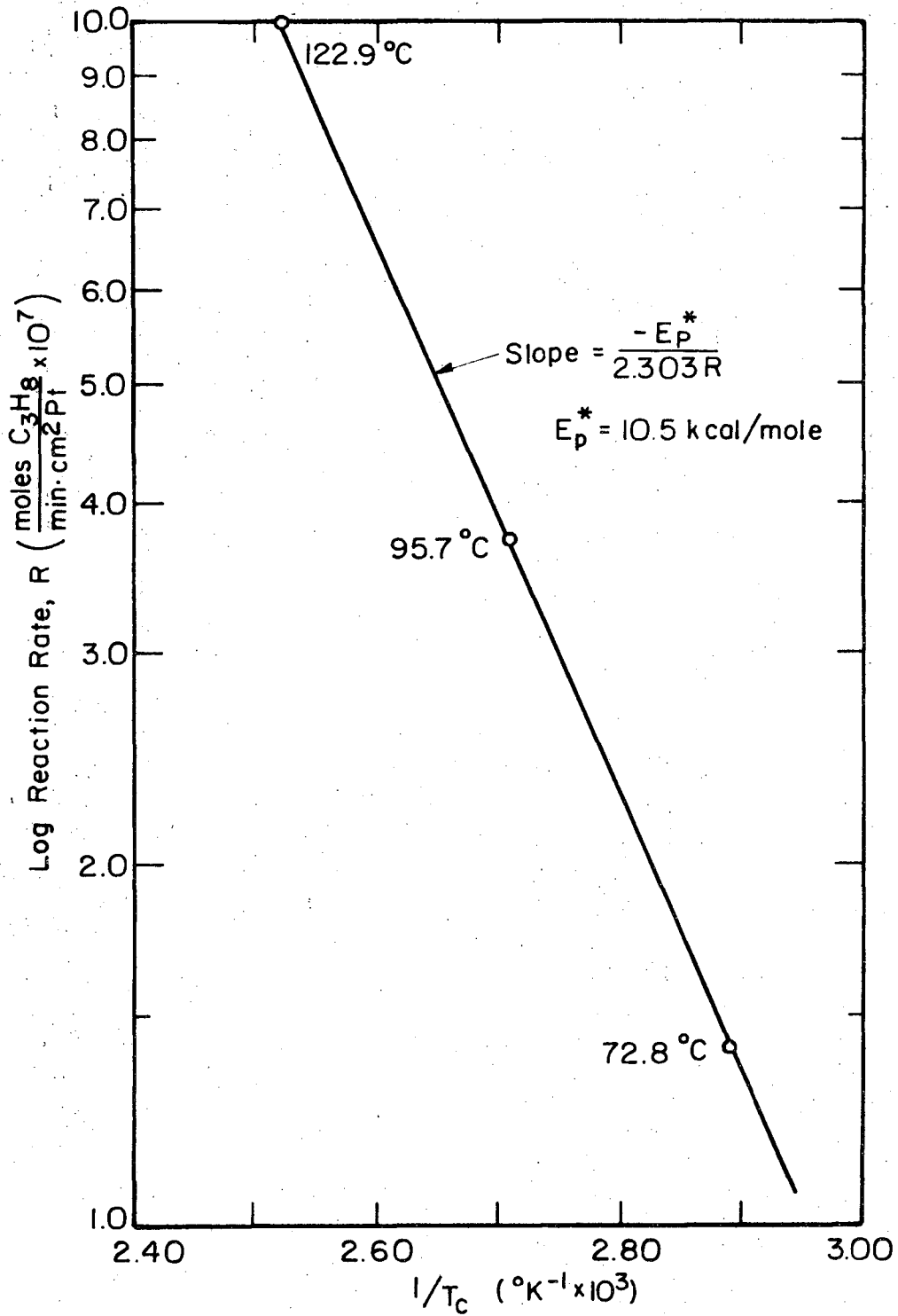
Hegedus⁵⁰ reported the cyclopropane hydrogenolysis reaction on an Al_2O_3 -supported platinum catalyst to be first order with respect to cyclopropane and some small negative order with respect to hydrogen at large H_2/CP ratios. A simple Langmuir-Hinshelwood mechanism can be written which approximately describes this behavior. For instance, assuming that H_2 dissociates on the surface and that the controlling step in the reaction is the surface reaction between adsorbed cyclopropane and a hydrogen atom, it can be shown⁵² that the initial rate of the unpoisoned reaction is given by:

$$r = \frac{k K_{H_2} K_{CP} C_{H_2} C_{CP}}{(1 + \sqrt{K_{H_2} C_{H_2}} + K_{CP} C_{CP})^3} \quad (1)$$

Table III - 7. Summary of rate data during the latter half of Run 14 - calculation of E_p^*

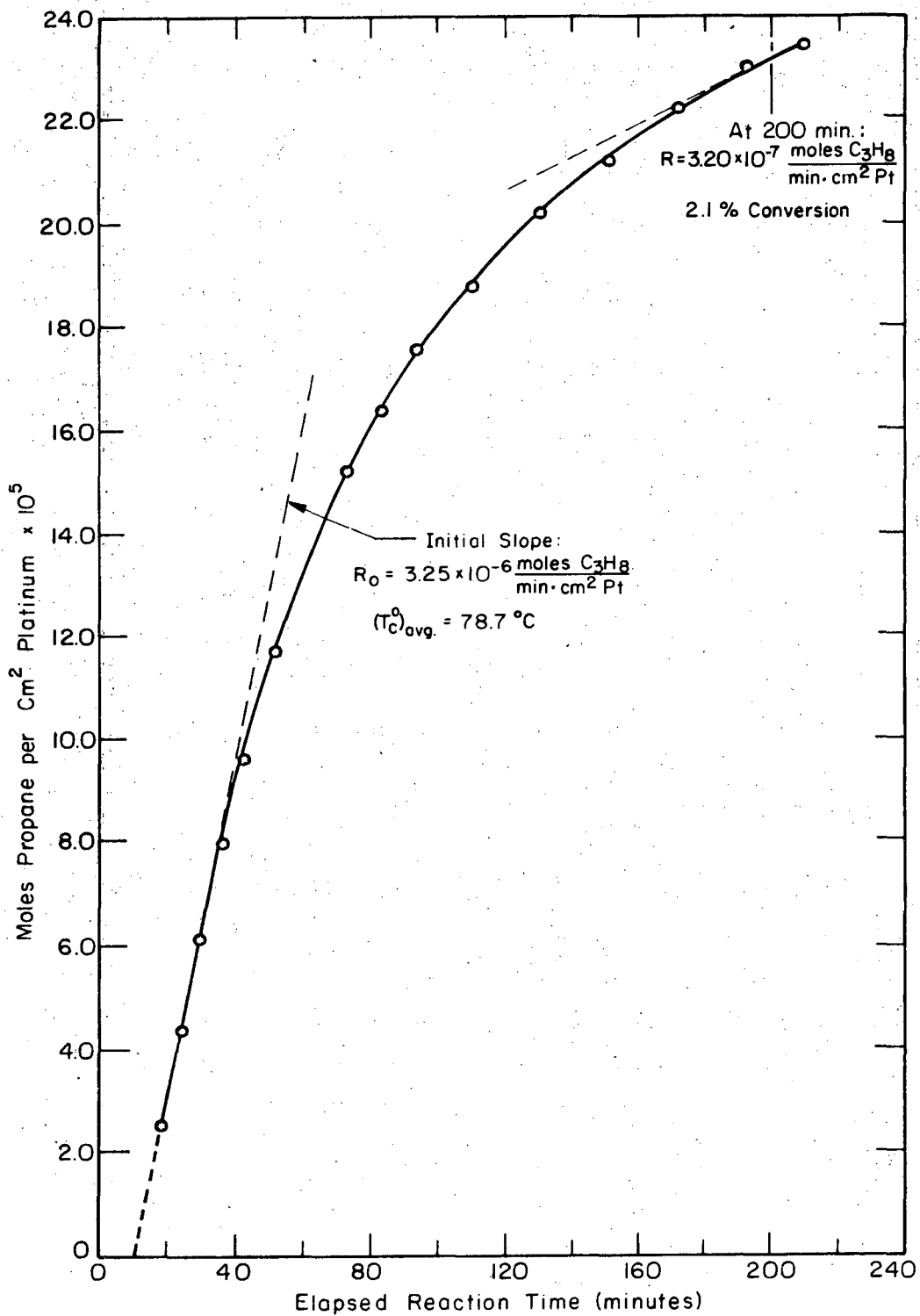
Time interval of rate measurement (minutes)	Reaction rate $\left(\frac{\text{moles C}_3\text{H}_8}{\text{min}\cdot\text{cm}^2\text{Pt}}\right)$	Average crystal temperature		$\frac{1}{T_c}$ ($^{\circ}\text{K}^{-1}\times 10^3$)
		T_c ($^{\circ}\text{C}$)	T_c ($^{\circ}\text{K}$)	
118.3 - 134.9	9.90×10^{-7}	122.9	396.1	2.52
151.6 - 168.0	3.71×10^{-7}	95.7	368.9	2.71
179.1 - 205.0	1.41×10^{-7}	72.8	346.0	2.89

-45-



XBL738-1645

Figure III-7. Run 14. Activation energy for the cyclopropane hydrogenolysis on the partially deactivated catalyst.



XBL738-1646

Figure III-8. Run 17. Cyclopropane hydrogenolysis on the Pt(S)-[6(111)×(100)] surface. $P_{\text{CP}}^\circ = 200 \text{ torr}$. $P_{\text{H}_2}^\circ = 675 \text{ torr}$.

If $\sqrt{K_{H_2} C_{H_2}} \gg (1 + K_{CP} C_{CP})$, then

$$r = k' C_{H_2}^{-1/2} C_{CP} \quad (2)$$

Other investigators have found orders ranging from zero to 1.0. For pumice-supported platinum catalysts, Bond⁵³ reports orders in cyclopropane between 0.2 and 1.0 depending on the catalyst reduction procedures. McKee⁴⁴ determined the hydrogenolysis reaction to be approximately zero order in cyclopropane concentration on unsupported platinum black. Dougharty⁴⁵ found the order with respect to cyclopropane to be in the range 0.2 to 0.6 on Al₂O₃-supported platinum catalysts.

Rewriting eqn. (1) in more general terms,

$$r = \frac{k K_{H_2} K_{CP} C_{H_2}^m C_{CP}^n}{[1 + K_{H_2} C_{H_2}^m + K_{CP} C_{CP}^n]^p} \quad (3)$$

Again assuming that $(K_{H_2} C_{H_2}^m) \gg (1 + K_{CP} C_{CP}^n)$,

$$r = \frac{k' K_{H_2} K_{CP} C_{H_2}^m C_{CP}^n}{K_{H_2} C_{H_2}^{m \cdot p}} \quad (4)$$

or

$$r = k'' C_{CP}^n \quad (5)$$

if the terms containing C_{H₂} are constant. Then,

$$\log r = n \log C_{CP} + \log k'' \quad (6)$$

A plot of the data at constant C_{H_2} in the form of eqn. (6) should therefore yield directly the order of the reaction with respect to cyclopropane.

Accordingly, Table III-8A lists the initial rates of the experimental runs used in the calculation. The hydrogen partial pressure in each run was held constant at 675 torr. The reaction temperature of Run 12A, namely 74.4°C, was arbitrarily chosen as the basis for the comparison. Table III-8B summarizes the results of the temperature correction,[†] where the upper and lower values of E^* have been included. Finally, Figure III-9 contains the averaged data of Table III-8B in the suggested form of eqn. (6). To within the scatter of the data using the best fit for the value of the activation energy, the order of the cyclopropane hydrogenolysis reaction with respect to cyclopropane was determined to be $n = 0.8 \pm 0.2$.

[†]Based on a form of the Arrhenius equation:

$$\log \left(\frac{r_2}{r_1} \right) = \frac{E^*}{2.303R} \left[\frac{T_2 - T_1}{T_1 T_2} \right],$$

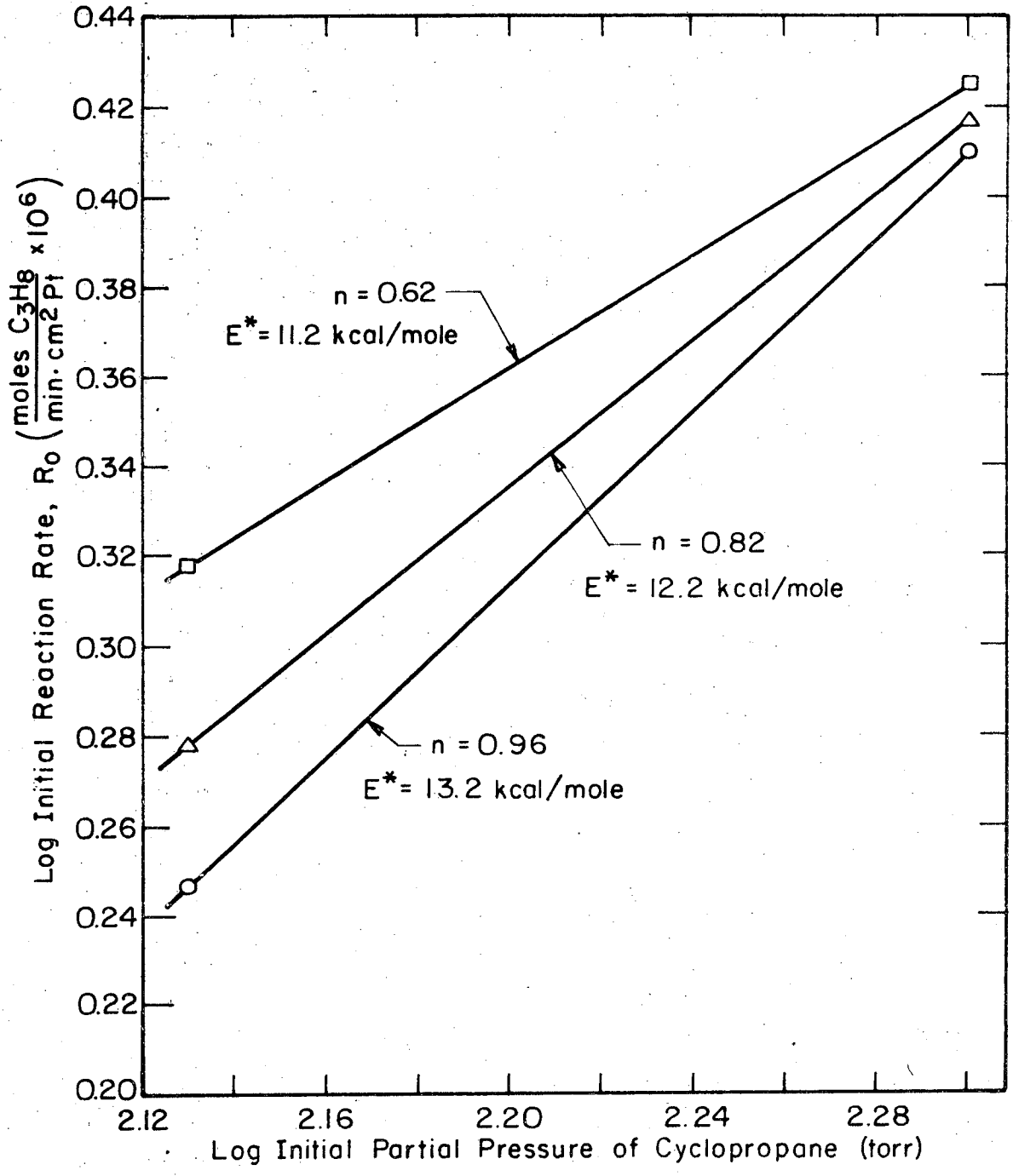
where E^* is the activation energy of the unpoisoned catalyst (12.2 ± 1.0 kcal/mole).

Table III - 8A. Calculation of reaction order with respect to cyclopropane

Run #	Average initial reaction temperature (T_c°) (T_c°) ($^{\circ}\text{C}$)	Initial cyclopropane partial pressure P_{CP}° (torr)	Initial reaction rate $\left(\frac{\text{moles } \text{C}_3\text{H}_8}{\text{min} \cdot \text{cm}^2 \text{Pt}}\right)$
10A	73.5	135	1.96×10^{-6}
12A	74.4	135	1.76×10^{-6}
15	100.2	135	5.98×10^{-6}
16	132.2	135	2.55×10^{-5}
17	78.7	200	3.25×10^{-6}

Table III - 8B

Activation energy E^* (kcal/mole)	Run #	Calculated rate based on temp. of Run 12A (74.4°C) $\left(\frac{\text{moles } C_3H_8}{\text{min} \cdot \text{cm}^2 \text{Pt}}\right)$	Average order with respect to cyclopropane n (Eqn. 6)
11.2	10A	2.05×10^{-6}	0.62
	12A	1.76×10^{-6}	
	15	2.05×10^{-6}	
	16	2.55×10^{-6}	
	17	2.66×10^{-6}	
12.2	10A	2.05×10^{-6}	0.82
	12A	1.76×10^{-6}	
	15	1.76×10^{-6}	
	16	2.06×10^{-6}	
	17	2.61×10^{-6}	
13.2	10A	2.06×10^{-6}	0.96
	12A	1.76×10^{-6}	
	15	1.60×10^{-6}	
	16	1.68×10^{-6}	
	17	2.57×10^{-6}	



XBL 738-1647

Figure III-9. Determination of reaction order with respect to cyclopropane.

7. Activation Energy for the Poisoning Process

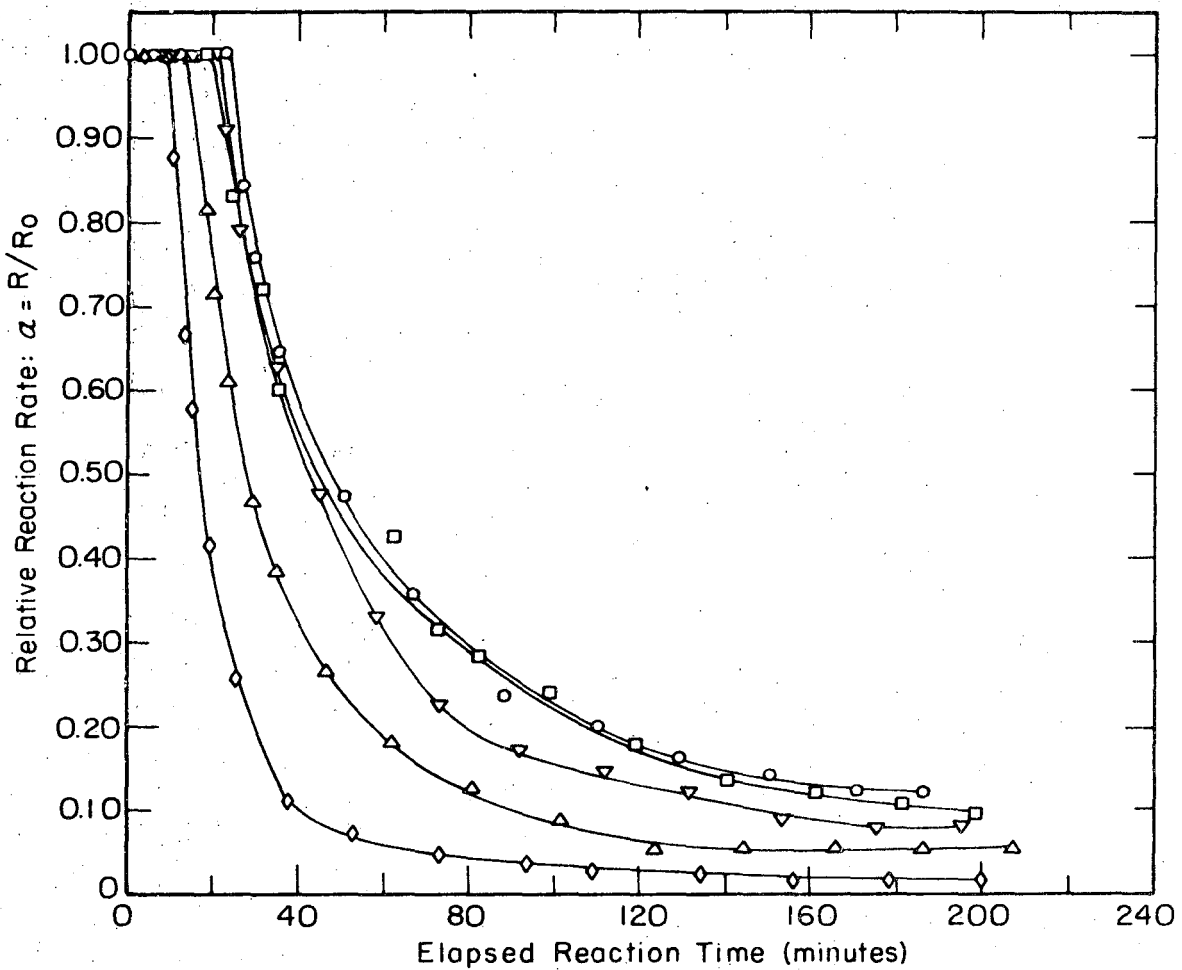
To understand better the nature of the poisoning process occurring during the hydrogenolysis of cyclopropane, the data of Runs 10A, 12A, 15, 16, and 17 were plotted on the same graph. In Figure III-10A a non-dimensionalized relative reaction rate, $\alpha = R/R_0$, is shown as a function of elapsed reaction time, where R_0 is the calculated initial rate listed in Table III-8A.[†]

The first point to note in Figure III-10A is that all five curves do not coincide. However the initial portions of the curves for Runs 10A, 12A, and 17 are very similar. Increasing the cyclopropane concentration from 135 torr to 200 torr therefore does not appear to change the relative rate of poisoning. This suggests that the poisoning process is zero-order with respect to the concentration of cyclopropane.

The second observation to be made is that as the crystal temperature is increased (Runs 15 and 16) at constant cyclopropane concentration, the poisoning process occurs sooner.

It was hoped that by non-dimensionalizing the time coordinate for each of the curves in Figure III-10A the data would be compressed onto a single line. The characteristic time chosen for this purpose was that corresponding to the point of inflection in each of the experimental curves, denoted here as t_p . Table III-9 summarizes the values of t_p determined for each experimental run. From Figure III-10A, $\alpha = 0.90$ was taken to be the point of inflection in all five cases. To check the sensitivity of this choice, t_p at $\alpha = 0.50$ has also been presented in Table III-9.

[†]The point rates of reaction for each experimental run presented in Figure III-10A are tabulated in Appendix J.



XBL 738-1648

Figure III-10A. Non-dimensionalized reaction rate data for the cyclopropane hydrogenolysis on the Pt(S)-[6(111)×(100)] single crystal.

Symbol	Run #	KEY			
		Average Initial Reaction Temp (°C)	Initial Cyclopropane Partial Pressure (torr)	Initial Reaction Rate $\frac{\text{moles } C_3H_8}{\text{min cm}^2 \text{ Pt}}$	Poisoning Time Constant (min)
▽	10A	73.5	135	1.96×10^{-6}	23.4
○	12A	74.4	135	1.76×10^{-6}	25.4
□	17	78.7	200	3.25×10^{-6}	23.0
△	15	100.2	135	5.98×10^{-6}	15.9
◇	16	132.2	135	2.55×10^{-5}	10.5

Table III -9. Summary of calculations for activation energy of the poisoning process $t_p = B \exp(-E_{pp}^*/RT)$

Run No. and figure code	CRYSTAL TEMPERATURE			POISONING TIME	
	T_c (°C)	T_c (°K)	$1/T_c$ (°K ⁻¹ × 10 ³)	t_p @ $\alpha = 0.90$ (min)	t_p @ $\alpha = 0.50$ (min)
10A ▽	73.5	346.7	2.884	23.4	43.3
12A ○	74.4	347.6	2.877	25.4	47.7
17 □	78.7	351.9	2.842	23.0	45.0
15 △	100.2	373.4	2.678	15.9	27.6
16 ◇	132.2	405.4	2.467	10.5	17.0

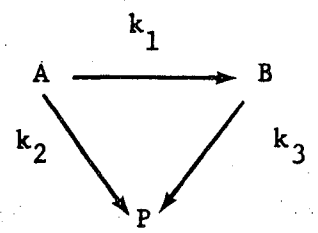
A plot of α versus a non-dimensionalized reaction time, $\tau = t/t_p$, is shown in Figure III-10B. The data points for each run between $\tau = 0$ and $\tau = 1.5$ practically coincide, with the scatter increasing as τ increases. Even on the completely non-dimensionalized plot it is evident that at the higher reaction temperatures (e.g., Run 16) the poisoning process occurs sooner than at the lower temperatures (e.g., Run 10A).

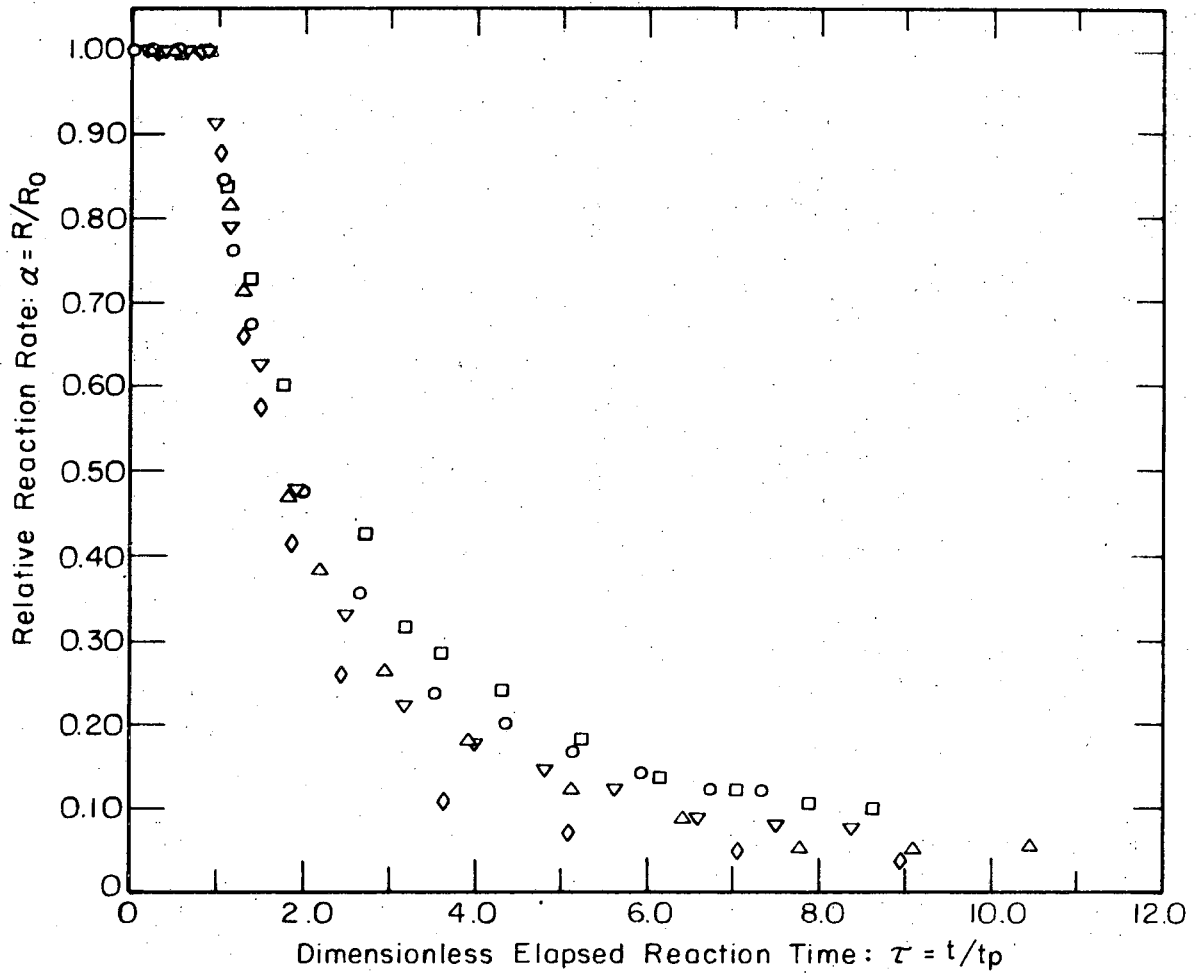
The characteristic poisoning time, t_p , has been represented as an exponential function following the Arrhenius form:

$$t_p = B e^{-E_{pp}^*/RT}$$

where E_{pp}^* is the apparent activation energy for the poisoning process. Using Table III-9 as a basis, $\log t_p$ vs $1/T_C$ has been plotted in Figure III-11 for both $\alpha = 0.90$ and $\alpha = 0.50$. The activation energy for the poisoning process based on this graphical procedure was found to be 4-5 kcal/mole. This is significantly less than the activation for the main reaction (12.2±1.0 kcal/mole).

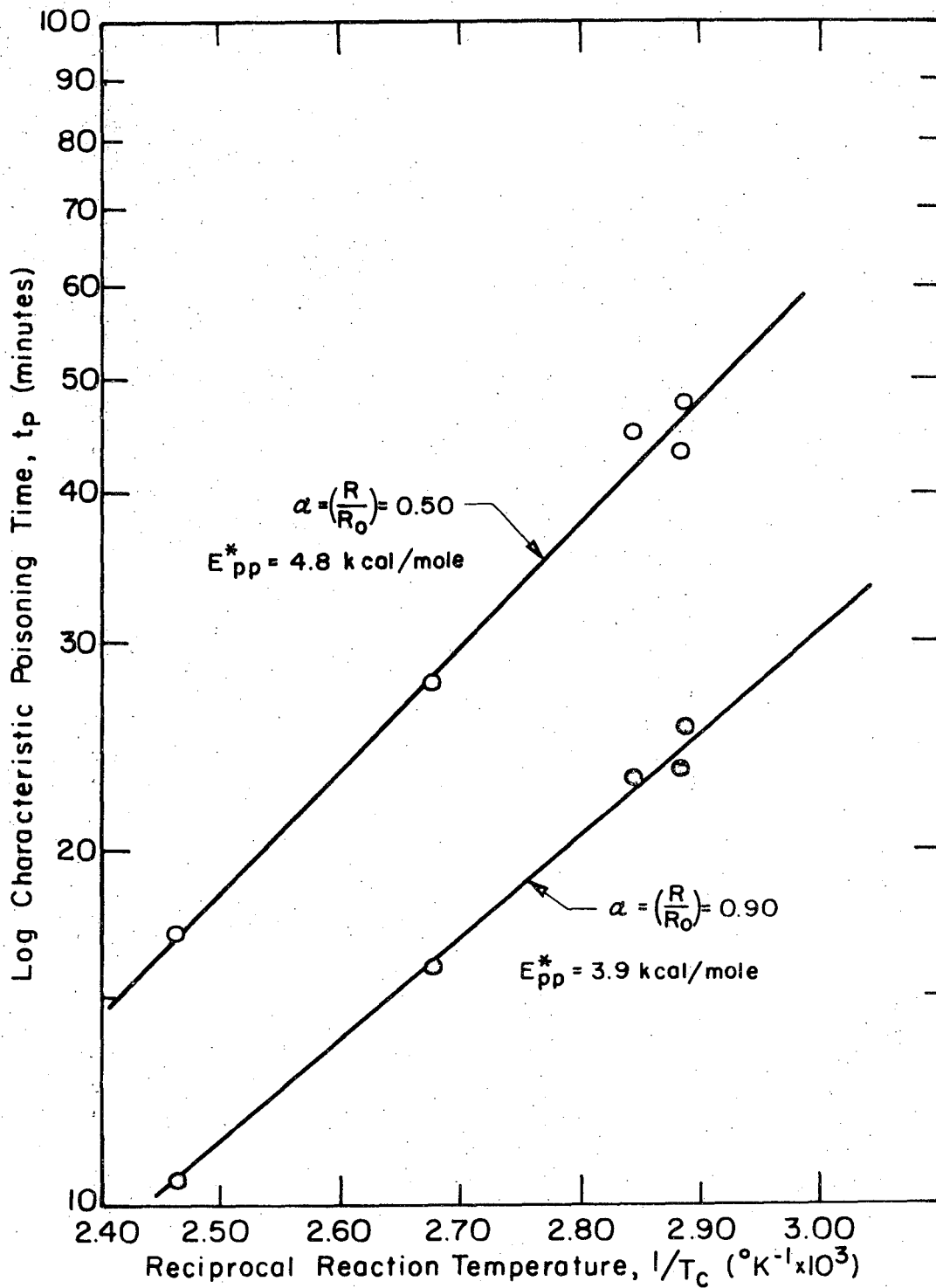
The mechanism of the poisoning process cannot be determined from the data cited above. If impurity poisoning is ruled out, the triangular poisoning mechanism postulated by Hegedus⁵¹ can be regarded as a good possibility:





XBL738-1649

Figure III-10B. Non-dimensionalized reaction rate versus time.
(Same key as in previous figure.)



XBL 738-1650

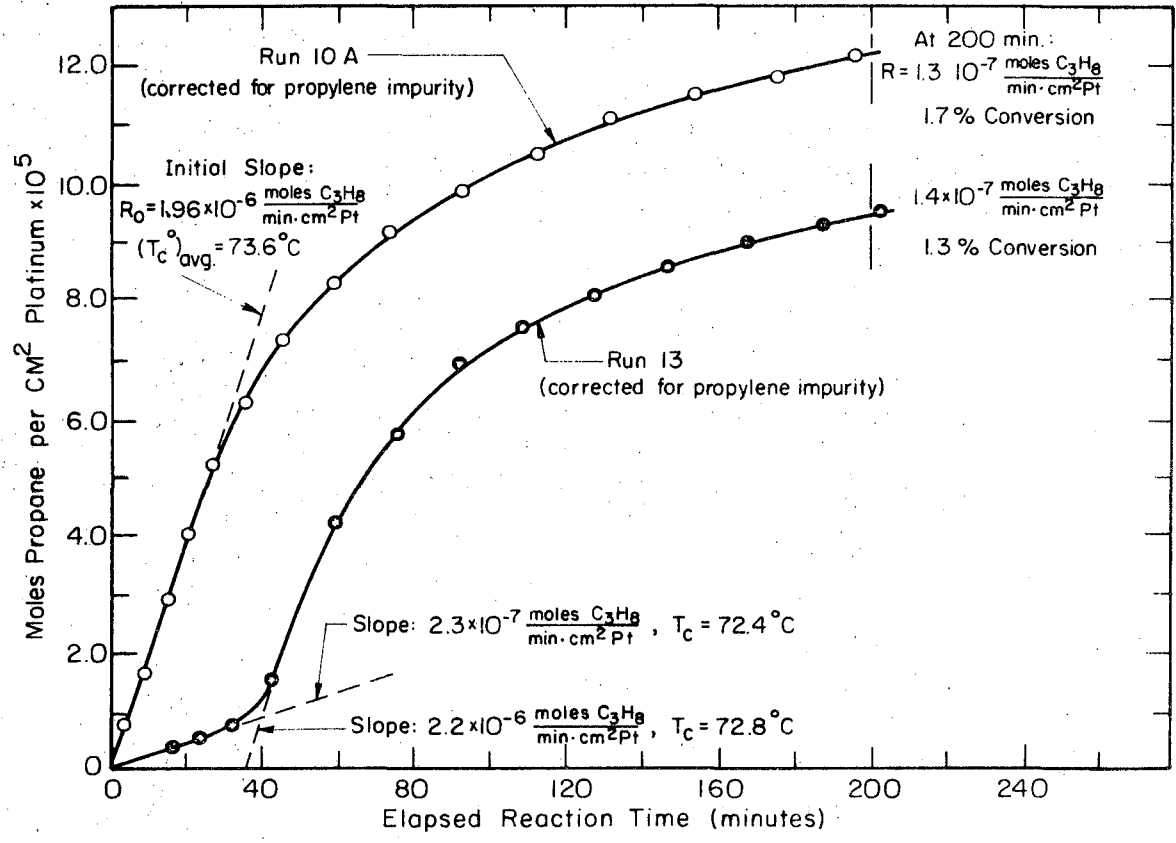
Figure III-11. Activation energy for the poisoning process during the cyclopropane hydrogenolysis on the Pt(S)-[6(111)×(100)] surface.

where A and B are reactant and product, respectively, and P is some form of partially dehydrogenated carbonaceous residue blocking surface sites. Hegedus⁵⁰ reported that the ratios (k_2/k_1) and (k_3/k_1) were not equal and in fact were far from unity. As the crystal temperature is increased from 73°C to 132°C in the present experiments, it is possible that the mechanism of the poisoning process is changing. This could explain the fact that the data in Figure III-10B does not lie along a single curve.

8. Catalyst Activity Following Minimal Hydrogen Pretreatment

To gain a better understanding of the importance of hydrogen pretreatment and its effect upon the initial rate of reaction, an additional experiment (Run 13) was carried out sharply reducing the time of hydrogen exposure. In all previous runs the platinum single crystal had been exposed to 780 torr H₂ at 75°C for 120 minutes prior to admitting the cyclopropane/hydrogen reaction mixture. Calculations appearing in Appendix H showed that based on literature data for the diffusivity of hydrogen in bulk platinum,³⁷ the single crystal would be saturated with H atoms at the end of this pretreatment period.

In Run 13 the pretreatment consisted of exposing the platinum crystal to approximately 50 torr H₂ for 110 seconds at 69°C. A plot of the reaction data of Run 13 with the propylene impurity subtracted out is shown in Figure III-12. Zero elapsed reaction time corresponds to filling the reactor with the standard 135 torr CP/675 torr H₂ mixture. There are several noteworthy features contained in this figure. During the first 30-35 minutes of elapsed reaction time the rate of



XBL 738-1651

Figure III-12. Effect of varying hydrogen pretreatment conditions. Upper curve: Run 10A with standard H₂ pretreatment (2 hrs at 75°C in 780 torr H₂). Lower curve: Run 13 with reduced H₂ exposure rate (110 sec at 69°C in 50 torr H₂). P_{cp}^o = 135 torr. P_{H₂}^o = 675 torr.

$2.3 \times 10^{-7} \frac{\text{moles } C_3H_8}{\text{min} \cdot \text{cm}^2 \text{ Pt}}$ at 72.4°C was about an order of magnitude lower than the initial rate for Run 10A (upper curve drawn in Figure III-12). At 35-40 minutes the rate suddenly increased about an order of magnitude. Thereafter the shape of the curve drawn through the remaining data points closely paralleled that of Run 10A.

It is difficult to determine the true shape of the experimental curve during the 35-60 minute reaction period from only three data points. Hence the extrapolated slope for the higher initial rate period cannot be drawn with certainty. It is clear however that following a 35-minute "induction" period the initial rate of the cyclopropane hydrogenolysis reaction in Run 13 was virtually the same as that in Run 10A (or Run 12A). Furthermore, the rate at 200 minutes elapsed reaction time ($1.4 \times 10^{-7} \frac{\text{moles } C_3H_8}{\text{min} \cdot \text{cm}^2 \text{ Pt}}$) was almost identical to the corresponding point rate in Run 10A ($1.3 \times 10^{-7} \frac{\text{moles } C_3H_8}{\text{min} \cdot \text{cm}^2 \text{ Pt}}$). The conversion at 200 minutes in Run 13 (1.30%) was less than that in Run 10A (1.66%) by virtue of the 35-minute delay period.

The data of Run 13 alone cannot explain the apparent induction period in the cyclopropane hydrogenolysis reaction curve as a result of the sharply reduced hydrogen pretreatment. If the surface reaction between an adsorbed cyclopropane species and an adsorbed hydrogen atom is indeed the rate-controlling step, then the concentration of one of these reactants may have been significantly lower during the initial rate period. Further experiments varying the thickness of the platinum crystal, the hydrogen pressure, and the duration of the pretreatment period are needed to completely understand this phenomenon.

9. Catalyst Activity Without Oxygen Pretreatment

The high temperature, UHV, oxygen treatment used to clean the platinum crystal of carbonaceous residues prior to each run was based on the LEED-Auger investigations of Joyner, Gland, and Somorjai.³⁵ There were no data found to suggest that heating the platinum single crystal in a hydrogen environment would also remove carbon from the surface. It is well known that partially deactivated polycrystalline supported platinum catalysts regain a large fraction of their initial activity after high temperature hydrogen treatment. Therefore, immediately following Run 12A, an experiment (Run 12B) was performed in an attempt to clean in a hydrogen environment the partially deactivated platinum single crystal.

A few minutes after the last data point of Run 12A had been taken, the reactor was flushed and filled with 800 torr H₂. After 14 hours at 25°C the reactor was again flushed with H₂ and filled to 780 torr H₂, whereupon the standard procedure for H₂ pretreatment was commenced (120 minutes at 75°C). Immediately following this period the reactor was filled to the same reactant partial pressures as in Run 12A (135 torr CP/675 torr H₂), and the formation of propane followed by periodic gas chromatographic sampling. It should be noted that the initial crystal temperature in Run 12B (77.7°C) was almost identical to the final temperature in Run 12A (78.0°C).

Figure III-2 previously shown in Section III-C-3 summarizes the data of Run 12, where the vertical line at 208.4 minutes separates the two parts of the experiment. During the first 90 minutes of Run

12B only the 0.20% propylene impurity ($1.54 \times 10^{-5} \frac{\text{moles}}{\text{cm}^2 \text{Pt}}$) reacted to propane. At approximately 300 minutes elapsed reaction time the cyclopropane-hydrogen reaction began to take place. The average rate of the cyclopropane hydrogenolysis reaction during the final 100 minutes of Run 12B, as indicated by the dashed curve, was about $1.6 \times 10^{-7} \frac{\text{moles C}_3\text{H}_8}{\text{min} \cdot \text{cm}^2 \text{Pt}}$. To compare directly this rate with the final rate in Run 12A the same dashed curve was drawn as an extension to the data of Run 12A. Note that it tends to give a very nearly smooth transition between the two parts of the run.

It seems clear that the low temperature hydrogen treatment following Run 12A did not reactivate the platinum single crystal. The data suggest that no appreciable removal of partially dehydrogenated carbonaceous species from the platinum surface occurred during the interval of time between Runs 12A and 12B. It is possible that the surface became even more covered with carbon residues during this period.

Additional experiments are needed to determine whether hydrogen alone can reactivate a platinum stepped single crystal surface. These should be done at progressively higher temperatures for longer periods of time.

10. Summary and Conclusions

The hydrogenolysis of cyclopropane was carried out on a Pt(S)-[6(111)×(100)] single crystal having a surface area of 0.76 cm². Prior to commencing each kinetic experiment the crystal was exposed to 1×10⁻⁶ torr O₂ at 900-925°C for 2 hours to remove carbonaceous surface residues and then pretreated in 780 torr H₂ at 75°C for an additional 2 hours.

At 75°C a blank run without the platinum crystal in the reactor resulted in no detectable conversion of cyclopropane to propane.

Two runs conducted under identical conditions showed that the data was reproducible to about 10%. The observation that the data points generally followed a smooth curve suggested that the experimental techniques were good and that the analysis of the gas chromatographic peak data was consistent.

Initial rate measurements made at several temperatures between 73°C and 132°C at constant initial reactant partial pressures gave an activation energy for the unpoisoned cyclopropane-hydrogen reaction of 12.2±1.0 kcal/mole. This value is just on the upper limit of activation energies reported in the literature for this reaction on supported platinum catalysts (8.0 to 12.2 kcal/mole). Furthermore, a comparison of specific rate data obtained by other investigators on polycrystalline platinum catalysts to the initial rates obtained in this study at 75°C and 135 torr cyclopropane showed that the stepped platinum single crystal behaves very much like a highly dispersed supported platinum catalyst.

Rate measurements made on the partially deactivated platinum crystal surface gave an activation energy of 10.5 kcal/mole, which was lower than that for the unpoisoned catalyst.

An experiment was carried out at a higher initial partial pressure of cyclopropane while maintaining the hydrogen pressure constant. From the initial rate data the order of the cyclopropane hydrogenolysis reaction with respect to cyclopropane was determined to be 0.8 ± 0.2 . Values reported in the literature range from zero to 1.0.

From a plot of relative reaction rate versus elapsed reaction time, the time constant for poisoning of each run was determined. Assuming that these characteristic times versus reaction temperature could be expressed by an equation of the Arrhenius form, the activation energy for the poisoning process was calculated to be 4-5 kcal/mole.

An additional experiment in which the standard hydrogen pretreatment exposure (pressure \times time) was reduced by a factor of 1000 resulted in two initial rate periods. The ratio of the rate of the second period to that of the first was approximately an order of magnitude, while the apparent "induction" time of the first rate period lasted 35-40 minutes.

Following the kinetics of the cyclopropane-hydrogen reaction on a platinum stepped single crystal having a surface area on the order of 1 cm^2 and using the thermal conductivity detector of a gas chromatograph proved to be feasible and rewarding. More experiments, however, are needed to understand the nature of the poisoning process and the effect of hydrogen pretreatment on the resultant kinetics. Finally, rate measurements on both low index and high index (stepped) single crystal

surfaces are necessary to check the assertion that the hydrogenolysis of cyclopropane is a "structure-insensitive" reaction.

CHAPTER IV

DISCUSSION OF RESULTS

The important result of this work is that at 1 atm total pressure a platinum single crystal behaves like a highly dispersed supported platinum catalyst for the cyclopropane hydrogenolysis. It was shown that initial reaction rates on the Pt(S)-[6(111)×(100)] surface were, to within a factor of two, the same as values reported in the literature for highly dispersed supported platinum catalysts. This would tend to verify Boudart's hypothesis that the cyclopropane hydrogenolysis is an example of a "facile" reaction.²³ It should be pointed out however that the H₂/D₂ exchange reaction has also been classified as "facile" by Poltorak and coworkers^{54,55} and by Boudart.²⁷ Yet Bernasek, Siekhaus, and Somorjai¹² clearly showed that the rate of exchange on a platinum stepped surface (Pt(S)-[9(111)×(111)]) was almost two orders of magnitude greater than on the low index Pt(111) surface. Until the cyclopropane hydrogenolysis can be carried out on a low index surface under conditions identical to that on the stepped platinum surface, the question remains whether the hydrogenolysis of cyclopropane is a "structure-insensitive" reaction.

One of the unexpected results obtained in this study in Run 14 was that the activation energy for the main reaction on the partially deactivated platinum stepped single crystal ($E_p^* = 10.5$ kcal/mole) was lower than the activation energy on the initially clean surface ($E^* = 12.2 \pm 1.0$ kcal/mole). Recall that to obtain E_p^* a downward temperature stepping procedure was used. This would result in the maximum possible slope

in the Arrhenius plot of Figure III-7, or the highest value obtainable for E_p^* . In addition, there was virtually no scatter in the data, as a straight line could be drawn through all three points. These facts confirm the result that E_p^* was definitely lower than E^* .

Consider now the rate equation written in the form

$$R = \frac{k_B T}{h} A_S e^{\Delta S^\ddagger / R} \times e^{-\Delta H^\ddagger / RT} \times \theta_{H_2} \theta_{CP}$$

where,

$$R = \text{reaction rate } \left(\frac{\text{molecules}}{\text{sec} \cdot \text{cm}^2} \right)$$

$$k_B = \text{Boltzmann's constant} = 1.380 \times 10^{-16} \frac{\text{ergs}}{^\circ\text{K}}$$

$$h = \text{Planck's constant} = 6.624 \times 10^{-27} \text{ ergs} \cdot \text{sec}$$

$$T = \text{reaction temperature } (^\circ\text{K})$$

$$A_S = \text{number of active sites per cm}^2 \text{ surface area}$$

$$\Delta S^\ddagger = \text{entropy change for the activated complex } \left(\frac{\text{cal}}{\text{mole} \cdot ^\circ\text{K}} \right)$$

$$\Delta H^\ddagger = \text{enthalpy change for the formation of the activated complex } \left(\frac{\text{cal}}{\text{mole}} \right)$$

and

θ_{H_2} , θ_{CP} = fractional surface coverages of hydrogen and cyclopropane, respectively.

Assume that during a catalytic run the temperature and concentration of reactant gases remain constant. As the poisoning progresses the rate (R) decreases and the activation enthalpy (ΔH^\ddagger) decreases, or the exponential term $e^{-\Delta H^\ddagger/RT}$ increases. Therefore the term $(A_S e^{\Delta S^\ddagger/R})$ must decrease faster than the rate of increase of the enthalpy term. Although no change was observed in the number or distribution of products formed before or during the poisoning process, it is not clear whether the entropy of activation for the activated complex (ΔS^\ddagger) remains constant or in fact decreases. Certainly a decrease in the number of catalytically active sites, represented by the area term A_S , could account for the net decrease in reaction rate as the poisoning process progresses. It should be pointed out that this interpretation is not consistent with experimental observations pertaining to the reactivity of the propylene impurity contained within the cyclopropane. In Runs 12A (initially clean surface, std. H_2 pretreatment), 12B (partially deactivated surface, std. H_2 pretreatment), and 13 (initially clean surface, minimal H_2 pretreatment), the 0.2% propylene impurity reacted completely to propane between 10 and 16 minutes of elapsed reaction time in each case. These times correspond to the second and third data points taken in each run. However this is not an entirely unexpected result, as the mechanism of the propylene hydrogenation may well involve different types of active sites than those needed for the cyclopropane hydrogenolysis.

Gland⁵⁶ has measured work function changes upon adsorbing various hydrocarbons on low index single crystal platinum surfaces in an ultra-high vacuum LEED system. For propane the work function change is measured within a few minutes after introducing the hydrocarbon, corresponding to approximately a monolayer coverage. Although cyclopropane was not investigated, one would expect that this compound would behave in very nearly the same manner. If the cyclopropane hydrogenolysis were to take place in the first carbon layer, the reaction should be approximately zero order with respect to cyclopropane. The data obtained in the present study showed that this dependency was almost first order (0.8 ± 0.2). This suggests that the reaction may not be occurring on the platinum metal itself, but on the first carbon overlayer. The work of Thomson and Wislade⁵⁷ tends to support this hypothesis. In their experimentation a monolayer of radioactive ethylene (C_{14}) was initially adsorbed on a nickel film, and the remainder of the gas was pumped out of the system. Nonradioactive ethylene and hydrogen then was admitted and the rate of ethylene hydrogenation as well as the radiation level of the nickel surface were monitored as a function of time. Only a fraction of the pre-adsorbed ethylene-C-14 was removed from the film during extensive hydrogenation of the inactive ethylene. Either the reaction was occurring in "holes" between carbon atoms in the first overlayer, or it was taking place on top of the carbon layer. Their data show that exchange of chemisorbed ethylene in the first layer with incoming gas-phase ethylene molecules was negligible.

The non-dimensionalized reaction rate plot of Figure III-10A provides another unusual result obtained in this study. Normally, one would expect a gradual decrease in reaction rate starting from zero reaction time. However, the first part of the figure represents a high initial rate period which is constant for a finite time. A rapid deactivation process follows and the rate falls off approximately an order of magnitude during 200 minutes of elapsed reaction time. The delay time is a function of temperature and has an activation energy of approximately 4-5 kcal/mole. The form of these curves suggests that two mechanisms are occurring here. The initial period might be termed the "precursor build-up" phenomenon in which the catalyst surface must be undergoing considerable change. This is followed by the "deactivation period" in which the number of active sites is reduced considerably. Further experiments are needed to determine whether a steady state rate is approached at much longer reaction times.

Decreasing the hydrogen pretreatment conditions in Run 13 produced another unanticipated result. The initial rate during the first 30-35 minutes of this run was approximately a factor of 10 lower than the initial rate corresponding to Run 10A, in which the standard hydrogen pretreatment conditions were used. At 35-40 minutes the rate suddenly increased by a factor of 10 and thereafter closely paralleled the reaction rate curve for Run 10A. If hydrogen protects the catalyst surface from forming carbon structures which are precursors to poison, then why wasn't the second portion of the rate curve in Run 13 lower than the curve corresponding to Run 10A? It seems reasonable to

assume that a much lower concentration of hydrogen on the surface would result in an increased number of surface sites available for hydrocarbon chemisorption. This would tend to accelerate the poisoning process and certainly not produce the dramatic rate increase after a 40-minute delay period.

Hegedus and Petersen⁵¹ have shown for a highly dispersed supported platinum catalyst that extended hydrogenation did not increase the catalyst activity for the cyclopropane hydrogenolysis, it merely delayed the poisoning. Both the mechanism and kinetics of the poisoning were the same, only the time scale was altered due to the extended hydrogenation period. Although their data cannot be compared directly to the result obtained in this study due to the possible influence of the alumina support, it is clear that the effect of hydrogen pretreatment is different in the two cases.

One possible explanation for the sudden increase in activity could be associated with residual oxygen left on the surface after the initial cleaning procedure. Perhaps one hour of pumping in UHV at 900°C was not sufficient to remove oxygen atoms adsorbed at the platinum step sites, contrary to the results of Joyner, Gland, and Somorjai.³⁵ In Run 10A there may have been sufficient time to react off all the remaining oxygen during the two-hour pretreatment procedure. In Run 13 with less than two minutes of hydrogen pretreatment, a finite period of time may have been required to remove the oxygen and expose surface sites which normally would have been available for the hydrocarbon catalysis. Auger spectroscopy measurements of the platinum crystal

combined with mass spectrometric analysis of the gas phase before and after hydrogen pretreatment are needed to check this hypothesis.

In conclusion, this work has raised many interesting questions about the nature of active sites in heterogeneous catalytic reactions. It has begun the task of bridging the gap between traditional heterogeneous catalytic studies and those using new analytical tools to probe the surface of a catalyst on an atomic scale. The data support the contention that single crystal surfaces are ideal models for polycrystalline supported catalysts. Finally, studies of this type appear to be well suited to discover the relationship between the morphology of the catalyst surface and its heterogeneous catalytic activity.

APPENDIX A

Design of the Experimental Apparatus1. Over-all Reactor Design Requirements

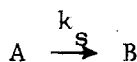
One of the stated goals of this study was to perform catalytic experiments on one (or more) platinum single crystal(s) both in ultra-high vacuum (UHV) and at 1 atmosphere total pressure. From the outset it was decided that both of these experiments should be done in one apparatus without physically altering the position of the catalyst crystal or severing any connections made to it. The latter includes suitable electrical connections for supporting or heating the crystal, and thermocouple connections for monitoring the catalyst temperature. With this objective the concept of a high pressure (1 atm.) reactor within an UHV reactor was developed which appeared to be the most flexible from an experimental standpoint. The single crystal could be heated in UHV to remove carbonaceous surface residues and provide a clean well-oriented surface for catalytic studies.^{35,36} Upon cooling to the proper temperature and leaking in a controlled flow of reactants, kinetic experiments in UHV could be made by monitoring the formation of products by a mass spectrometric technique.¹⁰ Alternatively upon cooling, the catalyst could be encased in a sealed small-volume chamber. Upon pressurizing the chamber to 1 atmosphere and admitting reactants, kinetic experiments could be carried out using a gas chromatograph to monitor the formation of products.

There were many design alternatives and problems which arose in transforming this concept into a working apparatus. In the present section only the details of the design finally adopted will be described. Included are the initial calculations for the high pressure reactor, the design and construction of the UHV and high pressure reactor chambers, and the design of the high pressure flow loop and gas manifold assembly.

2. Initial Calculations for the Design of the High Pressure Reactor

A recycle reactor operated in a batch mode was chosen as the basis for design. This consisted of the catalyst crystal suspended in a flow loop in which the contents were continuously circulated. When the conversion per pass is differential, this heterogeneous catalytic reactor is simply the analog of the well-stirred batch reactor in homogeneous catalytic studies. The mathematics for analyzing the performance of such a reactor thereby becomes greatly simplified.

Consider a continuously stirred, well-mixed, isothermal, constant volume reactor where the following first-order heterogeneous reaction takes place:



For the moment it will be assumed that there is no external diffusion influence. The conservation equation for species A is given by:

$$V \frac{dC_A}{dt} = -k_s A C_A \quad (A-1)$$

where,

- V = reactor volume (cm^3)
 C_A = reactant concentration (moles/cm^3)
 k_s = specific rate constant (cm/min)
 A = catalyst surface area (cm^2)
 t = elapsed reaction time (minutes)

With the boundary conditions that at $t=0$, $C_A = C_{A0}$, and as $t \rightarrow \infty$, $C_A \rightarrow 0$, the solution to Eq. (A-1) is:

$$C_A = C_{A0} \exp\left(-\frac{k_s A}{V} t\right) \quad (\text{A-2})$$

The concentration of product B formed is simply

$$C_B = \Delta C_A = C_{A0} - C_A \quad (\text{A-3})$$

or,

$$\Delta C_A = C_{A0} \left[1 - \exp\left(-\frac{k_s A}{V} t\right)\right] \quad (\text{A-4})$$

From Eq. (A-4) it is possible to calculate the time required for the minimum amount of product to be first detected by a gas chromatograph under a given set of experimental conditions. This is a crucial quantity in the present study when one considers the very small area of catalyst surface ($\sim 1 \text{ cm}^2$ per catalyst crystal) available for reaction. If this time is on the order of a few hours the reaction is probably too slow for the accurate determination of initial (unpoisoned) rate measurements. On the other hand, a minimum reaction

time on the order of a few minutes is a more realistic quantity on which to base reactor design calculations.

The cyclopropane hydrogenolysis reaction was chosen as the basis for the high pressure reactor design. According to Hegedus,⁵⁰ at large H₂/CP ratios the reaction is approximately first order in cyclopropane and fits the model described by Eq. (A-4). A considerable amount of data and experience has been amassed in our laboratory pertaining to this reaction.^{45,48,50,58,59} The rate is known to be relatively high at room temperature on bulk and supported platinum catalysts. Furthermore only one product (propane) is formed on platinum catalysts, thereby simplifying chromatographic detection.

In obtaining a specific rate constant, k_s, for the cyclopropane-hydrogen reaction the single pellet data of Hegedus⁵¹ summarized in Table A-1 was used. The rate constant reported can be expressed as

$$k_{a_0} = \frac{k_s A_s}{V_p} \quad (A-5)$$

where,

- A_s = platinum surface area (cm²)
- V_p = pellet volume (cm³)
- k_s = specific rate constant (cm/min)

Thus from Table A-1 and assuming 100% Pt dispersion on the η-Al₂O₃ support:

$$A_s = \frac{(4.0 \times 10^{-4} \frac{\text{grams Pt}}{\text{gram cat.}})(0.295 \text{ grams cat.})(6.023 \times 10^{23} \frac{\text{molecules}}{\text{mole}})}{(1.12 \times 10^{15} \frac{\text{molecules}}{\text{cm}^2 \text{ Pt}})(195 \frac{\text{grams Pt}}{\text{mole}})}$$

Table A-1

Rate Data from Hegedus^{50,51} for the Hydrogenolysis
of Cyclopropane on a Platinum/Alumina Catalyst

Physical Characteristics of the Platinum Catalyst Pellet

- 0.25 wt% Pt on $\eta\text{-Al}_2\text{O}_3$ diluted with $\eta\text{-Al}_2\text{O}_3$ to 0.04 wt% Pt
- Surface area of $\eta\text{-Al}_2\text{O}_3$ = 230 m²/gram
- Pellet weight = 0.295 grams
- Pellet density, = 1.14 grams/cm³

Initial Rate Data for the Cyclopropane Hydrogenolysis

- Catalyst calcined in 3% O₂ in N₂ @ 400-410°C for 2 hrs.
- Catalyst reduced in H₂ @ 300°C for 10 hrs.
- C_{H₂}^o = 41.4 × 10⁻⁶ moles/cm³ (P_{H₂}^o = 900 torr)
- C_{CP}^o = 3.45 × 10⁻⁶ moles/cm³ (P_{CP}^o = 75.0 torr)
- T_{rxn} = 75°C
- (k_a)_i = 2.61 sec⁻¹
- Order of reaction with respect to cyclopropane, n_{CP} = 1.0
- Activation energy, E_A^{*} = 10 kcal/mole

$$A_s = 326 \text{ cm}^2 \text{ Pt.}$$

A more realistic assumption as to the Pt dispersion would be roughly 50%. Then $A_s \approx 163 \text{ cm}^2 \text{ Pt}$. Using this result in Eq. (A-5),

$$(k_s)_{75^\circ\text{C}} = \frac{(2.61 \text{ sec}^{-1})(0.295 \text{ grams cat.})}{(163 \text{ cm}^2 \text{ Pt})(1.14 \frac{\text{grams cat}}{\text{cm}^3 \text{ cat}})} * (60 \frac{\text{sec}}{\text{min}})$$

$$(k_s)_{75^\circ\text{C}} = 2.49 \times 10^{-1} \frac{\text{cm}}{\text{min}}$$

A typical set of initial conditions to be employed in the cyclopropane hydrogenolysis reaction are the following:

$$\begin{aligned} P_{\text{CP}}^{\circ} &= 73 \text{ torr} \\ P_{\text{H}_2}^{\circ} &= 703 \text{ torr} \\ T_{\text{crystal}} = T_{\text{rxn}} &= 75^\circ\text{C} \\ T_{\text{gas}} &= 25^\circ\text{C} \end{aligned}$$

Hence,

$$C_{\text{CP}}^{\circ} = \frac{P_{\text{CP}}^{\circ}}{RT_{\text{gas}}} = \frac{(73/760) \text{ atm}}{(82.1 \frac{\text{atm} \cdot \text{cm}^3}{\text{mole} \cdot \text{K}})(298^\circ\text{K})} = 3.92 \times 10^{-6} \frac{\text{moles}}{\text{cm}^3}$$

The thermal conductivity detector used in the present study has a minimum sensitivity for propane of approximately 2×10^{-9} moles (See Appendix E). Choosing a sample volume of 0.5 cm^3 , the minimum

detectable product concentration (ΔC_A) would be 4×10^{-9} moles/cm³.

Substituting the values for k_s , C_{A_0} , and ΔC_A into Eq. (A-4) and solving for t_{\min} :

$$4.0 \times 10^{-4} = 3.92 \times 10^{-6} [1 - \exp(-0.249 \frac{A}{V} t_{\min})] \quad (\text{A-6})$$

$$t_{\min} = 4.04 \times 10^{-3} \frac{V}{A} \quad (\text{A-7})$$

For a reactor volume of 500 cm³ and using one single platinum crystal having a surface area of 1 cm², the minimum detection time would be approximately 2 minutes.

The parameters used in the above calculation were deemed to be realistic and experimentally feasible. The design and construction of the apparatus therefore proceeded on the basis of supporting one catalyst crystal ($A \approx 1 \text{ cm}^2$) within a high pressure reactor volume of approximately 500 cm³. In the event the reaction rate obtained was much lower than that obtained by Hegedus, there were sufficient numbers of variables which could be changed (the most important being the crystal temperature or the mode of G. C. detection) to insure that the first detectable amount of product could be monitored within a few minutes after commencing the reaction.

3. Criterion for Importance of External Mass Transfer

It was necessary to determine whether external transport resistances would be important in the high pressure, constant-volume reactor. The problem is simplified because the catalyst surface is uniformly accessible and there is no internal resistance to mass transfer, i.e., there is a very rapid heterogeneous chemical reaction occurring at the catalyst surface. The mathematical analysis is identical to that used by Petersen⁶⁰ in which he considered the system of a single, nonporous, spherical catalyst pellet immersed within and in steady state with a large medium of stagnant reactant. The reactant diffuses up to the surface, reacts catalytically, and the product diffuses away. For a first-order reaction ($A \xrightarrow{k_1} B$) the criterion for which the system is in the kinetic control regime is given by

$$\boxed{\frac{k_1'}{\beta_m} < 0.1} \quad (A-8)$$

where,

k_1' = heterogeneous first-order rate constant based upon external surface area (cm/min).

β_m = local coefficient of mass transfer, which is constant over the entire surface of the pellet (cm/min).

Equation (A-8) is a criterion corresponding to a value of the concentration at the catalyst surface approaching the bulk stream value, whereupon

the over-all reaction rate is determined by the rate of chemical reaction at the surface.

In calculating the values of k_1' and β_m in Eq. (A-8) for the cyclopropane hydrogenolysis reaction, a reference of 25°C was used. The data of Hegedus corrected to 25°C gave the value for k_1' :

$$\log \left(\frac{k_{S2}}{k_{S1}} \right) = \frac{E_a^*}{2.303R} \left[\frac{T_2 - T_1}{T_1 T_2} \right] \tag{A-9}$$

where,

- $k_{S1} = k_1'$ (cm/min) in Eq. (A-8)
- $k_{S2} = 2.49 \times 10^{-1}$ cm/min (Eq. A-6)
- $E_a^* = 10$ kcal/mole
- $T_2 = 75^\circ\text{C}$
- $T_1 = 25^\circ\text{C}$

Solving,

$$(k_S)_{25^\circ\text{C}} = k_1' = 2.22 \times 10^{-2} \text{ cm/min} .$$

The most conservative estimate for β_m was chosen where there is no flow within the reactor (simple diffusion), namely that the Nusselt number for mass transfer (Nu_m) is unity:

$$Nu_m = \frac{\beta_m r_o}{\mathcal{D}_{AB}} = 1$$

or,

$$\frac{\beta_m d}{\mathcal{D}_{AB}} = 2$$

(A-10)

where

d_p = characteristic particle diameter (cm)

\mathcal{D}_{AB} = mass diffusivity for the binary hydrogen-cyclopropane mixture (cm^2/sec).

Foust et.al.⁶¹ outline the procedure for estimating the mass diffusivity for binary mixtures based on a Lennard-Jones model. At 25°C and a total pressure of 803 torr, the diffusivity for the H_2/CP system was calculated to be $\mathcal{D}_{\text{H}_2/\text{CP}} = 0.435 \text{ cm}^2/\text{sec}$. Taking the characteristic particle diameter to be approximately 6.5 mm and substituting these values into Eq. (A-10),

$$\beta_m = \frac{(2) (0.435 \frac{\text{cm}^2}{\text{sec}}) (60 \frac{\text{sec}}{\text{min}})}{(0.65 \text{ cm})} = 80.4 \frac{\text{cm}}{\text{min}} \quad (\text{A-11})$$

Thus,

$$\left(\frac{k_1'}{\beta_m} \right) = \frac{2.22 \times 10^{-2} \frac{\text{cm}}{\text{min}}}{0.804 \times 10^2 \frac{\text{cm}}{\text{min}}} = 2.8 \times 10^{-4} \quad (\text{A-12})$$

or approximately three orders of magnitude lower than the limit necessary for the system to be within the kinetic-controlled regime. This means that diffusion is extremely fast compared to reaction and that there will be no external transport resistance to consider in the analysis of the kinetic data.

4. Design of the UHV-High Pressure Reactor System

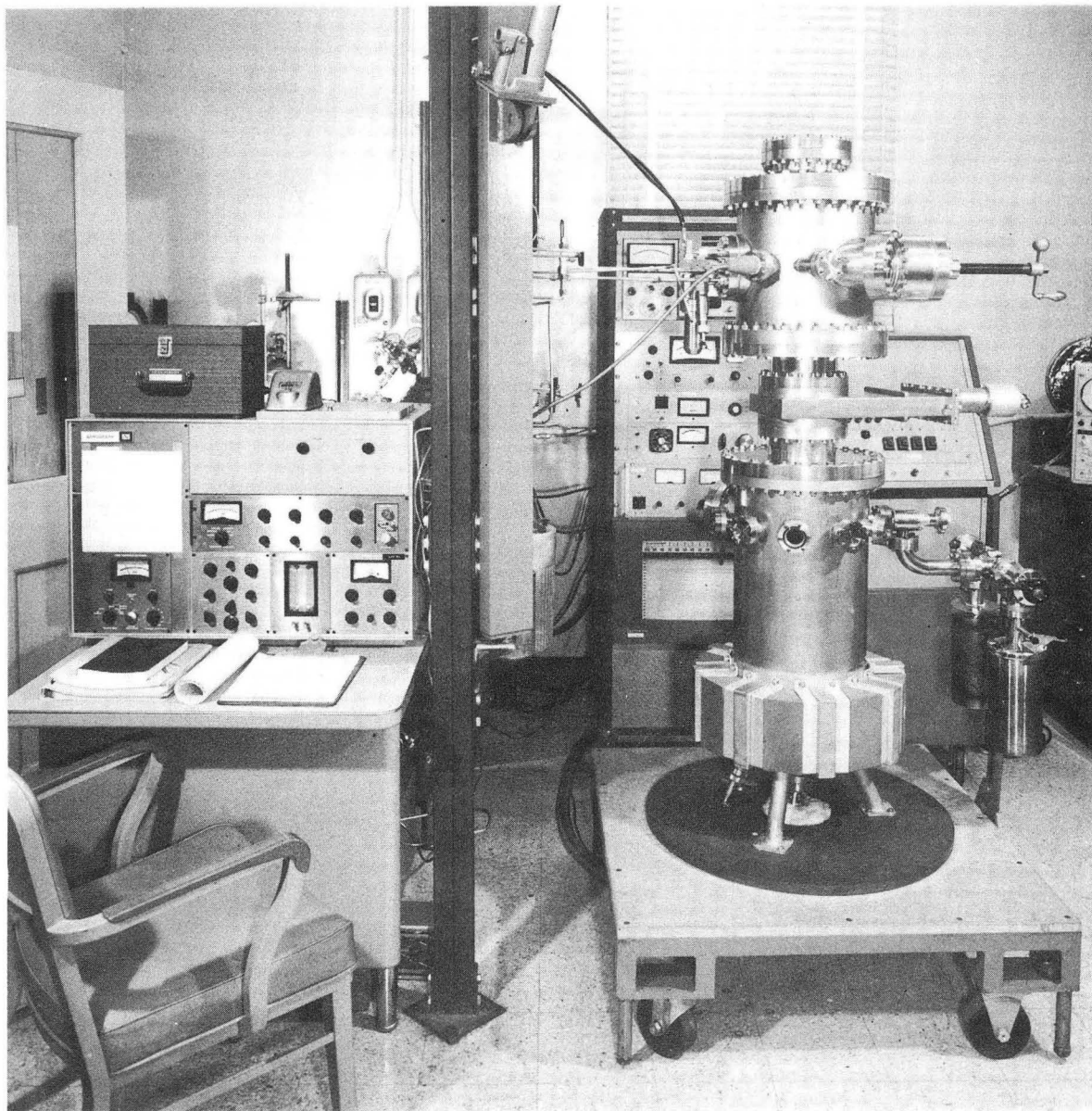
An over-all view of the completed apparatus for the UHV-high pressure studies is presented in Fig. A-1 to indicate the relative scale of the equipment.

A close-up of the 304 stainless-steel UHV-high pressure assembly is shown in Fig. A-2. The lower UHV chamber consists of a 12-inch dia., multi-flanged vessel housing a 200 liter/sec Ultek D-I ion pump and a titanium sublimation pump capable of reducing the pressure in the system to 5×10^{-10} torr with a moderate bakeout. The pumping unit is controlled by an Ultek Combination Ion Pump-TSP Power Supply (Model No. 224-0620). Additional details concerning the design of this chamber can be found elsewhere.⁶²

Separating the upper and lower chambers is a 6-inch i.d. stainless-steel, viton-sealed gate valve manufactured by Thermionics.

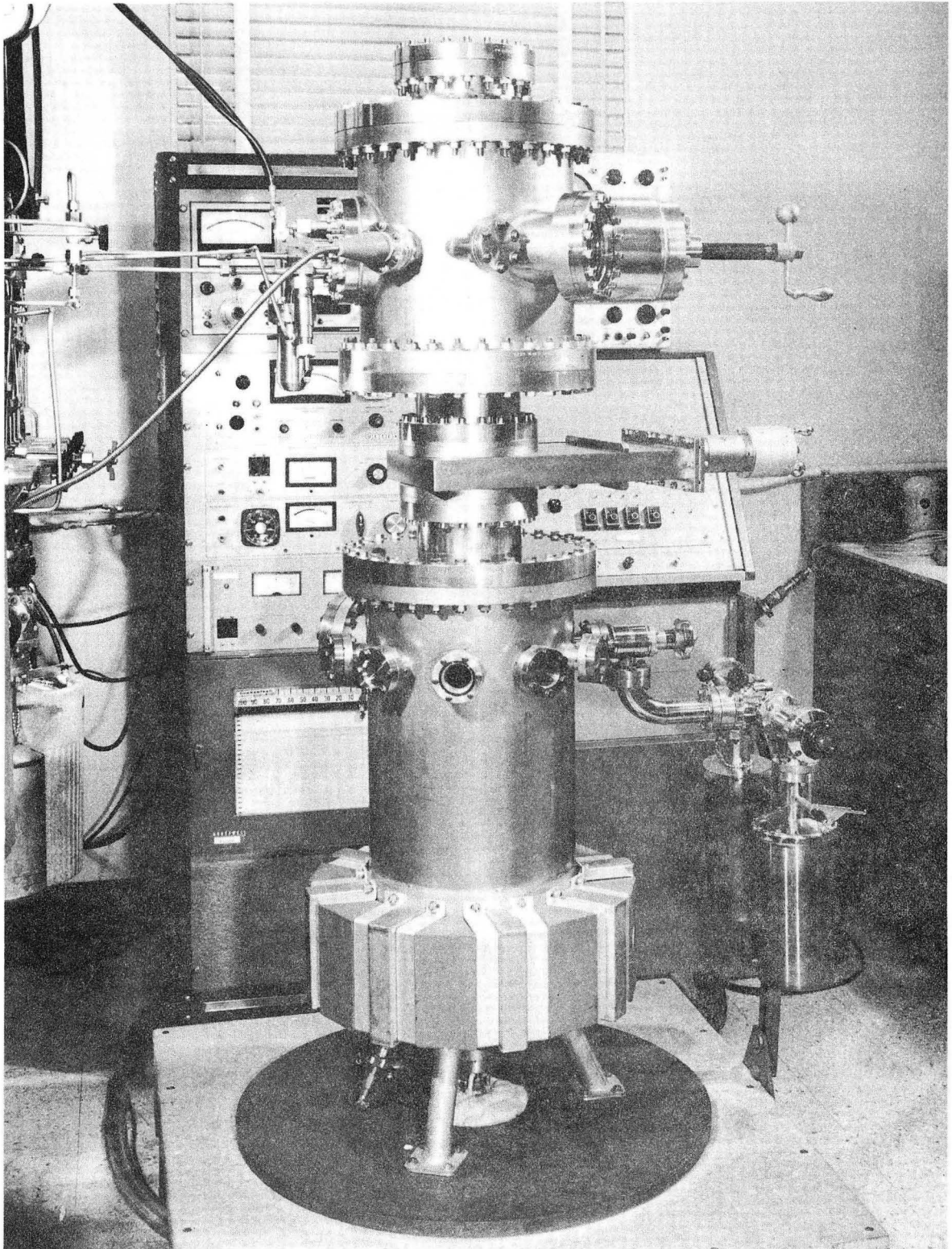
The upper 12-inch diameter, multi-flanged chamber shown in Fig. A-3 comprises both the UHV and high-pressure reactors. Proceeding in a counter-clockwise direction the outer flange arrangement (presented schematically in Fig. II-1) consists of the following:

- A 2 3/4-inch flange for a nude Varian ion guage.
- A 2 3/4-inch flange for an Auger electron gun control assembly.
- A 6-inch flange for a Varian viewing port.
- A 6-inch flange for a movable bellows-cup assembly
- A 2 3/4-inch flange for a quadrupole mass spectrometer head and accessories to a Granville-Phillips Spectra Scan 750 Residual Gas Analyzer.



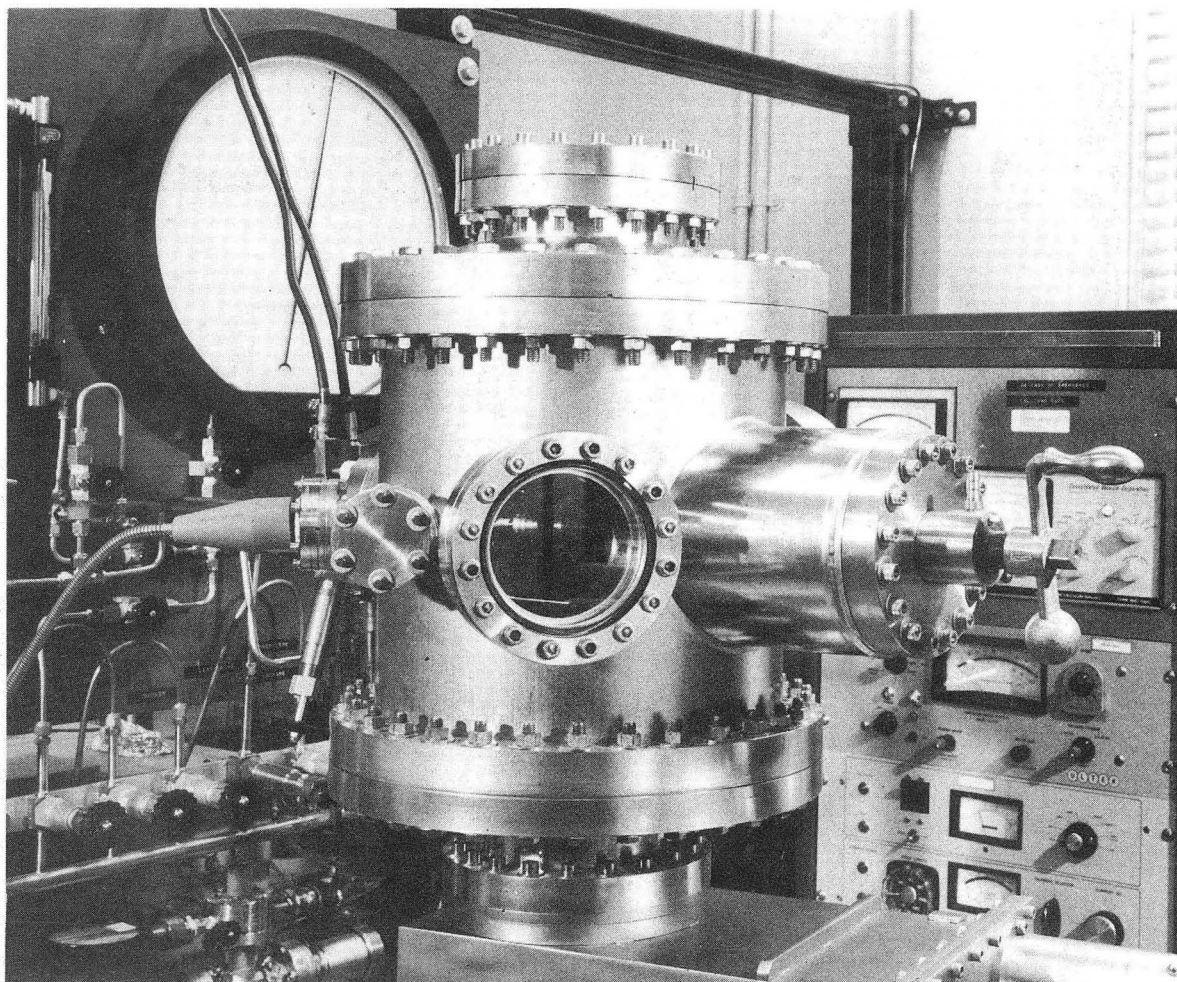
XBB 732-787

Figure A-1. Over-all view of equipment for UHV and high pressure studies, including reactors, mass spectrometer, gas chromatograph, and associated electronics.



XBB 732-788

Figure A-2. Close-up of the UHV-high pressure reactor assembly.



XBB 732-789

Figure A-3. Close-up of UHV-high pressure reactor fabricated for the present studies. Flanges visible include, from left to right, those for a nude ion gauge, an Auger electron gun assembly (not shown), a viewing port, and the "bellows-cup" assembly.

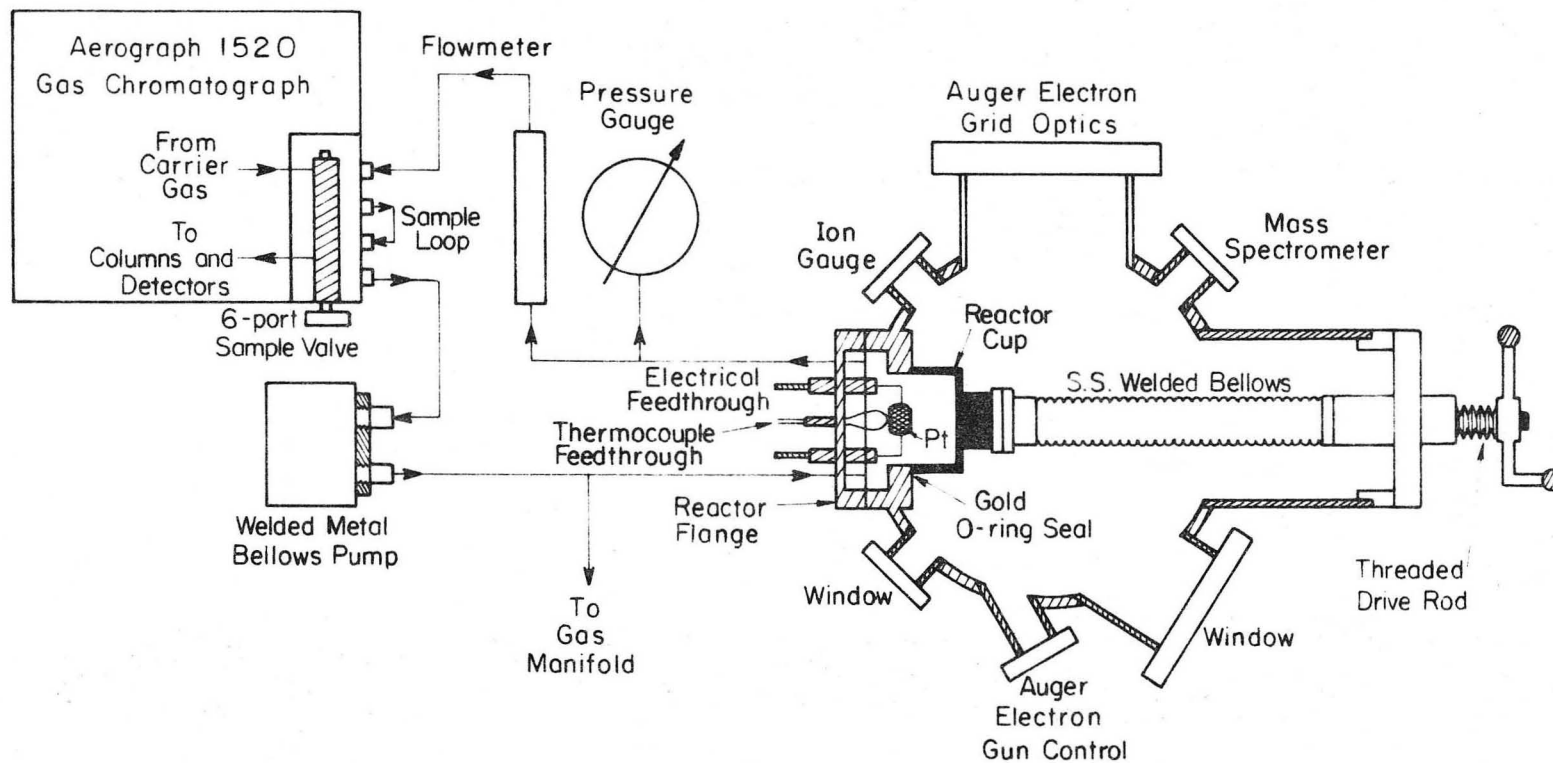


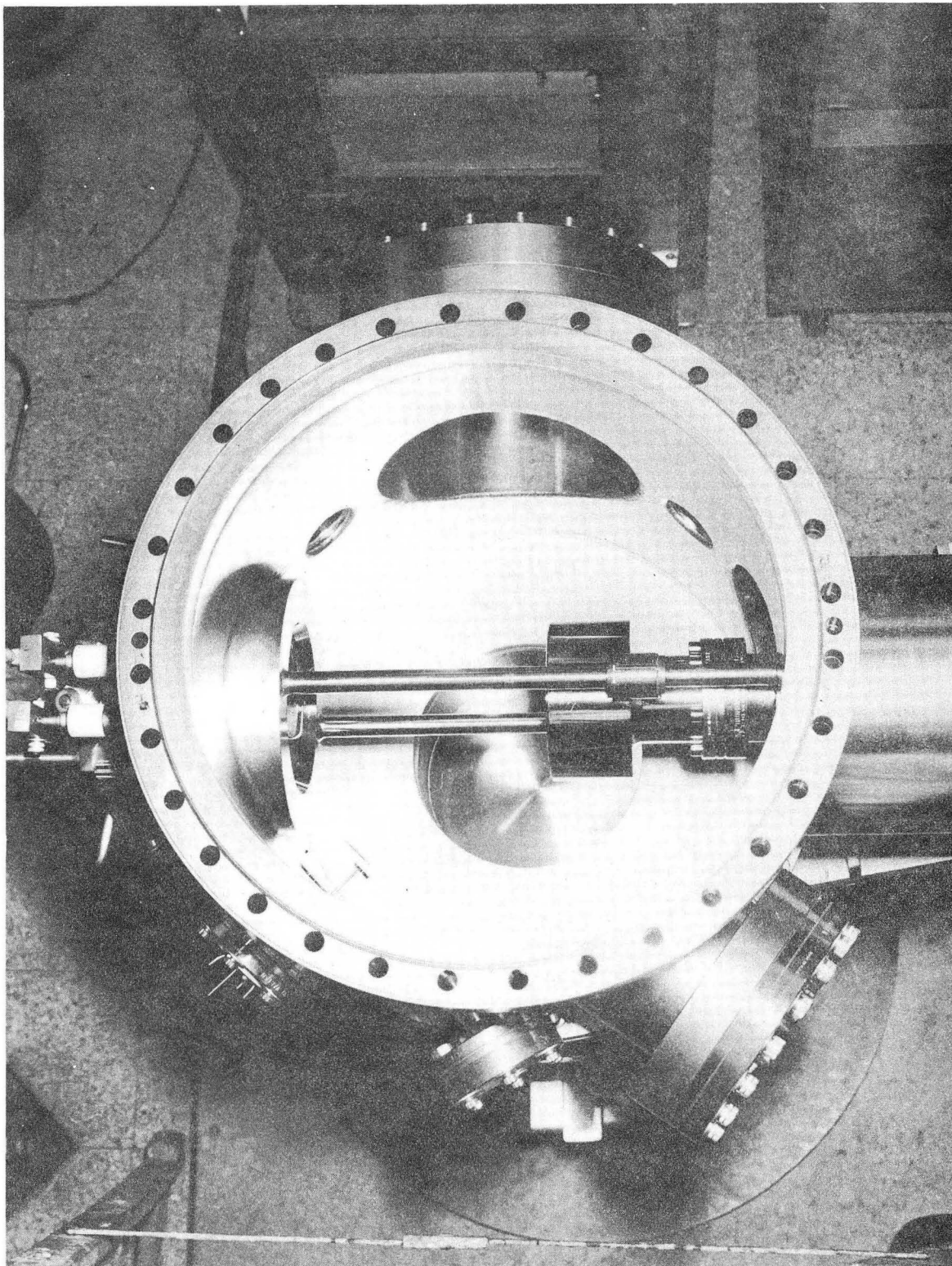
Figure II-1. SCHEMATIC OF FLOW LOOP FOR HIGH PRESSURE (1 ATM.) CATALYSIS ON SINGLE CRYSTAL PLATINUM SURFACES

XBL 734 - 5969

00003908089

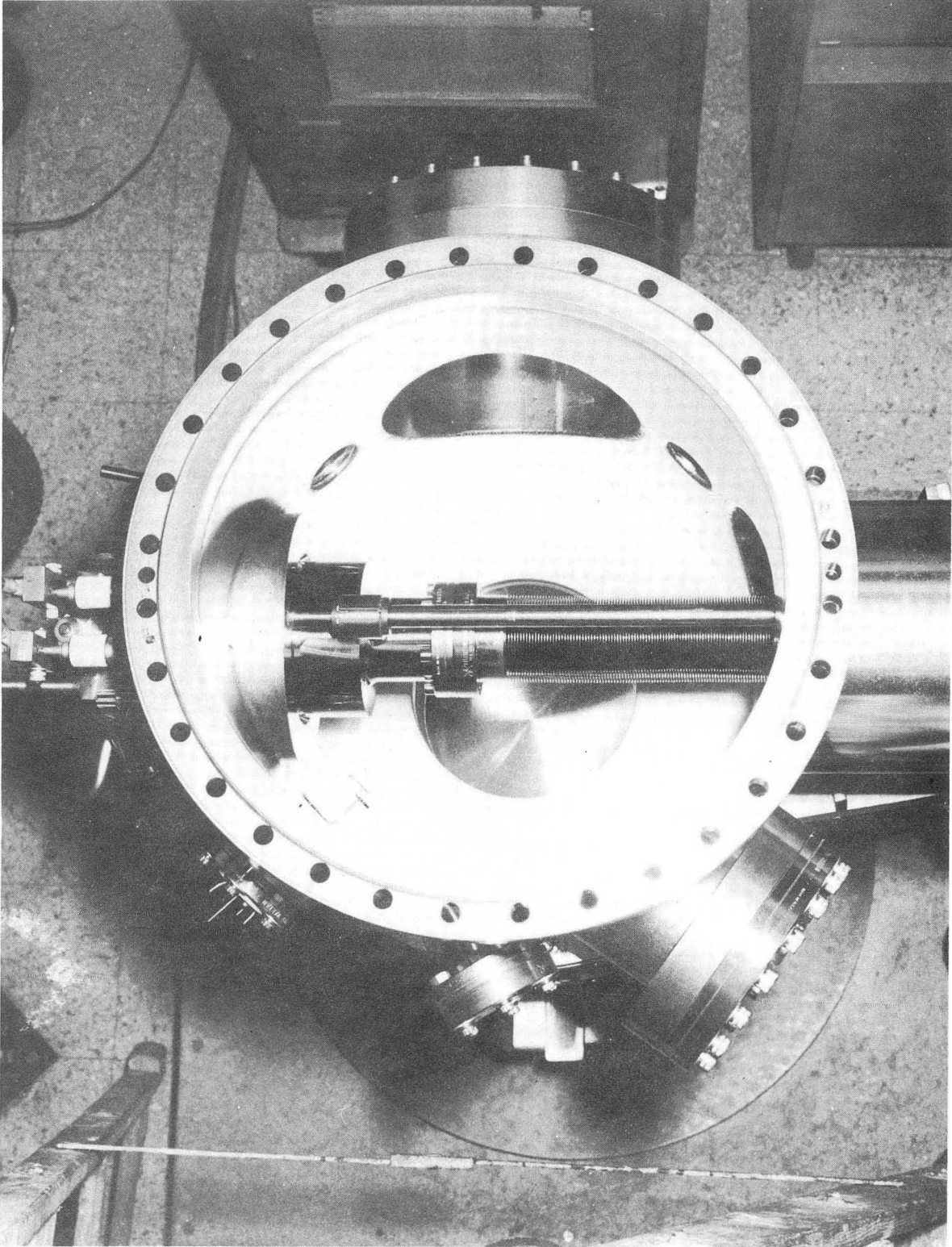
- An 8-inch flange for housing Auger electron grid optics and accessories.
- A 2 3/4-inch flange for optional use.
- A 6-inch flange, denoted as the reactor flange, consisting of seven symmetrically spaced 1.33-inch dia. mini-flanges for electrical feedthroughs (2), an 8-pin thermocouple feedthrough, a Varian variable leak valve, inlet and outlet Hoke S. S. bellows valves (2), and a viewing port.

The main feature of the upper chamber is the movable bellows-cup mechanism, which is shown in more detail in Figs. A-4a and A-4b. It is comprised of a 1-inch dia. threaded drive rod which extends through a bronze sleeve incorporated into the right 6-inch o.d. flange, a 2-inch o.d. stainless-steel flexible welded bellows, and finally into the rear compartment of the high pressure reactor "cup" which houses a series of thrust bearings. Thus the reactor cup attached to the bellows drive mechanism is capable of traversing the total internal diameter of the reactor. The high pressure reactor ($V \sim 560 \text{ cm}^3$) is formed by seating the finely machined 3 3/8-inch dia. knife edge of the reactor cup onto a gold O-ring in the wall of the left 6-inch o.d. flange. The two case-hardened 1/2-inch diameter stainless steel rods welded to the 6-inch reactor flange and bellows flange above and below the cup serve not only to guide the cup in its transverse path, but also to prevent deformation of the upper chamber when applying the necessary force to seal the high pressure reactor.



XBB 732-796

Figure A-4a. Top view of UHV-high pressure reactor with bellows-cup assembly withdrawn to expose catalyst single crystal to UHV.

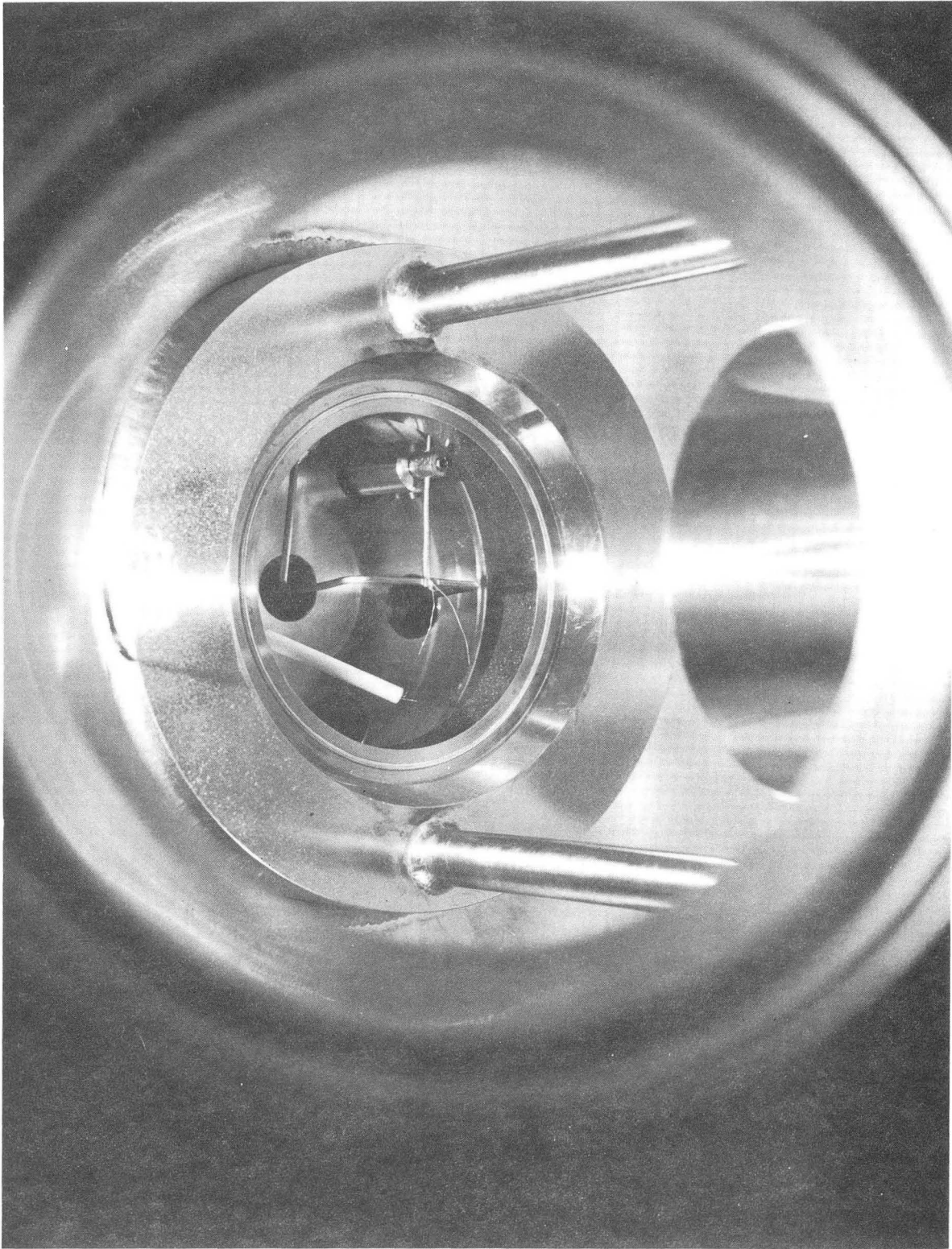


XBB 732-797

Figure A-4b. Top view of UHV-high pressure reactor with bellows-cup assembly extended to enclose catalyst single crystal in a small volume for high pressure studies.

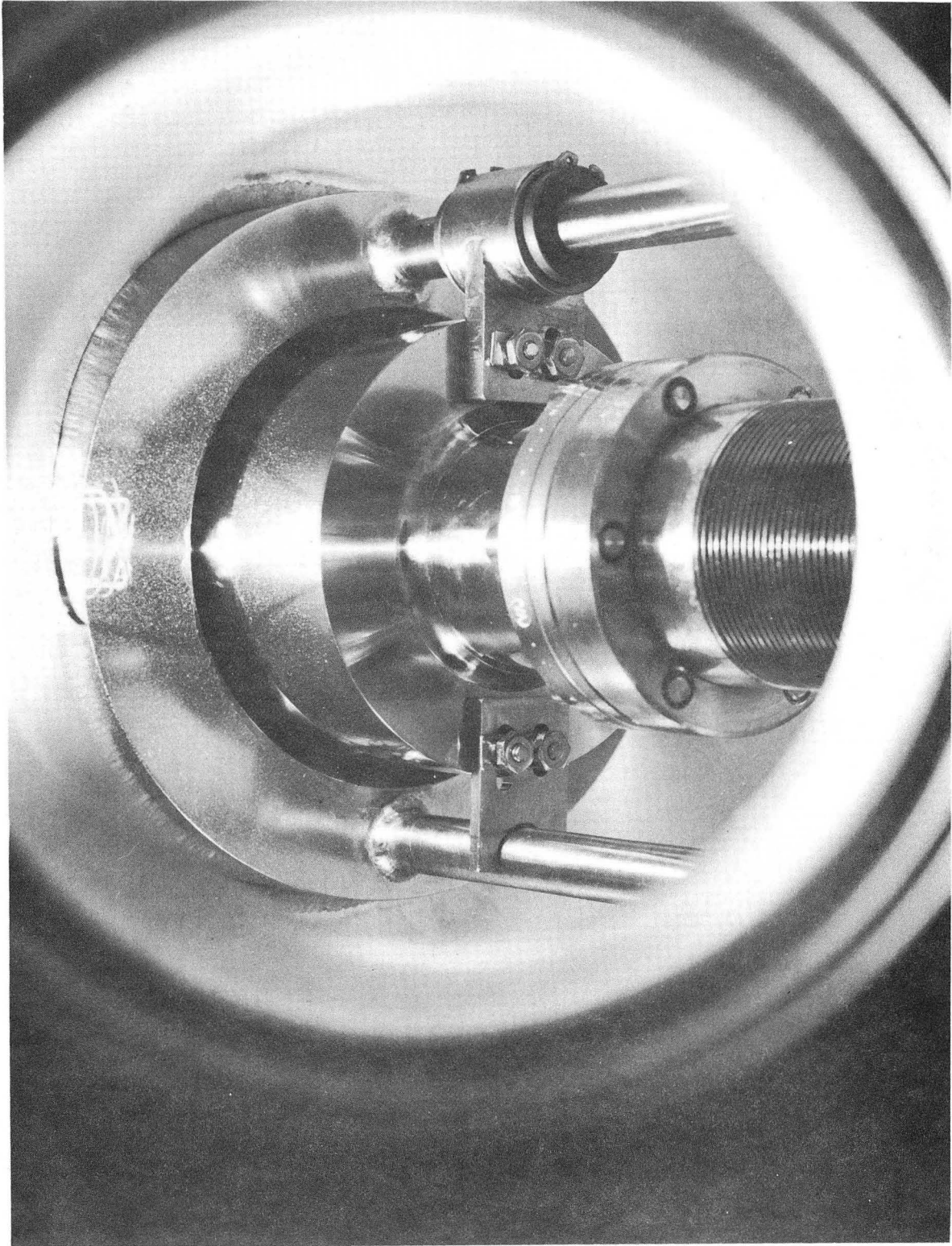
A close-up of the reactor flange as seen through the 6-inch viewing-port flange is provided in Figs. A-5a and A-5b. In the former photograph note the 3 3/8-inch dia. gold O-ring which has been pressed into the finely machined 1/16-inch groove in the reactor flange wall. A knife edge has also been machined within the groove to provide two sealing surfaces on the gold O-ring upon closing the reactor cup. Experiments conducted to check the cup seal during high pressure experiments (800-1000 torr) indicated that negligible amounts of reactant and product would be leaked into the UHV system during the course of a run. The constant leakage flow normally increased the pressure in the outer UHV chamber from 5×10^{-9} torr to 1×10^{-8} torr. As many as 20 cup closures have been obtained using one gold O-ring.

Although the photograph in Fig. A-5a was taken at a time when the platinum crystal had been removed to make a series of blank runs, the manner in which the crystal is supported is clearly evident. The two 0.070-inch dia. tantalum electrodes extend from copper sleeves connected to the electrical feedthroughs to approximately the center and leading edge of the reactor flange sealing surface. As shown the tantalum electrodes are spot-welded together. However for the catalytic runs the Pt crystal was spot-welded to the flattened ends of the two tantalum electrodes. External leads connecting the electrical feedthroughs to a Harrison 6260 A d.c. power supply (0-10 volts, 0-100 amps) enabled the single crystal to be heated routinely and accurately from room temperature to 1000°C.



XBB 732-791

Figure A-5a. Close-up of reactor flange, detailing the gold O-ring seated in the reactor flange wall, the tantalum electrodes, and the Pt/Pt-10% Rh thermocouple wires.



XBB 732-795

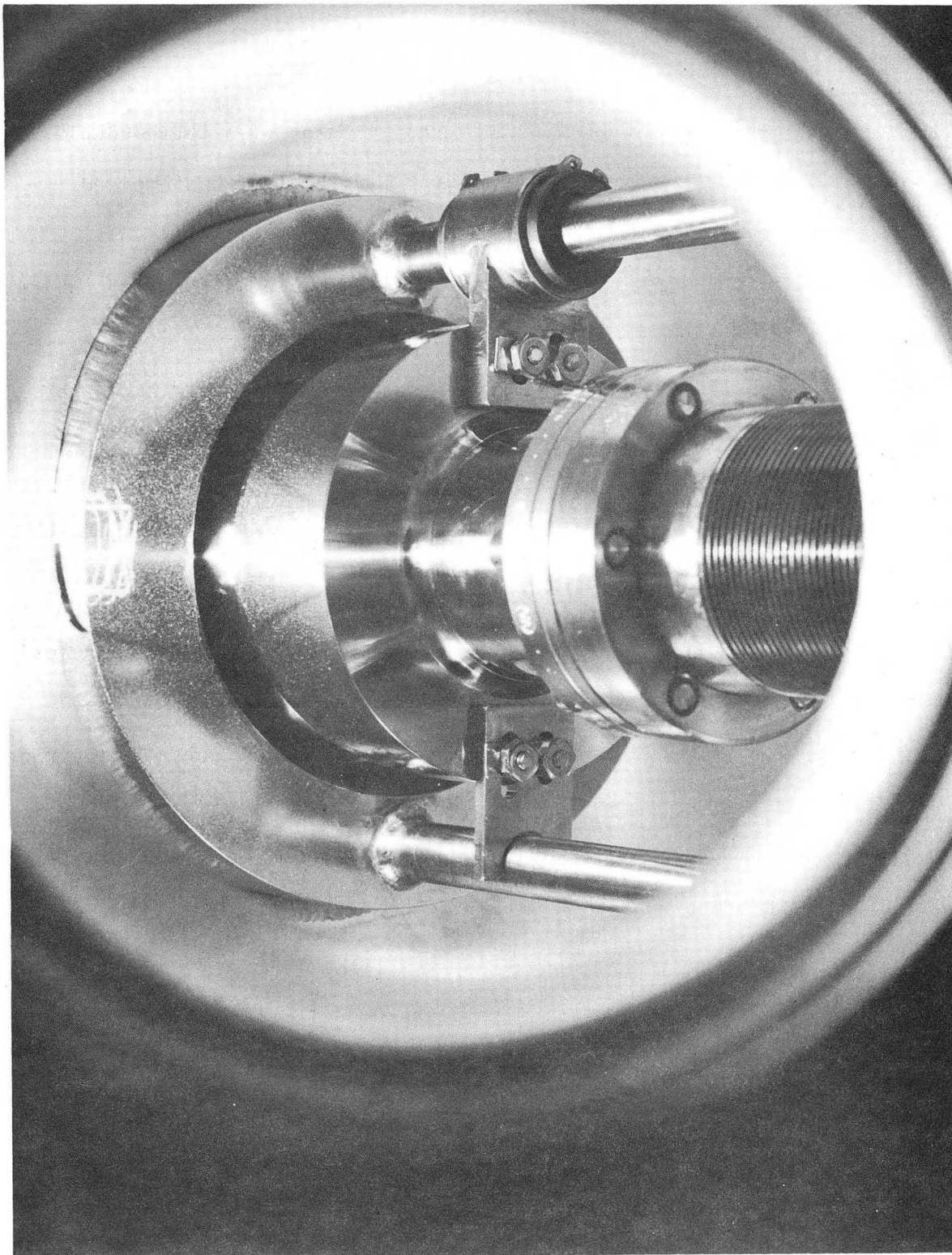
Figure A-5b. Close-up of reactor flange, with reactor cup seated on the gold O-ring to form the high pressure reactor.

The crystal temperature was measured by means of a thermocouple junction composed of 0.010-inch dia. Pt/Pt-10%Rh wires spot-welded to the lower edge of the Pt crystal. Using a Honeywell millivolt potentiometer (Model 2732) and standard thermocouple calibration tables, the crystal temperature could be monitored to within $\pm 0.1^\circ\text{C}$. In Fig. A-5a a 2-holed ceramic tube insulates the thermocouple wires to within 1 inch of the junction.

5. Construction of the High Pressure Flow Loop and Gas Manifold Assembly

A schematic of the high pressure flow loop has been given in Fig. II-1. To minimize possible sources of contamination the principal material of construction is stainless steel. Viton O-rings are used in the flowmeter and the sample valve, while Teflon is used as a packing material in the flow valves.

The reactor pressure is monitored by a 0-1500 torr Heise gauge measuring absolute pressure to within ± 0.25 torr. The flow rate within the loop is measured by a Fisher-Porter rotameter consisting of a variable area 1/8-inch tri-flat glass tube (FP-1/8-20-G-5/84). Using a stainless steel float, the range of flow for a 3/1 hydrogen to cyclopropane mixture (sp.gr. = 0.415 @ 800 torr and 20°C) is 0-4800 scc/min. Composition of the gas mixture is achieved by routing the flow through a 6-port sample valve housed in a 1520 Varian Aerograph gas chromatograph containing dual thermal conductivity and flame ionization detectors. Details of the analytical system are presented in Appendix E.



XBB 732-795

Figure A-5b. Close-up of reactor flange, with reactor cup seated on the gold O-ring to form the high pressure reactor.

The crystal temperature was measured by means of a thermocouple junction composed of 0.010-inch dia. Pt/Pt-10%Rh wires spot-welded to the lower edge of the Pt crystal. Using a Honeywell millivolt potentiometer (Model 2732) and standard thermocouple calibration tables, the crystal temperature could be monitored to within $\pm 0.1^\circ\text{C}$. In Fig. A-5a a 2-holed ceramic tube insulates the thermocouple wires to within 1 inch of the junction.

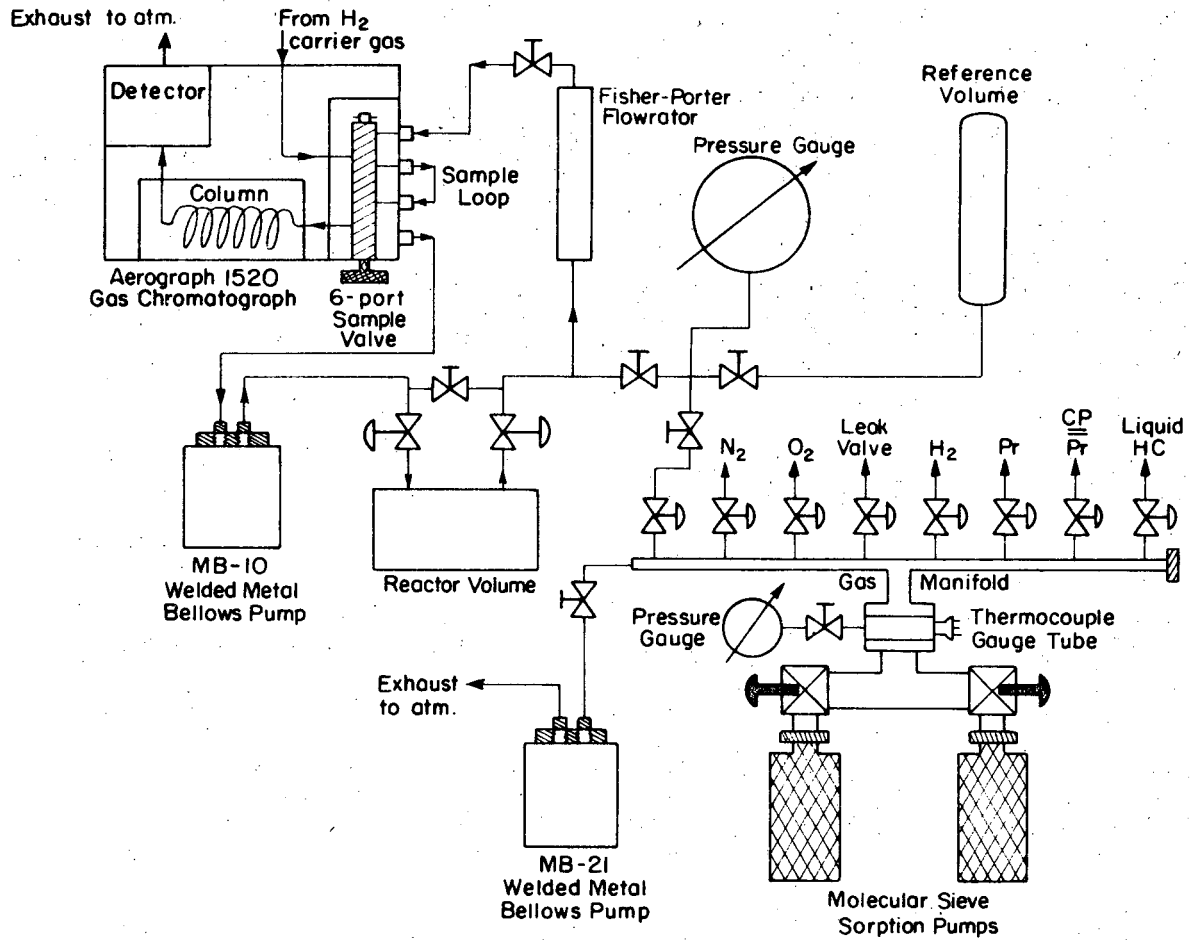
5. Construction of the High Pressure Flow Loop and Gas Manifold Assembly

A schematic of the high pressure flow loop has been given in Fig. II-1. To minimize possible sources of contamination the principal material of construction is stainless steel. Viton O-rings are used in the flowmeter and the sample valve, while Teflon is used as a packing material in the flow valves.

The reactor pressure is monitored by a 0-1500 torr Heise gauge measuring absolute pressure to within ± 0.25 torr. The flow rate within the loop is measured by a Fisher-Porter rotameter consisting of a variable area 1/8-inch tri-flat glass tube (FP-1/8-20-G-5/84). Using a stainless steel float, the range of flow for a 3/1 hydrogen to cyclopropane mixture (sp.gr. = 0.415 @ 800 torr and 20°C) is 0-4800 scc/min. Composition of the gas mixture is achieved by routing the flow through a 6-port sample valve housed in a 1520 Varian Aerograph gas chromatograph containing dual thermal conductivity and flame ionization detectors. Details of the analytical system are presented in Appendix E.

A model MB-10 stainless steel welded bellows pump (Metal Bellows Corp.) provides the gas circulation within the flow loop when the total pressure is between 400 torr and 1200 torr. Although the pump is rated at 2800 scc/min of air under zero pressure drop, the pressure drop across the sample valve limits the maximum flow rate to about one-fourth of its maximum value. Throughout the experimental runs the circulation within the flow loop was sufficient to give a gas residence time ($\tau = V/v_0$) of approximately 1 minute. Hence the contents of the reactor and flow loop can be considered to be "well-stirred" within the time frame of sampling. This simplifies the mathematical analysis of the kinetic data, as all fluid elements within the flow system are considered to have the same reactant or product concentration at a given point in time.

A schematic of the gas manifold assembly is shown in Fig. A-6. The manifold itself is fabricated from a 3/4-inch o.d. (0.065-inch wall) 304 S.S. tube to which are welded seven teflon-seated 316 S.S. Hoke valves (# 4251 N6Y). All gases to be admitted into the reactor system are first expanded into the manifold via these valves. An auxiliary 316 S.S. Hoke valve (# 4234 Q6Y) connects the manifold to the UHV variable leak valve. The manifold can be evacuated to approximately 400 torr by means of an MB-21 stainless steel welded bellows pump (Metal Bellows Corp.) which is vented to the atmosphere. Two liquid nitrogen chilled molecular-sieve sorption pumps further reduce the pressure to less than 5 μ Hg. The vacuum level is measured by means of a thermal conductivity gauge tube (connected to a CVC 110 C



XBL 738-1652

Figure A-6. Schematic representation of the high pressure flow loop and gas manifold assembly.

ion gauge) inserted into the system between the manifold and sorption pumps. In practice it is not possible to remove hydrogen completely from the system with the sorption pumps. Therefore nitrogen is used as a purge gas to sweep most of the hydrogen out of the manifold or reactor flow loop via the MB-21 bellows pump, whereupon the sorption pumps are opened to remove the remaining nitrogen.

APPENDIX B

Preparation of Platinum Single Crystals

The platinum used in this study was purchased from Materials Research Corporation (Orangeburg, N.Y.) in the form of 1/4-inch dia. single crystal rods grown by electron-beam zone refining (Marz grade). A typical mass spectrographic analysis of Marz grade platinum is given in Table B-1. The properties of various contaminants in platinum have been described elsewhere.^{35,36}

Platinum stepped surfaces are generated by cutting a platinum crystal at small angles from low index planes. The resulting high Miller index surfaces as determined by LEED studies have been shown to consist of low index terraces of constant width linked by steps of monatomic height.^{8,33} The Pt(S)-[7(111)×(111)] surface was obtained by sparkmachining at 8.5° from the (111) face towards the (110) plane. The nomenclature⁸ indicates that the terrace is of (111) orientation, 7 atomic rows in width, while the step is also of (111) orientation and one atom in height. The Pt(S)-[6(111)×(100)] surface was cut at 9.5° from the (111) face towards the (100) plane. It consists of terraces 6 atoms wide with (111) orientation and a step geometry of (100) orientation. The accuracy of the sparkmachining process is ± 0.5°. A schematic representation of the atomic structure of these two stepped surfaces has been shown previously in Fig. II-2.

After cutting, the crystals were mechanically polished with a series of abrasives, the final polish being 1/4 μm alumina. They were

Table B - 1. Typical mass spectrographic analysis
of "Marz" grade platinum³²

Element	Content (ppm)	Element	Content (ppm)
Li	<0.0002	Rh	15.0
Be	<0.02	Pd	0.6
B	0.0003	Ag	0.012
C	10.0	Cd	<0.025
H ₂	1.5	In	0.03
O ₂	10.0	Sb	<0.004
N ₂	3.0	Sn	0.08
F	<0.003	Te	<0.008
Na	<0.06	I	<0.002
Mg	<0.06	Cs	<0.002
Al	7.0	Ba	<0.003
Si	7.0	La	<0.002
P	0.002	Ce	<0.002
S	0.2	Pr	<0.002
Cl	0.4	Nd	<0.01
K	0.1	Sm	<0.01
Ca	0.05	Eu	<0.005
Sc	<0.03	Gd	<0.01
Ti	2.5	Tb	<0.003
V	0.25	Dy	<0.01
Cr	2.5	Ho	<0.003
Mn	0.6	Er	<0.008
Fe	30.0	Tm	<0.003
Co	0.3	Yb	<0.06
Ni	2.5	Lu	<0.003
Cu	0.05	Hf	0.05
Zn	0.05	Ta	< 5.0
Ga	0.01	W	5.0
Ge	<0.004	Re	< 0.02

Table B - 1 (continued)

Element	Content (ppm)	Element	Content (ppm)
As	0.01	Os	<0.08
Se	<0.003	Ir	0.3
Br	0.008	Au	<0.3
Rb	<0.01	Hg	<0.15
Sr	<0.003	Tl	<0.15
Y	<0.01	Pb	<0.6
Zr	2.5	Bi	<0.06
Nb	1.0	Th	<0.07
Mo	<0.3	U	<0.07
Ru	0.3		

then etched in hot 50% aqua regia for 5-15 minutes prior to introduction into the vacuum system.

Both stepped single crystals were approximately elliptical in shape. Table B-2 summarizes the calculation of the total geometric surface area for each elliptical disc. This area is composed of an elliptical area having the orientation of the stepped surface and a circumferential area of unknown orientation, presumably polycrystalline in nature. The total area values were used in all calculations involving specific rates of reaction. It has been assumed that the surface roughness is unity, i.e., the platinum surface area available for reaction is the total geometric surface area.

Cleaning techniques have been developed to remove impurities from low index and stepped crystal faces of platinum.^{35,36} From this work, the major contaminant in the high purity platinum single crystal is carbon. In a freshly prepared stepped single crystal having a (111) terrace orientation, carbon can be removed by heating the crystal to 1000°C for 6 hours at a pressure of 5×10^{-6} torr. A slightly contaminated surface containing only a surface layer of carbon can be cleaned by heating the crystal to 800°C in 1×10^{-6} torr oxygen for 5 minutes. It is known that oxygen chemisorbs readily on platinum stepped surfaces at the step sites.⁹ Hence it was found that these surfaces should be heated for an additional hour at 800°-1000°C in vacuum, after removing oxygen from the gas phase.

Table B - 2. Platinum single crystal surface area.

Platinum single crystal	Major axis	Minor axis	Crystal thick- ness	Elliptical surface area	Circumferential surface area	Total surface area	% Unknown orientation
	2a	2b	t	A_s (cm ²)	A_c (cm ²)	A_T (cm ²)	$\left(\frac{A_C}{A_T} \times 100\right)$
	(mm)	(mm)	(mm)	(2 π ab)	$\left(2\pi t \sqrt{\frac{a^2+b^2}{2}}\right)$		
Pt(s) - [7(111)X(111)]	7.0	6.0	0.7	0.66	0.14	0.80	18
Pt(s) - [6(111)X(100)]	7.0	6.0	0.5	0.66	0.10	0.76	13

These cleaning techniques, based upon Auger electron spectroscopy to monitor the surface contaminant concentration down to 1% of a monolayer, were used as a basis for the crystal pretreatment procedures employed in this study (See Appendix G). The Pt(S)-[6(111)×(100)] single crystal was cleaned for 13 hours in 1×10^{-6} torr oxygen at 903-913°C prior to its use in Run 10A. Thereafter before each experimental run, the crystal was heated in 1×10^{-6} torr oxygen at 900-925°C for 2 hours. The oxygen was pumped out of the UHV system for an additional 60 minutes while maintaining the crystal temperature at 900-925°C. Prior to closing the reactor cup and filling it with 200 torr hydrogen, the crystal temperature was not allowed to drop below 250°C at a pressure of 5×10^{-9} torr. This was done to avoid chemisorption of CO which takes place on platinum stepped surfaces having (111) terraces below 200°C.^{9,35} Carbon monoxide is a major background contaminant in UHV systems.

APPENDIX C

Purity of Materials

1. Gases

The cyclopropane was obtained from Matheson and contained less than 0.4% impurities. Propylene accounted for approximately two-thirds of this impurity. The gas was passed through a bed of activated $MgClO_4$ to remove traces of water. During early experiments on the Pt(S)-[7(111)×(111)] single crystal, the cyclopropane was also frozen out in a liquid N_2 cold finger, evacuated, melted, degassed, and distilled. The middle distillate fraction was then expanded into the reactor flow loop. Gas chromatographic analysis indicated that the propylene concentration in the distilled cyclopropane was somewhat greater than that in the undistilled cyclopropane. Hence this purification procedure was eliminated in all subsequent runs.

Hydrogen was obtained from the Lawrence Berkeley Laboratory and had a minimum purity of 99.99%, the major impurity being oxygen. This was also passed through activated $MgClO_4$ prior to introduction into the gas chromatograph or reactor flow loop.

2. Calcium Impurity in the Platinum Single Crystals

It was pointed out in Chapter III that a calcium impurity within the bulk of the Pt(S)-[7(111)×(111)] single crystal had segregated to the surface and was in some way responsible for the lack of data reproducibility on this surface. The evidence for this assertion is indirect but nonetheless convincing.

After heating the single crystal to 850-950°C several times, a thin circumferential ring appeared on the surface. At room temperature the ring appeared faint and milky-white in color. Upon heating the crystal to 900°C, the ring was clearly visible and glowed considerably brighter than the bulk platinum. Prolonged high-temperature oxygen treatment had no effect in diminishing the intensity of the ring.

Meanwhile, independent Auger electron spectroscopy (AES) analysis of several other platinum single crystals cut from the same single crystal rod as the Pt(S)-[7(111)×(111)] crystal indicated that the platinum contained a considerable amount of calcium. The impurity probably segregates on the surface as a calcium oxide rather than the pure element. Efforts to completely remove calcium impurities from platinum crystals by ion bombardment or other in situ techniques have not been successful.⁶³

Because the experimental apparatus was not equipped for AES analyses, it was decided that the Pt(S)-[7(111)×(111)] single crystal would be used only for qualitative order of magnitude reactivities. Indeed the contaminated surface was still highly active for the cyclopropane hydrogenolysis and propylene hydrogenation reactions.

The Pt(S)-[6(111)×(100)] single crystal used for the cyclopropane hydrogenolysis reaction in Runs 9 through 17 was cut from a different MRC platinum rod and was shown by AES analysis to contain only a very small amount of calcium impurity.³⁴

3. Sulfur Impurity in the Tantalum Electrodes

Tantalum was chosen as the metal to support the platinum single crystals directly because of its lack of reactivity, low oxide vapor pressure, and high melting point. For the preliminary experiments on the Pt(S)-[7(111)×(111)] single crystal, 0.060-inch dia. tantalum rods having a purity of 99.9% were used. Prior to inserting the support rods into the UHV system, they were thoroughly degreased in solvents and etched for 10 minutes in a 50% bath of nitric and hydrofluoric acids. Blank runs for the cyclopropane hydrogenolysis and propylene hydrogenation reactions indicated that the tantalum was not reactive.

Independent AES analysis of tantalum samples obtained from the same source and cleaned in a similar manner revealed that there was a sulfur impurity contained within the metal.³⁴ Upon heating the tantalum to 1000°C in vacuum, practically a monolayer of sulfur covered the surface after a couple of hours. Furthermore when a previously cleaned platinum stepped single crystal was spotwelded to the impure tantalum and the assembly heated in vacuum to 1000°C, the sulfur was found to diffuse from the tantalum to the platinum surface. It was possible to remove the sulfur adsorbed on the platinum by heating the crystal in 1×10^{-6} torr oxygen at 900-1000°C for prolonged periods (4-10 hours). It should be noted here that sulfur is known to form well-ordered structures on low index platinum surfaces.⁶⁴

The immediate goal of the preliminary experiments was to determine order of magnitude reactivities for a number of reactions using the thermal conductivity detector of the gas chromatograph. Hence reaction rates which could be measured on a surface containing a sulfur impurity would also be measurable on a clean platinum surface. This is certainly the case for the cyclopropane hydrogenolysis reaction. However the fact that no reactivity could be measured for the "demanding" n-heptane/H₂ and neopentane/H₂ reactions could have been a result of the blockage of step sites by the sulfur impurity.

New 0.068-inch dia. tantalum rods were prepared for the cyclopropane/H₂ experiments in Runs 9 through 17. A three-pass zone refining procedure was used to increase the tantalum purity to 99.999%. The rods were also etched for 10 minutes in an 80% solution containing nitric and hydrofluoric acids prior to their insertion into the vacuum system.

Several samples of the newly purified tantalum were subjected to AES analysis to check the effectiveness of the zone refining procedure.⁶⁵ In one experiment a platinum foil (10-20 μ thickness) was spot-welded between two tantalum electrodes. Only platinum, carbon, and oxygen could be detected on the initially cold platinum surface. Heating the foil to 900°C in vacuum for only 5 minutes resulted in considerable mass transport of sulfur to the platinum surface to the extent that the identity of the AES platinum peak was lost due to the sulfur coverage. The maximum sulfur signal was an order of magnitude lower than that found for tantalum alone. When the foil was heated in

1×10^{-6} torr oxygen for 2 hours at 900°C , the Pt/S signal ratio was approximately 0.1. Prolonged heating at these conditions (16 hours) did not increase this ratio. However pumping out the oxygen for 1 hour, while maintaining the same temperature, increased the Pt/S ratio to 1.0.

It is clear that the tantalum electrodes used in Runs 9-17 were not sulfur-free and could very well have contaminated the platinum crystal surface with sulfur prior to each run. Yet the fact that the data was reproducible to about 10% and that the initial reaction rates were comparable to those on highly dispersed supported platinum catalysts suggest that the extent of poisoning was not severe. It is possible the activation energy based upon initial reaction rates was increased by the sulfur coverage, as it was slightly higher than values reported in the literature. If the actual catalysis occurs on a carbon overlayer rather than on the platinum (or platinum-sulfided) surface, it is possible that the shape of the reaction rate curves would not be very different had there been no sulfur present.

An Auger electron gun control and grid optics unit is presently being fabricated for installation into the present apparatus. It is hoped that this additional analytical tool will help to resolve the sulfur impurity question and provide added insight into the nature of the true catalytic surface.

APPENDIX D

Volume Calibrations for the High Pressure Flow Loop

A series of experiments were conducted to determine the volume of each component of the high pressure flow loop. Figure D-1 is a schematic of the flow loop and manifold assembly identifying each of these volume segments, where

V_{REF} = Reference volume

V_{GC} = Volume of the flow loop, excluding the reactor, composed of three segments (V_{GC1} , V_{GC2} , V_{GC3})

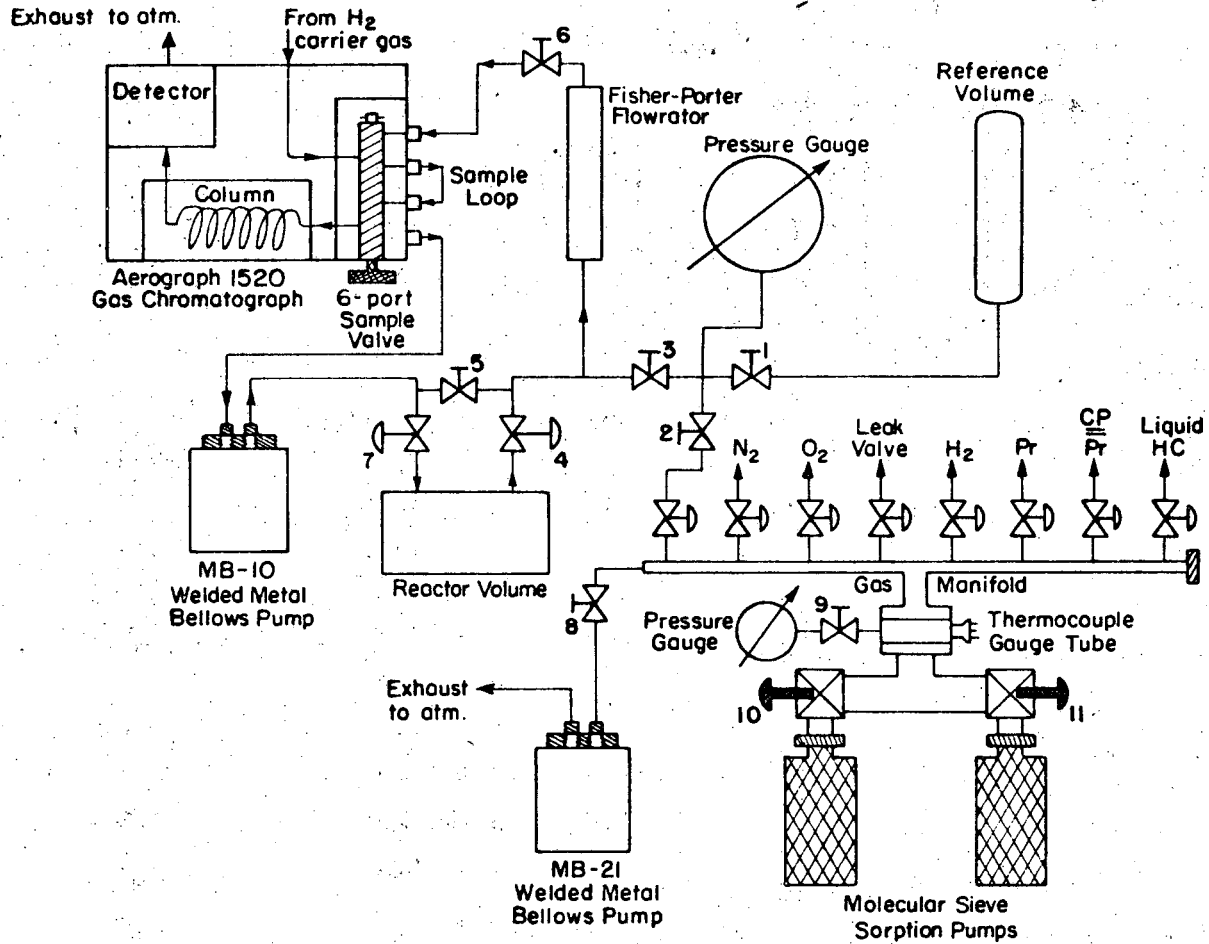
V_R = Reactor volume

V_{SL} = Sample loop volume (contained within V_{GC})

V_M = Manifold volume

The volume of the reference cylinder was determined first by a gravimetric method. The cylinder was weighed on an Ohaus triple beam balance (2610 gram capacity) and a tare weight established. The cylinder was then filled with hot distilled water, cooled to room temperature, and then weighed several times to obtain an average weight. After four separate filling trials, the average net weight of water contained in the reference cylinder was found to be 507.6 ± 0.5 gms. Using the density of water at 23°C ($\rho_{\text{H}_2\text{O}} = 0.9976 \text{ gm/cm}^3$), the reference cylinder volume was calculated to be 508.8 cm^3 . Correcting this value for the short length of tubing leading up to the Hoke valve, the total reference volume is $515.0 \pm 1.0 \text{ cm}^3$.

The remaining volumes of the flow loop were obtained by simple expansion experiments using the ideal gas law. Knowing one volume and



XBL 738-1652

Figure D-1. Schematic of high pressure flow loop and gas manifold assembly.

Key to identification of reactor system volumes

Volume Designation	Valves Isolating Designated Volume
V_{REF}	Reference cylinder up to valve 1
V_{GC1}	Valves 1, 2, 3
V_{GC2}	Valves 3, 4, 5, 6
V_{GC3}	Valves 5, 6, 7 (including V_{SL})
V_{GC}	Valves 1, 2, 3, 7
V_R	Valves 4, 7
V_M	Valves 2, 8, 9, 10, 11
$V_R + V_{GC}$	Valves 1, 2

both initial and final pressures using the Heise gauge, the unknown volume was calculated.

Table D-1 summarizes the results of these trials. All volumes reported have been determined to within 1% error, with the exception of V_{SL} which has been estimated to within 2.5%.

Table D - 1. Summary of high-pressure reactor system volumes

V_{ref}	=	515.0 cm ³
V_{GC1}	=	72.9 cm ³
V_{GC2}	=	36.9 cm ³
V_{GC3}	=	79.1 cm ³
V_{GC}	=	188.9 cm ³
V_{SL}	=	0.78 cm ³
V_{R}	=	570.5 cm ³
V_{M}	=	472.4 cm ³
$V_{\text{R}} + V_{\text{GC}}$	=	$V_{\text{system}} = 759.4 \text{ cm}^3$
$\frac{V_{\text{system}}}{V_{\text{SL}}}$	=	973.6
$\frac{V_{\text{R}}}{V_{\text{GC}}}$	=	3.02

APPENDIX E

Analytical System: Calibration of the Gas Chromatograph for
the Cyclopropane Hydrogenolysis Reaction

The concentration of reactants and products in the high pressure loop for the hydrogenolysis of cyclopropane was measured by a gas chromatographic sampling technique. The components involved in the analysis are propane, propylene, and cyclopropane. The propylene appears as an impurity in the cyclopropane and must be known for initial rate calculations.

The gases in the circulation loop were routed through a viton-sealed, 6-port sample valve housed in a Varian Aerograph 1520 gas chromatograph containing dual thermal conductivity detectors (TCD). Although dual flame ionization detectors were also available, these were not used as the TCD produced a more stable baseline and provided adequate sensitivity for the detection of propane.

The carrier gas chosen for this study was hydrogen (H_2). Early experiments using helium as a carrier gas confirmed the anomalous behavior of He/H_2 mixtures described by Purcell and Ettore.³⁸ It was decided that H_2 was a more logical choice from a number of standpoints. The sensitivity of the TCD is maximized using H_2 as a carrier gas. Analysis of the gas chromatograms is simplified because no H_2 peak appears when using the dual TCD set-up. With the 6-port sample valve each sample taken results in a small amount of carrier gas being admitted into the reactor flow loop. By using the same source of H_2 for both the G.C. carrier gas and as a reactant, the progressive addition of a new component into the reactor system is eliminated.

Sampling is accomplished by depressing the spindle of the 6-port valve, enabling the carrier gas to sweep the volume of reactor gases contained in the sample loop into the column and then to the detector filaments. Using a sample volume of 0.78 cm^3 and a carrier gas flow rate of 30 cc/min, experiments showed that a 10 sec injection time was sufficient for this purpose.

The G.C. operating conditions and column specifications used in the analysis of the cyclopropane hydrogenolysis reaction are given in Table E-1.

The output from the chromatograph was recorded on a Honeywell Elektronik 15 strip chart recorder. The chromatographic peaks were integrated by the triangulation method, where the peak area is given by the peak height multiplied by the peak width at half height. Since the peak widths for propane and cyclopropane were virtually constant at all attenuations throughout a run, the peak area was proportional to the peak height. Tables E-2 and E-3 summarize the peak area data for a series of calibration mixtures containing propane, propylene, and cyclopropane. The moles of hydrocarbon calculated were based upon the sample loop volume of 0.78 cm^3 . The average peak sensitivities listed in the last column of Table E-2 were used in all subsequent calculations to convert peak areas to hydrocarbon concentrations.

Table E-1. Summary of operating conditions
for the analytical system.

Column Specification:

1/8 in. o.d. × 20 ft stainless steel tubing packed with 30% bis
2-methoxyethyl adipate on 60/80 mesh acid-washed chromosorb P
for use in Aerograph 1520 gas chromatograph (type A column bend).

Detector Filaments:

Gow Mac type W2 (3% Rh/W).

Operating Conditions:

Carrier gas flow rate (hydrogen):	30 ml/min
Carrier gas delivery pressure:	40 psig
Filament current:	230 ma
Detector temperature:	118°C
Column temperature:	34°C
Injection time:	10.0 sec
Recorder speed:	2 in./min
Sample Loop Volume:	0.78 cm ³

Table E - 2. Summary of G. C. calibrations for the cyclopropane hydrogenolysis reaction

Hydrocarbon component	Pressure range (torr)	Average G. C. peak sensitivity $\left(\frac{\text{moles component}}{\text{mV}\cdot\text{sec}}\right)$
Cyclopropane	0 - 135	2.40×10^{-8}
Propylene	0 - 135	2.40×10^{-8}
Propane	0 - 21	2.33×10^{-8}

Table E-3. Component G. C. peak sensitivities at various pressures

<u>Component</u>		: <u>Cyclopropane</u>			
Pressure (torr)	Moles $\times 10^8$	Peak area (mV. sec)	Sensitivity S ($\frac{\text{moles} \times 10^8}{\text{mV. sec}}$)	$S_{\text{avg.}}$	Detector temp. (°C)
135.0	557.4	232.4	2.398	2.40	115
	555.1	231.1	2.402		
	552.8	230.1	2.402		
135.0	557.3	236.0	2.361	2.38	117
	555.2	234.0	2.373		
	553.1	231.4	2.390		
	550.8	230.1	2.394		
100.0	413.9	167.9	2.465	2.46	117
	412.3	167.6	2.460		
	410.6	167.3	2.454		
65.0	270.3	110.9	2.437	2.44	118
	269.0	109.5	2.457		
	268.0	109.8	2.441		
	266.6	109.8	2.428		
30.0	125.2	49.74	2.517	2.51	115
	124.7	49.74	2.507		
	124.2	49.58	2.505		
	123.8	49.58	2.497		

Table E-3. (continued)

<u>Component</u>		<u>Propylene</u>			
Pressure (torr)	Moles $\times 10^8$	Peak area (mV. sec)	Sensitivity S ($\frac{\text{moles} \times 10^8}{\text{mV. sec}}$)	$S_{\text{avg.}}$	Detector temp. (°C)
135.0	558.7	234.2	2.386	2.38	118
	553.9	232.9	2.378		
	551.8	232.0	2.378		
101.0	420.0	180.2	2.331	2.33	116
	418.2	179.5	2.330		
	416.6	179.1	2.326		
	415.0	178.6	2.324		
65.0	270.8	111.2	2.435	2.42	118
	269.6	110.4	2.442		
	268.6	111.2	2.415		
	267.3	111.7	2.393		
30.0	125.1	48.89	2.559	2.56	117
	124.7	48.79	2.556		
	124.2	48.48	2.562		
15.0	62.14	26.81	2.318	2.31	118
	61.89	26.71	2.317		
	61.61	26.71	2.307		
	61.36	26.61	2.306		

Table E-3. (continued)

<u>Component</u>		<u>Propane</u>			
<u>Pressure</u> (torr)	<u>Moles</u> $\times 10^8$	<u>Peak area</u> (mV. sec)	<u>Sensitivity</u> S ($\frac{\text{moles} \times 10^8}{\text{mV. sec}}$)	$S_{\text{avg.}}$	<u>Detector temp.</u> (°C)
21.0	87.12	36.72	2.373	2.37	116
	86.76	36.64	2.368		
	86.40	36.31	2.380		
15.0	64.07	28.19	2.273	2.29	115
	63.81	27.87	2.290		
	63.57	27.74	2.292		
	63.33	27.66	2.290		
11.0	46.84	19.87	2.357	2.35	118
	46.61	19.75	2.360		
	46.43	19.79	2.346		
	46.19	19.83	2.329		
5.0	21.19	10.20	2.077	2.05	117
	21.11	10.30	2.050		
	21.03	10.36	2.030		
1.0	4.14	2.31	1.79	1.78	117
	4.12	2.31	1.78		
	4.10	2.31	1.77		
	4.08	2.30	1.77		

APPENDIX F

EXPERIMENTAL DATA FOR THE PRELIMINARY RUNS
ON THE Pt(s)-[7(111)×(111)] SINGLE CRYSTAL

RUN NO. 2A

PROCEDURAL NOTES AND OBSERVATIONS

- (1) Crystal cleaned in 3×10^{-6} torr O_2 @ 920-950°C for 2 hours.
- (2) Oxygen pumped out for 15 minutes prior to cooling crystal.
- (3) Crystal allowed to cool rapidly; at 4.0 minutes, $T_c = 100^\circ C$ and reactor cup closed.
- (4) At 5.6 minutes, 172.5 torr H_2 introduced into the reactor cup.
- (5) For the next 9.4 minutes, the crystal was heated to 74°C in H_2 .
- (6) Following this period, 135 torr cyclopropane was added to the reactor system. Additional H_2 was added to give a total system pressure of $P_T = 803$ torr.
- (7) Zero elapsed reaction time corresponds to the introduction of the cyclopropane into the reactor system.

0000390027

RUN NO. 2A G.C. OPERATING CONDITIONS AND CHROMATOGRAPHIC PEAK DATA

Filament Current: 230 ma
 Detector Temperature: 115°C
 Column Temperature: 35°C
 Room Temperature: 23.2°C
 Initial Mixture Composition: 135 torr Cyclopropane; 668 torr H₂

Hydrogen Regulator Pressure: 41 psig
 Column A Flow Rate (% Max): 40
 Column B Flow Rate (% Max): 18
 Injection Time: 10.0 sec

Chromat. Number	Elapsed Rxn. Time (min)	Reactor Pressure (torr)	Crystal Temp (°C)	Propane Peak Area (mv·sec)	Moles C ₃ H ₈ in V _{SL} ×10 ⁸	Total Moles C ₃ H ₈ per cm ² Pt × 10 ⁵
127	3.5	804.5	74	0.38	0.91	1.10
128	8.6	806.5	74	0.49	1.18	1.43
129	13.8	808.0	74	0.59	1.42	1.72
130	19.1	810.0	74	0.68	1.64	1.99
131	24.6	812.0	74	0.81	1.93	2.34
132	30.4	814.0	74	0.99	2.39	2.90
133	36.2	816.0	73	1.18	2.83	3.44
134	42.0	818.0	72	1.28	3.06	3.71
135	47.6	820.5	73	1.45	3.48	4.22
136	53.5	822.5	73	1.57	3.76	4.56
137	59.2	824.5	73	1.61	3.87	4.70
138	65.0	827.0	73	1.66	3.99	4.84
139	70.9	829.0	73	1.78	4.26	5.17
140	77.0	831.0	73	1.83	4.39	5.33
141	82.7	833.0	73	1.89	4.54	5.51
142	88.8	835.0	73	1.93	4.63	5.62
143	94.7	837.0	73	1.98	4.75	5.77
144	100.6	839.0	73	2.02	4.85	5.89
145	107.0	840.5	73	2.03	4.87	5.91
146	112.9	842.5	73	2.07	4.97	6.03

RUN NO. 2A G.C. OPERATING CONDITIONS AND CHROMATOGRAPHIC PEAK DATA

Filament Current:	Hydrogen Regulator Pressure:
Detector Temperature:	Column A Flow Rate (% Max):
Column Temperature: Ibid.	Column B Flow Rate (% Max): Ibid.
Room Temperature:	Injection Time:
Initial Mixture Composition:	

Chromat. Number	Elapsed Rxn. Time (min)	Reactor Pressure (torr)	Crystal Temp (°C)	Propane Peak Area (mv·sec)	Moles C ₃ H ₈ in V _{SL} × 10 ⁸	Total Moles C ₃ H ₈ per cm ² Pt × 10 ⁵
147	118.8	844.5	73	2.10	5.04	6.12
148	130.7	846.5	73	2.18	5.23	6.35
149	142.4	848.0	72	2.20	5.29	6.42
150	156.0	850.0	72	2.28	5.46	6.63
151	169.3	852.0	70	2.33	5.58	6.77
152	183.4	854.0	73	2.38	5.71	6.93
153	200.2	856.0	73	2.44	5.85	7.10

00003900028

RUN NO. 3

PROCEDURAL NOTES AND OBSERVATIONS

- (1) Crystal cleaned in 1×10^{-6} torr O_2 @ $906-952^\circ C$ for 2 hours.
- (2) Oxygen pumped out of UHV system for 20 minutes prior to cooling crystal.
- (3) Crystal allowed to cool rapidly; at 4.0 minutes, $T_c = 100^\circ C$ and reactor cup closed.
- (4) At 6.8 minutes, H_2 was already introduced and additional H_2 added to give a total reactor pressure of $P_T = 50.7$ torr.
- (5) Crystal heated in H_2 @ $77-79^\circ C$ for 1 hour.
- (6) An error in filling the reactor cup with the cyclopropane/hydrogen reactant mixture resulted in a total initial reactor system pressure of $P_T = 680$ torr. As a result during the experimental run the air peak increased very gradually.
- (7) The crystal temperature was increased to $T_c = 109^\circ C$ just prior to chromatographic sampling.

RUN NO. 3 G.C. OPERATING CONDITIONS AND CHROMATOGRAPHIC PEAK DATA

Filament Current: 230 ma Hydrogen Regulator Pressure: 41 psig
 Detector Temperature: 116°C Column A Flow Rate (% Max): 40
 Column Temperature: 35°C Column B Flow Rate (% Max): 20
 Room Temperature: 22.0°C Injection Time: 10.0 sec
 Initial Mixture Composition: 135 torr Cyclopropane; 545 torr H₂

Chromat. Number	Elapsed Rxn. Time (min)	Reactor Pressure (torr)	Crystal Temp (°C)	Propane Peak Area (mv·sec)	Moles C ₃ H ₈ in V _{SL} × 10 ⁸	Total Moles C ₃ H ₈ per cm ² Pt × 10 ⁵
182	2.7	688.0	109	0.88	2.04	2.48
183	7.7	690.0	113	3.13	7.28	8.84
184	12.8	691.5	112	5.48	12.76	15.49
185	18.0	693.0	112	7.30	17.02	20.66
186	23.2	695.0	112	8.69	20.25	24.58
187	28.3	697.0	112	9.77	22.77	27.64
188	33.4	699.0	112	10.51	24.48	29.72
189	38.7	701.5	112	11.02	25.67	31.16
190	44.4	704.0	111	11.67	27.19	33.00
191	49.8	706.0	112	11.98	27.90	33.87
192	58.5	708.0	111	12.87	29.99	36.40
193	71.4	710.0	111	13.44	31.32	38.02
194	86.9	712.0	111	14.42	33.61	40.80
195	100.5	713.5	111	15.08	35.13	42.65
196	115.4	715.5	111	15.75	36.69	44.54
197	129.2	717.5	111	16.36	38.12	46.28
198	144.0	719.5	109	17.10	39.83	48.35
199	159.6	721.0	109	17.52	40.83	49.57
200	174.7	723.5	109	18.07	42.11	51.12
201	189.1	725.5	109	18.81	43.82	53.20
202	205.7	727.5	109	19.34	45.06	54.70

0000390029

RUN NO. 4

PROCEDURAL NOTES AND OBSERVATIONS

Run 4A:

- (1) Crystal cleaned in 1×10^{-6} torr O_2 @ $910-950^\circ C$ for 2 hours.
- (2) Oxygen pumped out for 25 minutes.
- (3) Crystal pretreated in 705 torr H_2 @ $74^\circ C$ for 68.0 minutes.
- (4) Prior to introduction of CP/ H_2 mixture, $T_c = 74^\circ C$. Following introduction of reactant mixture, $T_c = 81^\circ C$.

Run 4B: Exact same procedure used as in Run 4A, except:

- (1) Crystal cleaned @ $924-968^\circ C$.
- (2) Oxygen pumped out for 27 minutes.
- (3) Crystal pretreated in 765 torr H_2 @ $74-79^\circ C$ for 68.0 minutes.
- (4) Crystal temperature before reaction, $T_c = 79^\circ C$. Following introduction of CP/ H_2 mixture, $T_c = 88^\circ C$.

RUN NO. 4A G.C. OPERATING CONDITIONS AND CHROMATOGRAPHIC PEAK DATA

Filament Current: 230 ma Hydrogen Regulator Pressure: 40 psig
 Detector Temperature: 116°C Column A Flow Rate (% Max): 43
 Column Temperature: 35°C Column B Flow Rate (% Max): 18
 Room Temperature: 23.4°C Injection Time: 10.0 sec
 Initial Mixture Composition: 135 torr Cyclopropane; 668 torr H₂

Chromat. Number	Elapsed Rxn. Time (min)	Reactor Pressure (torr)	Crystal Temp (°C)	Propane Peak Area (mv·sec)	Moles C ₃ H ₈ in V _{SL} × 10 ⁸	Total Moles C ₃ H ₈ per cm ² Pt × 10 ⁵
224	6.6	814.0	81	0.24	0.57	0.69
225	11.9	816.5	81	0.37	0.86	1.04
226	17.3	819.0	81	0.54	1.25	1.52
227	23.0	821.0	81	0.63	1.46	1.77
228	29.2	823.0	81	0.78	1.81	2.20
229	40.9	825.0	81	1.00	2.33	2.83
230	53.9	827.0	81	1.22	2.83	3.44
231	68.3	829.0	81	1.40	3.26	3.96
232	83.5	830.5	81	1.52	3.55	4.31
233	98.4	832.5	81	1.60	3.72	4.52
234	112.4	834.5	81	1.73	4.04	4.90
235	133.0	836.0	81	1.91	4.44	5.39
236	153.9	838.0	81	2.04	4.76	5.78
237	175.0	839.0	81	2.21	5.16	6.26
238	195.6	841.0	81	2.34	5.45	6.62

0000390030

RUN NO. 4B G.C. OPERATING CONDITIONS AND CHROMATOGRAPHIC PEAK DATA

Filament Current: 230 ma
 Detector Temperature: 115°C
 Column Temperature: 35°C
 Room Temperature: 22.0°C
 Initial Mixture Composition: 135 torr Cyclopropane; 668 torr H₂

Hydrogen Regulator Pressure: 40 psig
 Column A Flow Rate (% Max): 45
 Column B Flow Rate (% Max): 19
 Injection Time: 10.0 sec

Chromat. Number	Elapsed Rxn. Time (min)	Reactor Pressure (torr)	Crystal Temp (°C)	Propane Peak Area (mv·sec)	Moles C ₃ H ₈ in V _{SL} × 10 ⁸	Total Moles C ₃ H ₈ per cm ² Pt × 10 ⁵
241	8.2	808.5	88	0.46	1.08	1.31
242	13.7	810.0	88	0.81	1.89	2.29
243	19.5	812.0	88	1.33	3.11	3.78
244	25.1	814.0	88	1.83	4.26	5.17
245	31.0	815.5	88	2.32	5.39	6.54
246	36.5	817.5	88	2.62	6.11	7.42
247	42.4	819.0	88	2.99	6.96	8.45
248	48.5	821.0	88	3.30	7.69	9.34
249	63.2	822.5	88	3.98	9.27	11.25
250	76.1	824.0	88	4.45	10.37	12.59
251	92.1	825.5	87	4.95	11.53	14.00
252	107.3	827.0	87	5.23	12.19	14.80
253	122.9	829.0	87	5.61	13.07	15.87
254	137.7	830.5	87	5.92	13.78	16.73
255	152.8	832.5	87	6.19	14.43	17.52
256	168.3	834.5	88	6.41	14.93	18.12
257	182.4	936.5	88	6.59	15.35	18.63

N-HEPTANE/HYDROGEN REACTION

- (1) Columns: 10'x1/8" s.s. filled with 10% tetracyanoethylated pentaerythritol (TCEPE) on 60/80 mesh Chrom. W.
- (2) Filament current: 230 ma
Detector temperature: 115°C
Column temperature: 62°C (Toluene peak elution at 2.4 minutes)
Room temperature: 22.4°C
Hydrogen regulator pressure: 32.5 psig
Column A flow rate: 69% max
Column B flow rate: 66% max
Injection time: 10.0 sec
- (3) Initial mixture composition: 7.9 torr n-heptane
79.0 torr hydrogen
713.0 torr nitrogen

Reactant purity: n-heptane, MCB "Spectroquality" reagent 99+ % purity (0.03% maximum water content)
- (4) No measurable toluene formed at any time during the 140-minute experimental run. It should be noted that the width of the n-heptane peak was obscured by the elution of the very large nitrogen peak. Nitrogen was used as an inert gas to enable the reaction to be carried out at 800 torr total pressure.

RUN NO. 7B

PROCEDURAL NOTES AND OBSERVATIONS

NEOPENTANE/HYDROGEN REACTION

- (1) Column A: 14'x1/4" s.s. filled with 20% dimethylsulfolane on 60/80 Chrom. W.
Column B: 10'x1/4" s.s. filled with 20% dimethylsulfolane on 45/60 Chrom. W.
- (2) Filament current: 230 ma
Detector temperature: 117°C
Column temperature: 35°C
Room temperature: 22.6°C
Hydrogen regulator pressure: 33 psig
Column A flow rate: 62% max) Approx. 35 ml/minute
Column B flow rate: 56% max)
Injection time: 10.0 sec
- (3) Initial Mixture Composition: 135.0 torr neopentane
668.0 torr hydrogen
- (4) No observable products measured during 60 minutes of elapsed reaction time. Spot weld to crystal breaks and run terminated at 80 minutes of elapsed reaction time.

00003900032

RUN NO. 8A

PROCEDURAL NOTES AND OBSERVATIONS

___ Initial Mixture Composition: 135 torr cyclopropane; 664 torr H₂

___ Crystal Temperature: 82°C

- (1) First amount of propane observed at 11.4 minutes.
- (2) Propylene and propane peaks about equal at about 90 minutes.
- (3) Approximately 75% of the propylene impurity reacted at 163 minutes.
- (4) Approximately 90% of the propylene reacted at 190 minutes.

RUN NO. 8B G.C. OPERATING CONDITIONS AND CHROMATOGRAPHIC PEAK DATA

Filament Current: 230 ma
 Detector Temperature: 118°C
 Column Temperature: 37°C
 Room Temperature: 24.0°C
 Initial Mixture Composition: 135.0 torr Propylene; 668.0 torr H₂

Hydrogen Regulator Pressure: 40 psig
 Column A Flow Rate (% Max): 38
 Column B Flow Rate (% Max): 18
 Injection Time: 10.0 sec

Chromat. Number	Elapsed Rxn. Time (min)	Reactor Pressure (torr)	Crystal Temp (°C)	Propane Peak Area (mv·sec)	Moles C ₃ H ₈ in V _{SL} ×10 ⁸	Total Moles C ₃ H ₈ per cm ² Pt × 10 ⁵
361	2.7	810.0	78.6	1.59	0.80	0.97
362	7.9	809.0	83.8	2.65	2.22	2.70
363	13.8	810.5	82.4	3.57	3.46	4.20
364	19.3	811.5	82.9	4.45	4.65	5.65
365	25.4	813.0	82.9	5.28	5.77	7.00
366	32.7	814.5	82.9	6.23	7.05	8.56
367	44.1	816.0	82.4	7.73	9.07	11.01
368	55.0	817.0	82.4	9.10	10.91	13.24
369	69.8	818.0	82.2	10.63	12.96	15.73
370	87.0	819.0	82.2	12.46	15.44	18.74
371	101.5	820.0	82.2	13.91	17.39	21.11
372	118.4	821.0	82.2	15.52	19.56	23.75
373	134.9	822.0	82.2	17.22	21.84	26.51
374	153.6	823.0	82.2	18.89	24.09	29.25

00003900333

APPENDIX G

Experimental Procedure for a Standard Run During
the Cyclopropane Hydrogenolysis on the
Pt(s)-[6(111)×(100)] Single Crystal

In what will be termed a "standard run", the platinum crystal is first pretreated in 1×10^{-6} torr oxygen at 900-925°C for 120 minutes with the reactor cup open. The oxygen is then pumped out of the ultra-high vacuum system for an additional 60 minutes, reducing the pressure to approximately 5×10^{-9} torr while maintaining the crystal at 900-925°C. After 180 minutes have elapsed, the current supplied to the crystal is shut off and the crystal allowed to cool rapidly. When the crystal temperature reaches 300°C (approximately 1.6 minutes later), the reactor cup is closed onto the gold O-ring embedded in the reactor flange wall. Immediately thereafter the reactor Hoke valves are opened, and hydrogen stored in the G.C. loop (V_{GC}) is expanded into the reactor cup, bringing the system pressure to approximately 200 torr. The time elapsed from the point where the crystal is at 300°C and 5×10^{-9} torr, to 200 torr hydrogen and approximately room temperature, is on the order of 30 seconds. The reactor cup is then filled to 780 torr with additional hydrogen from the gas manifold. The reactor valves are closed and the crystal heated to 75°C for a period of 120 minutes. †

During the stagnant hydrogen pretreatment period a mixture of hydrogen and cyclopropane is prepared in the G.C. loop, such that when expanded into the total system volume ($V_{GC} + V_R$), the initial partial pressure of hydrogen and cyclopropane will be 675 torr and 135 torr, respectively. After stirring the mixture for at least

† An analysis of the hydrogen pretreatment conditions is presented in Appendix H.

10 minutes with the MB-10 bellows pump, two "pre-reaction" chromatograms are taken to check the initial purity of the hydrocarbon reactant.

Just prior to the end of the hydrogen pretreatment, the crystal temperature is reduced to approximately 69°C. This will offset the 6°C rise in the crystal temperature when the reactor valves are opened, due to the decrease in the thermal conductivity of the gas mixture surrounding the crystal.

At the conclusion of the 120 minute hydrogen pretreatment period with the MB-10 bellows pump on, the reactor valves are opened and the reactor bypass valve closed, thereby routing the flow directly through the reactor cup. Several minutes are allowed to elapse before the first chromatogram is taken. Thereafter the system is sampled approximately every 5-6 minutes during the initial reaction period. During the latter portion of a run, a 30 minute sampling interval is sufficient for analysis. When the elapsed reaction time exceeds 200 minutes, the run is arbitrarily ended, although there is usually measurable catalytic activity remaining.

APPENDIX H

Analysis of Hydrogen Pretreatment

The solubility and diffusion of hydrogen in bulk platinum has been reported by Ebisuzaki et al.³⁷ At 1 atm total pressure, the permeability, diffusivity, and solubility are, respectively,

$$(1) \quad P = (7.6 \pm 3.0) \times 10^{-7} * \exp \left(\frac{-16.9 \pm 0.5 \text{ kcal}}{RT} \right) \frac{\text{gm-atom}}{\text{cm} \cdot \text{sec}}$$

$$(2) \quad D = (6.0 \pm 3.5) \times 10^{-3} * \exp \left(\frac{-5.9 \pm 1.0 \text{ kcal}}{RT} \right) \frac{\text{cm}^2}{\text{sec}}$$

and

$$(3) \quad S = \frac{Pv}{D}$$

where v = molal volume of platinum = 9.15 cm^3 . Substituting (1) and

(2) into (3) gives

$$(4) \quad S = 1.2 \times 10^{-3} * \exp \left(\frac{-11.0 \text{ kcal}}{RT} \right) \frac{\text{gm-atom H}}{\text{gm-atom Pt}}$$

The hydrogen pretreatment conditions for nearly all the cyclopropane hydrogenolysis runs on the Pt(s)-[6(111)×(100)] single crystal were identical, namely 75°C and 780 torr H₂. For these values of temperature and pressure the average diffusivity is

$$D = 6.0 \cdot 10^{-3} * \exp \left(\frac{-5.9 \times 10^3 \text{ kcal}}{1.987 \frac{\text{cal}}{\text{mole} \cdot \text{K}} \cdot 348 \text{K}} \right)$$

$D_{75^\circ\text{C}} = 11.8 \times 10^{-7} \text{ cm}^2/\text{sec}$
--

As outlined in Appendix B, the thickness of the Pt(s)-[6(111)×(100)] single crystal was 0.50 mm. One time constant for the diffusion of H₂ into the bulk metal can be calculated from:

$$\tau = \frac{Dt}{L^2} = 1$$

$$t_{\tau} = \frac{L^2}{D} = \frac{\left[\frac{1}{2} (0.50 \text{ mm})\right]^2}{11.8 \times 10^{-7} \frac{\text{cm}^2}{\text{sec}}} = \frac{(2.5 \times 10^{-2} \text{ cm})^2}{11.8 \times 10^{-7} \frac{\text{cm}^2}{\text{sec}}}$$

$$t_{\tau} = 530 \text{ sec} \approx 9 \text{ minutes}$$

or

$$5t_{\tau} \approx 45 \text{ minutes}$$

Thus it would take approximately 45 minutes for the center of the bulk platinum crystal to attain 99% of its maximum hydrogen concentration. Since the pretreatment was extended for a total of 120 minutes at 75°C, it has been assumed that the platinum crystal is saturated with H atoms at the conclusion of the pretreatment period.

An interesting question arises as to the relative importance of the hydrogen atoms in the bulk platinum versus the surface concentration of hydrogen species. From Eq. (4),

$$S = \text{atom fraction} \left(\frac{H}{Pt} \right) = 1.2 \times 10^{-3} * \exp \left(\frac{-11.0 \times 10^3 \text{ cal}}{RT} \right)$$

At 75°C,

$$S = 1.2 \times 10^{-3} * \exp \left(\frac{-11.0 \times 10^3 \text{ cal}}{1.987 \frac{\text{cal}}{\text{mole}^\circ\text{K}} * 348^\circ\text{K}} \right)$$

$$S_{75^\circ\text{C}} = \frac{M_{\text{H}}}{M_{\text{Pt}}} = 1.46 \cdot 10^{-10} \frac{\text{atoms H}}{\text{atom Pt}}$$

The number of platinum atoms in the crystal can be calculated from

$$M_{\text{Pt}} = \frac{A_c t \rho_{\text{Pt}} N_o}{M_{\text{Pt}}}$$

where,

$$\begin{aligned} A_c &= \text{total elliptical surface area of the Pt crystal} \\ &= 0.66 \text{ cm}^2 \end{aligned}$$

$$t = \text{crystal thickness} = 0.50 \text{ mm}$$

$$\rho_{\text{Pt}} = \text{platinum density} = 21 \text{ gms/cm}^3$$

$$M_{\text{Pt}} = \frac{(0.66 \text{ cm}^2)(5 \times 10^{-2} \text{ cm})(21 \frac{\text{gm}}{\text{cm}^3})(6.02 \times 10^{23} \frac{\text{g} \cdot \text{atoms}}{\text{g} \cdot \text{mole}})}{195 \frac{\text{gms}}{\text{g} \cdot \text{mole}}}$$

$$M_{\text{Pt}} = 2.14 \times 10^{21} \text{ atoms Pt} \cdot$$

Then,

$$\begin{aligned} M_{\text{H}} &= M_{\text{Pt}} * S \\ &= (2.14 \times 10^{21} \text{ atoms Pt})(1.46 \times 10^{-10} \frac{\text{atoms H}}{\text{atom Pt}}) \end{aligned}$$

$$M_{\text{H}} = 3.12 \times 10^{11} \text{ atoms H} \cdot$$

or an equivalent of 1.56×10^{11} molecules of H_2 . Suppose that no other hydrogen was available for the cyclopropane hydrogenolysis reaction other than the amount contained in the platinum crystal as a result of pretreatment. For this hypothetical case, a maximum of 1.56×10^{11} molecules, or 2.6×10^{-13} moles, of propane could be formed. However, this amount could not be measured using a thermal conductivity detector. The minimum sensitivity of the t.c.d. used in the present study for propane is approximately 2×10^{-9} moles, or four orders of magnitude higher than this hypothetical propane value.

It is apparent from the above computation that we are indeed measuring true catalytic reaction rates. The hydrogen reacting on the surface with adsorbed cyclopropane must originate from the gas phase and not from the bulk platinum. The surface concentration of hydrogen species, and not the bulk concentration, is therefore the more important quantity. Because hydrogen pretreatment is necessary for achieving relatively high rates of reaction on platinum for hydrogenolysis and hydrogenation processes, it follows that the main function of the metal surface in this regard is to provide a source of highly mobile, dissociated hydrogen molecules.

APPENDIX I

EXPERIMENTAL DATA FOR THE CYCLOPROPANE HYDROGENOLYSIS
ON THE Pt(s)-[6(111)×(100)] SINGLE CRYSTAL

RUN NO. 9A

PROCEDURAL NOTES AND OBSERVATIONS

Initial Mixture Composition: 135.0 torr cyclopropane; 675.0 torr H₂

Crystal Temperature (T_c): 75°C

- (1) First amount of propane formed at 56.1 minutes.
- (2) First definitive propane peak measured at 170.6 minutes.
- (3) After 190 minutes of elapsed time, no reactivity of cyclopropane was detected. Propane which was formed could be attributed completely to the reaction of the 0.22% propylene impurity (approximately 45% conversion).

RUN NO. 9B G.C. OPERATING CONDITIONS AND CHROMATOGRAPHIC PEAK DATA

Filament Current: 230 ma
 Detector Temperature: 117°C
 Column Temperature: 35°C
 Room Temperature: 23.2°C
 Initial Mixture Composition: 134 torr Propylene; 676 torr H₂

Hydrogen Regulator Pressure: 40 psig
 Column A Flow Rate (% Max): 39
 Column B Flow Rate (% Max): 18
 Injection Time: 10.0 sec

Chromat. Number	Elapsed Rxn. Time (min)	Reactor Pressure (torr)	Crystal Temp (°C)	Propane Peak Area (mv·sec)	Moles C ₃ H ₈ in V _{SL} ×10 ⁸	Total Moles C ₃ H ₈ per cm ² Pt × 10 ⁵
464	4.1	821.0	73.6	1.81	1.74	2.23
465	8.9	823.0	74.0	2.61	3.65	4.68
466	13.6	824.5	74.0	3.38	5.52	7.07
467	18.2	826.0	74.0	4.07	7.17	9.18
468	24.5	827.5	73.7	5.01	9.43	12.08
469	31.5	829.0	73.9	5.92	11.60	14.86
470	40.8	830.5	73.7	7.15	14.56	18.65
471	51.8	831.5	73.9	8.53	17.87	22.89
472	64.7	832.5	74.1	9.87	21.10	27.03
473	79.2	834.0	74.1	11.57	25.16	32.23
474	98.3	835.0	74.1	13.46	29.71	38.06
475	116.6	835.5	74.0	15.26	34.02	43.58
476	135.6	836.5	74.0	17.03	38.28	49.04
477	155.9	837.5	74.0	18.99	42.98	55.06
478	176.3	839.0	74.0	20.24	45.97	58.89
479	198.3	840.0	74.1	22.03	50.28	64.41

RUN NO. 10A G.C. OPERATING CONDITIONS AND CHROMATOGRAPHIC PEAK DATA

Filament Current: 230 ma Hydrogen Regulator Pressure: 40 psig
 Detector Temperature: 119°C Column A Flow Rate (% Max): 44
 Column Temperature: 35°C Column B Flow Rate (% Max): 18
 Room Temperature: 22.3°C Injection Time: 10.0 sec
 Initial Mixture Composition: 135.0 torr CP; 675.0 torr H₂

Chromat. Number	Elapsed Rxn. Time (min)	Reactor Pressure (torr)	Crystal Temp (°C)	Propane Peak Area (mv·sec)	Moles C ₃ H ₈ in V _{SL} × 10 ⁸	Total Moles C ₃ H ₈ per cm ² Pt × 10 ⁵
482	3.45	820.0	74.8	0.556	0.61	0.78
483	9.06	822.0	73.9	1.061	1.28	1.64
484	15.04	823.5	73.6	1.576	2.27	2.91
485	20.61	825.5	73.5	1.953	3.15	4.04
486	26.61	827.0	73.5	2.351	4.08	5.23
487	35.12	829.0	73.5	2.693	4.87	6.24
488	45.20	831.0	75.5	3.055	5.72	7.33
489	58.61	832.5	75.5	3.386	6.49	8.31
490	73.84	834.5	75.5	3.672	7.16	9.17
491	92.84	836.5	75.6	3.907	7.70	9.86
492	112.25	838.0	75.6	4.106	8.17	10.47
493	131.33	840.0	75.2	4.310	8.64	11.07
494	153.61	841.5	74.9	4.447	8.96	11.48
495	175.33	843.0	74.9	4.544	9.19	11.77
496	195.34	845.0	74.9	4.667	9.47	12.13

0.000390330

RUN NO. 12A G.C. OPERATING CONDITIONS AND CHROMATOGRAPHIC PEAK DATA

Filament Current: 230 ma
 Detector Temperature: 116°C
 Column Temperature: 34°C
 Room Temperature: 22.0°C
 Initial Mixture Composition: 135.0 torr CP; 675.0 torr H₂

Hydrogen Regulator Pressure: 40 psig
 Column A Flow Rate (% Max): 42
 Column B Flow Rate (% Max): 19
 Injection Time: 10.0 sec

Chromat. Number	Elapsed Rxn. Time (min)	Reactor Pressure (torr)	Crystal Temp (°C)	Propane Peak Area (mv·sec)	Moles C ₃ H ₈ in V _{SL} × 10 ⁸	Total Moles C ₃ H ₈ per cm ² Pt × 10 ⁵
524	3.74	820.0	75.3	0.318		
525	9.28	822.0	74.6	0.444		
526	15.02	824.0	74.3	0.525	0.01	0.01
527	20.76	825.5	74.3	0.796	0.64	0.82
528	27.39	827.5	74.5	1.260	1.73	2.22
529	37.98	829.0	74.5	1.877	3.16	4.05
530	50.51	831.0	74.5	2.468	4.54	5.82
531	66.25	832.5	77.7	2.984	5.74	7.35
532	82.33	834.0	77.7	3.376	6.66	8.53
533	103.84	836.0	78.4	3.723	7.47	9.57
534	125.25	838.0	78.1	3.988	8.08	10.35
535	144.77	840.0	78.4	4.223	8.63	11.06
536	165.67	841.5	77.8	4.417	9.08	11.63
537	185.92	843.5	77.8	4.559	9.41	12.05
538	201.34	845.0	78.0	4.672	9.67	12.39

RUN NO. 12B

PROCEDURAL NOTES AND OBSERVATIONS

After 208.4 minutes of Run 12A had elapsed, the crystal heating supply and the MB-10 bellows pump were turned off. The total reactor volume ($V_R + V_{GC}$) was flushed ten times with 1200 torr portions of hydrogen to remove cyclopropane and propane, and then filled to 800 torr with hydrogen. The crystal remained in a stagnant hydrogen environment at 25°C overnight (14 hours).

Following this period, the reactor was flushed with several 1200 torr portions of hydrogen and then filled to 780 torr, whereupon the standard procedure for hydrogen pretreatment was commenced (120 minutes at 75°C). The same partial pressures of cyclopropane and hydrogen as in Run 12A were mixed in the G.C. loop. At the 120-minute mark, the reactor valves were opened to begin Run 12B.

00003900000

RUN NO. 12B G.C. OPERATING CONDITIONS AND CHROMATOGRAPHIC PEAK DATA

Filament Current: 230 ma
 Detector Temperature: 116°C
 Column Temperature: 33°C
 Room Temperature: 22.2°C
 Initial Mixture Composition: 135.0 torr CP; 675.0 torr H₂

Hydrogen Regulator Pressure: 40 psig
 Column A Flow Rate (% Max): 41
 Column B Flow Rate (% Max): 18
 Injection Time: 10.0 sec

Chromat. Number	Elapsed Rxn. Time (min)	Reactor Pressure (torr)	Crystal Temp (°C)	Propane Peak Area (mv·sec)	Moles C ₃ H ₈ in V _{SL} × 10 ⁸	Total Moles C ₃ H ₈ per cm ² Pt × 10 ⁵
541	211.8	837.0	77.7	0.054	0.126	0.16
542	217.6	839.0	77.7	0.194	0.452	0.58
543	223.8	841.5	77.8	0.345	0.804	1.03
544	230.0	843.5	77.2	0.391	0.911	1.17
545	239.9	846.0	77.2	0.420	0.979	1.25
546	255.6	848.5	77.0	0.438	1.021	1.31
547	278.8	851.0	77.5	0.400	0.932	1.19
548	298.9	853.5	77.5	0.502	1.170	1.50
549	371.0	856.5	77.8	0.938	2.186	2.80
550	388.6	858.5	77.8	0.989	2.304	2.95

RUN NO. 13

PROCEDURAL NOTES AND OBSERVATIONS

The pretreatment procedure used in Run 13 will be described here, as it deviates substantially from the steps outlined in Appendix G.

The platinum crystal was first oxygen treated in the standard way (120 minutes at 900-925°C in 1×10^{-6} torr O_2). At the 120-minute mark, the leak valve was closed, the gate valve opened, and the oxygen pumped out of the UHV system. Meanwhile, a 543 torr CP/357 torr H_2 mixture was prepared in the G.C. loop, while the leak valve was filled to 6 psig (1070 torr) with H_2 . At the 185-minute mark, the crystal heating supply was turned off and the crystal allowed to cool. At a crystal temperature of 200°C, the reactor cup was closed, whereupon the leak valve was immediately opened, bringing the reactor cup pressure to approximately 50 torr H_2 . The crystal temperature was then increased to 69°C over a period of 40 sec. After maintaining the crystal at 69°C in 50 torr H_2 for an additional 70 seconds, the leak valve was closed, the reactor valves opened (expanding the CP/ H_2 mixture into the reactor cup), and additional hydrogen admitted into the reactor system ($V_{GC} + V_R$) to bring the total system pressure to 810 torr. The MB-10 bellows pump was immediately started and the reactor bypass valve closed. A total of 30 seconds then elapsed from the time the reactor valves were opened to the closure of the reactor by-pass valve.

RUN NO. 13 G.C. OPERATING CONDITIONS AND CHROMATOGRAPHIC PEAK DATA

Filament Current: 230 ma
 Detector Temperature: 117°C
 Column Temperature: 35°C
 Room Temperature: 23.7°C
 Initial Mixture Composition: 135.0 torr CP; 675 torr H₂

Hydrogen Regulator Pressure: 40 psig
 Column A Flow Rate (% Max): 39
 Column B Flow Rate (% Max): 18
 Injection Time: 10.0 sec

Chromat. Number	Elapsed Rxn. Time (min)	Reactor Pressure (torr)	Crystal Temp (°C)	Propane Peak Area (mv·sec)	Moles C ₃ H ₈ in V _{SL} × 10 ⁸	Total Moles C ₃ H ₈ per cm ² Pt × 10 ⁵
553	4.7	809.0	75.2	0.366		
554	10.0	810.5	73.9	0.513		
555	16.3	812.0	72.0	0.571	0.29	0.37
556	23.9	814.0	72.5	0.632	0.43	0.55
557	32.0	816.0	72.7	0.694	0.58	0.74
558	42.6	818.0	72.7	0.959	1.19	1.52
559	59.7	819.0	73.0	1.846	3.26	4.18
560	75.8	821.0	73.9	2.299	4.48	5.74
561	92.0	-	73.3	2.851	5.41	6.93
562	108.9	823.5	73.5	2.880	5.88	7.53
563	127.2	825.0	70.5	3.249	6.31	8.08
564	146.6	826.5	70.7	3.211	6.68	8.56
565	167.9	828.0	70.5	3.465	7.03	9.01
566	187.3	830.0	69.5	3.549	7.23	9.26
567	202.6	832.0	69.8	3.733	7.40	9.48

RUN NO. 14

PROCEDURAL NOTES AND OBSERVATIONS

Just prior to opening the reactor valves, the crystal temperature was reduced to approximately 35°C (10.0 amps). Three data points, each 5-6 minutes apart, were taken at this temperature. Immediately after injecting the third G.C. sample the crystal current was increased to 14.0 amps. After three data points at approximately 55°C, the temperature was reduced to the base level (35°C).

The above procedure was repeated at successively higher temperatures until a maximum crystal temperature of 125°C was attained. Thereafter the crystal temperature was progressively decreased until at 75°C, the 200-minute mark had elapsed and the run terminated.

00005900041

RUN NO. 14 G.C. OPERATING CONDITIONS AND CHROMATOGRAPHIC PEAK DATA

Filament Current: 230 ma Hydrogen Regulator Pressure: 40 psig
 Detector Temperature: 118°C Column A Flow Rate (% Max): 38
 Column Temperature: 35°C Column B Flow Rate (% Max): 18
 Room Temperature: 22.7°C Injection Time: 10.0 sec
 Initial Mixture Composition: 135.0 torr CP; 675.0 torr H₂

Chromat. Number	Elapsed Rxn. Time (min)	Reactor Pressure (torr)	Crystal Temp (°C)	Propane Peak Area (mv·sec)	Moles C ₃ H ₈ in V _{SL} × 10 ⁸	Total Moles C ₃ H ₈ per cm ² Pt × 10 ⁵
570	3.08	815.0	38.7	0.117	0.273	0.35
571	8.40	816.5	38.3	0.209	0.487	0.62
572	13.82	818.0	38.0	0.297	0.692	0.89
573	19.20	822.0	57.4	0.313	0.730	0.94
574	24.67	824.0	57.4	0.378	0.881	1.13
575	30.33	825.5	56.3	0.399	0.930	1.19
576	35.86	825.0	37.2	0.459	1.07	1.37
577	41.57	826.5	37.3	0.405	0.944	1.21
578	47.84	828.0	37.3	0.421	0.981	1.26
579	53.39	834.5	74.5	0.481	1.12	1.43
580	58.87	837.0	74.6	0.612	1.43	1.83
581	64.81	839.1	74.2	0.933	2.17	2.78
582	71.67	836.0	36.5	0.989	2.31	2.96
583	77.85	837.5	36.0	0.969	2.26	2.90
584	83.98	839.0	35.3	1.100	2.35	3.01
585	89.37	848.5	90.6	1.285	2.99	3.83
586	95.10	851.0	90.5	1.525	3.55	4.55
587	100.66	853.5	90.4	1.770	4.12	5.28
588	106.36	848.0	35.2	1.728	4.03	5.16
589	111.77	850.0	35.2	1.728	4.03	5.16

RUN NO. 14 G.C. OPERATING CONDITIONS AND CHROMATOGRAPHIC PEAK DATA

Filament Current: Hydrogen Regulator Pressure:
 Detector Temperature: Column A Flow Rate (% Max):
 Column Temperature: Ibid. Column B Flow Rate (% Max): Ibid.
 Room Temperature: Injection Time:
 Initial Mixture Composition:

Chromat. Number	Elapsed Rxn. Time (min)	Reactor Pressure (torr)	Crystal Temp (°C)	Propane Peak Area (mv·sec)	Moles C ₃ H ₈ in V _{SL} × 10 ⁸	Total Moles C ₃ H ₈ per cm ² Pt × 10 ⁵
590	117.81	851.5	35.0	1.703	3.97	5.08
591	123.36	863.0	122.8	1.906	4.44	5.68
592	128.87	866.0	122.8	2.089	4.87	6.24
593	134.40	868.5	123.1	2.272	5.29	6.77
594	139.84	860.0	36.2	2.267	5.28	6.76
595	145.71	861.5	35.8	2.247	5.24	6.70
596	151.14	863.0	35.7	2.242	5.22	6.69
597	156.58	872.0	95.7	2.333	5.44	6.96
598	162.00	874.5	95.7	2.371	5.52	7.07
599	167.50	876.5	95.7	2.434	5.67	7.26
600	172.98	871.0	35.2	2.495	5.81	7.45
601	178.57	872.5	34.8	2.443	5.69	7.29
602	184.18	878.5	72.7	2.462	5.74	7.35
603	194.59	881.0	72.1	2.520	5.87	7.52
604	204.47	883.0	73.6	2.563	5.97	7.65

00003900342

RUN NO. 15 G.C. OPERATING CONDITIONS AND CHROMATOGRAPHIC PEAK DATA

Filament Current: 230 ma
 Detector Temperature: 117°C
 Column Temperature: 35°C
 Room Temperature: 22.7°C
 Initial Mixture Composition: 135.0 torr CP; 675.0 torr H₂

Hydrogen Regulator Pressure: 40 psig
 Column A Flow Rate (% Max): 38
 Column B Flow Rate (% Max): 19
 Injection Time: 10.0 sec

Chromat. Number	Elapsed Rxn. Time (min)	Reactor Pressure (torr)	Crystal Temp (°C)	Propane Peak Area (mv·sec)	Moles C ₃ H ₈ in V _{SL} × 10 ⁸	Total Moles C ₃ H ₈ per cm ² Pt × 10 ⁵
607	3.13	819.5	100.6	0.93	1.39	1.78
608	8.00	821.0	100.6	2.07	3.70	4.74
609	13.00	823.0	100.6	3.14	6.19	7.93
610	18.05	824.5	99.3	4.10	8.43	10.80
611	23.44	826.0	99.3	4.86	10.20	13.07
612	29.06	828.0	98.8	5.28	11.18	14.32
613	34.67	829.5	98.8	5.89	12.61	16.15
614	46.80	831.0	92.8	6.67	14.43	18.48
615	62.10	833.5	93.2	7.32	15.95	20.43
616	81.20	836.0	93.6	7.97	17.45	22.35
617	102.18	838.0	93.8	8.29	18.21	23.33
618	123.36	840.0	95.0	8.66	19.06	24.42
619	144.18	842.0	94.7	8.83	19.46	24.93
620	166.00	845.0	96.2	9.16	20.22	25.90
621	186.91	847.5	97.0	9.33	20.62	26.41
622	207.02	850.0	97.1	9.56	21.16	27.11

RUN NO. 16 G.C. OPERATING CONDITIONS AND CHROMATOGRAPHIC PEAK DATA

Filament Current: 230 ma Hydrogen Regulator Pressure: 40 psig
 Detector Temperature: 118°C Column A Flow Rate (% Max): 38
 Column Temperature: 35°C Column B Flow Rate (% Max): 18
 Room Temperature: 21.5°C Injection Time: 10.0 sec
 Initial Mixture Composition: 135.0 torr CP; 675.0 torr H₂

Chromat. Number	Elapsed Rxn. Time (min)	Reactor Pressure (torr)	Crystal Temp (°C)	Propane Peak Area (mv·sec)	Moles C ₃ H ₈ in V _{SL} × 10 ⁸	Total Moles C ₃ H ₈ per cm ² Pt × 10 ⁵
625	3.29	825.0	132.1	3.37	6.99	8.85
626	8.31	826.0	132.4	7.55	16.54	21.19
627	13.88	827.0	132.1	11.28	25.24	32.33
628	19.93	828.0	131.2	14.20	32.08	41.09
629	25.66	829.0	130.8	15.85	35.88	45.96
630	38.21	831.0	130.9	17.95	40.78	52.24
631	53.27	833.0	130.9	18.97	43.15	55.28
632	73.81	835.0	131.5	19.99	45.53	58.32
633	93.89	837.5	131.9	20.60	46.96	60.16
634	114.81	840.0	132.1	21.26	48.48	62.10
635	134.48	843.0	133.2	21.75	49.62	63.56
636	156.32	845.0	133.5	22.11	50.47	64.65
637	178.42	847.0	133.8	22.36	51.05	65.40
638	200.04	849.0	133.8	22.68	51.81	66.37

00003908043

RUN NO. 17 G.C. OPERATING CONDITIONS AND CHROMATOGRAPHIC PEAK DATA

Filament Current: 230 ma
 Detector Temperature: 117°C
 Column Temperature: 35°C
 Room Temperature: 23.2°C
 Initial Mixture Composition: 200.0 torr CP; 675.0 torr H₂

Hydrogen Regulator Pressure: 40 psig
 Column A Flow Rate (% Max): 39
 Column B Flow Rate (% Max): 18
 Injection Time: 10.0 sec

Chromat. Number	Elapsed Rxn. Time (min)	Reactor Pressure (torr)	Crystal Temp (°C)	Propane Peak Area (mv·sec)	Moles C ₃ H ₈ in V _{SL} × 10 ⁸	Total Moles C ₃ H ₈ per cm ² Pt × 10 ⁵
641	3.42	887.5	79.0	0.524	0.55	0.71
642	13.76	889.5	79.0	-	-	-
643	18.70	891.0	79.0	1.479	1.97	2.52
644	24.18	893.0	78.1	2.096	3.40	4.36
645	29.70	894.5	79.0	2.683	4.77	6.11
646	36.31	896.0	-	3.300	6.21	7.96
647	42.64	898.0	77.8	3.856	7.50	9.61
648	51.82	899.5	77.8	4.549	9.12	11.68
649	73.54	900.5	78.3	5.732	11.88	15.22
650	83.87	902.0	78.6	6.120	12.78	16.37
651	93.94	903.5	78.6	6.528	13.73	17.59
652	110.08	905.5	79.1	6.926	14.66	18.78
653	130.82	906.5	79.3	7.405	15.77	20.20
654	151.82	907.5	79.3	7.742	16.56	21.21
655	172.58	909.0	78.6	8.078	17.34	22.21
656	192.38	910.5	78.6	8.354	17.98	23.03
657	209.65	911.5	78.3	8.507	18.34	23.49

APPENDIX J

SUMMARY OF CALCULATIONS FOR OBTAINING
DIMENSIONLESS DATA PLOTS IN FIGURE III-10

EXPERIMENTAL RUN NUMBER 10A

Chromat. Number	Crystal Temp (°C)	Net Reaction Time (min)	Corrected Moles of C ₃ H ₈ in V _{SL} × 10 ⁸	Point Rate of Reaction (moles C ₃ H ₈ /min)	R/R ₀ (α)	t/t _p @ α = 0.90 (t _p = 23.4)
482	74.8	3.4	0.61	1.532 × 10 ⁻⁹	1.000	0.15
483	73.9	9.1	1.28	1.532 × 10 ⁻⁹	1.000	0.39
484	73.6	15.0	2.27	1.532 × 10 ⁻⁹	1.000	0.64
485	73.5	20.6	3.15	1.532 × 10 ⁻⁹	1.000	0.88
486	73.5	26.6	4.08	1.210 × 10 ⁻⁹	0.790	1.14
487	73.5	35.1	4.87	9.58 × 10 ⁻¹⁰	0.625	1.50
488	75.5	45.2	5.72	7.30 × 10 ⁻¹⁰	0.476	1.93
489	75.5	58.6	6.49	5.02 × 10 ⁻¹⁰	0.328	2.50
490	75.5	73.8	7.16	3.42 × 10 ⁻¹⁰	0.223	3.15
491	75.6	92.8	7.70	2.60 × 10 ⁻¹⁰	0.1695	3.97
492	75.6	112.2	8.17	2.24 × 10 ⁻¹⁰	0.1460	4.79
493	75.2	131.3	8.64	1.870 × 10 ⁻¹⁰	0.1220	5.61
494	74.9	153.6	8.96	1.376 × 10 ⁻¹⁰	0.0897	6.56
495	74.9	175.3	9.19	1.212 × 10 ⁻¹⁰	0.0790	7.49
496	74.9	195.3	9.47	1.212 × 10 ⁻¹⁰	0.0790	8.35
Extra data point:		23.0		1.393 × 10 ⁻⁹	0.910	0.98

EXPERIMENTAL RUN NUMBER 12A

Chromat. Number	Crystal Temp (°C)	Net Reaction Time (min)	Corrected Moles of C ₃ H ₈ in V _{SL} × 10 ⁸	Point Rate of Reaction (moles C ₃ H ₈ /min)	R/R ₀ (α)	t/t _p @ α = 0.90 (t _p = 25.4)
526	74.3	0.0	0.01	1.370 × 10 ⁻⁹	1.000	0.00
527	74.3	5.7	0.64	1.370 × 10 ⁻⁹	1.000	0.22
528	74.5	12.4	1.73	1.370 × 10 ⁻⁹	1.000	0.49
529	74.5	23.0	3.16	1.370 × 10 ⁻⁹	1.000	0.91
530	74.5	35.5	4.54	9.20 × 10 ⁻¹⁰	0.671	1.40
531	77.7	51.2	5.74	6.48 × 10 ⁻¹⁰	0.473	2.02
532	77.7	67.3	6.66	4.85 × 10 ⁻¹⁰	0.354	2.65
533	78.4	88.8	7.47	3.24 × 10 ⁻¹⁰	0.236	3.50
534	78.1	110.2	8.08	2.73 × 10 ⁻¹⁰	0.199	4.34
535	78.4	129.8	8.63	2.27 × 10 ⁻¹⁰	0.166	5.11
536	77.8	150.6	9.08	1.93 × 10 ⁻¹⁰	0.141	5.93
537	77.8	170.9	9.41	1.640 × 10 ⁻¹⁰	0.120	6.73
538	78.0	186.3	9.67	1.640 × 10 ⁻¹⁰	0.120	7.77
Extra data points:						
		27.0		1.15 × 10 ⁻⁹	0.840	1.06
		30.0		1.037 × 10 ⁻⁹	0.757	1.18
		(Minus time delay of 15 min.)				

000009000000

EXPERIMENTAL RUN NUMBER 15

Chromat. Number	Crystal Temp (°C)	Net Reaction Time (min)	Corrected Moles of C ₃ H ₈ in V _{SL} × 10 ⁸	Point Rate of Reaction (moles C ₃ H ₈ /min)	R/R ₀ (α)	t/t _p @ α = 0.90 (t _p = 15.9)
607	100.6	3.1	1.39	4.67 × 10 ⁻⁹	1.000	0.20
608	100.6	8.0	3.70	4.67 × 10 ⁻⁹	1.000	0.50
609	100.6	13.0	6.19	4.67 × 10 ⁻⁹	1.000	0.82
610	99.3	18.0	8.43	3.81 × 10 ⁻⁹	0.815	1.13
611	99.3	23.4	10.20	2.84 × 10 ⁻⁹	0.608	1.47
612	98.8	29.1	11.18	2.18 × 10 ⁻⁹	0.466	1.83
613	98.8	34.7	12.61	1.78 × 10 ⁻⁹	0.381	2.18
614	92.8	46.8	14.43	1.235 × 10 ⁻⁹	0.264	2.94
615	93.2	62.1	15.95	8.35 × 10 ⁻¹⁰	0.179	3.91
616	93.6	81.2	17.45	5.77 × 10 ⁻¹⁰	0.124	5.11
617	93.8	102.2	18.21	4.09 × 10 ⁻¹⁰	0.0875	6.43
618	95.0	123.4	19.06	2.50 × 10 ⁻¹⁰	0.0535	7.76
619	94.7	144.2	19.46	2.50 × 10 ⁻¹⁰	0.0535	9.07
620	96.2	166.0	20.22	2.50 × 10 ⁻¹⁰	0.0535	10.44
621	97.0	186.9	20.62	2.50 × 10 ⁻¹⁰	0.0535	11.75
622	97.1	207.0	21.16	2.50 × 10 ⁻¹⁰	0.0535	13.02
Extra data point:		20.5		3.33 × 10 ⁻⁹	0.713	1.29

EXPERIMENTAL RUN NUMBER 16

Chromat. Number	Crystal Temp (°C)	Net Reaction Time (min)	Corrected Moles of C ₃ H ₈ in V _{SL} × 10 ⁸	Point Rate of Reaction (moles C ₃ H ₈ /min)	R/R ₀ (α)	t/t _p @ α = 0.90 (t _p = 10.5)
625	132.1	3.3	6.99	1.99 × 10 ⁻⁸	1.000	0.31
626	132.4	8.3	16.54	1.99 × 10 ⁻⁸	1.000	0.79
627	132.1	13.9	25.24	1.314 × 10 ⁻⁸	0.660	1.32
628	131.2	19.9	32.08	8.22 × 10 ⁻⁹	0.413	1.90
629	130.9	25.7	35.88	5.14 × 10 ⁻⁹	0.258	2.45
630	130.9	38.2	40.78	2.18 × 10 ⁻⁹	0.1095	3.64
631	130.9	53.3	43.15	1.38 × 10 ⁻⁹	0.0694	5.08
632	131.5	73.8	45.53	0.962 × 10 ⁻⁹	0.0484	7.03
633	131.9	93.9	46.96	0.745 × 10 ⁻⁹	0.0374	8.94
634	132.1	114.8	48.48	0.570 × 10 ⁻⁹	0.0286	10.93
635	133.2	134.5	49.62	0.478 × 10 ⁻⁹	0.0240	12.81
636	133.5	156.3	50.47	3.07 × 10 ⁻¹⁰	0.0154	14.89
637	133.8	178.4	51.05	3.07 × 10 ⁻¹⁰	0.0154	16.99
638	133.8	200.0	51.81	3.07 × 10 ⁻¹⁰	0.0154	19.05
Extra data points:						
		11.0		1.740 × 10 ⁻⁸	0.875	1.05
		16.0		1.146 × 10 ⁻⁸	0.575	1.52

00006900045

EXPERIMENTAL RUN NUMBER 17

Chromat. Number	Crystal Temp (°C)	Net Reaction Time (min)	Corrected Moles of C ₃ H ₈ in V _{SL} × 10 ⁸	Point Rate of Reaction (moles C ₃ H ₈ /min)	R/R ₀ (α)	t/t _p @ α = 0.90 (t _p = 23.0)
643	79.0	7.7	1.97	2.54 × 10 ⁻⁹	1.000	0.33
644	78.1	13.2	3.40	2.54 × 10 ⁻⁹	1.000	0.57
645	79.0	18.7	4.77	2.54 × 10 ⁻⁹	1.000	0.81
646	-	25.3	6.21	2.12 × 10 ⁻⁹	0.833	1.10
647	77.8	31.6	7.50	1.841 × 10 ⁻⁹	0.725	1.37
648	77.8	40.8	9.12	1.520 × 10 ⁻⁹	0.598	1.77
649	78.3	62.5	11.88	1.076 × 10 ⁻⁹	0.424	2.72
650	78.6	72.9	12.78	8.00 × 10 ⁻¹⁰	0.315	3.17
651	78.6	82.9	13.73	7.20 × 10 ⁻¹⁰	0.283	3.60
652	79.1	99.1	14.66	6.40 × 10 ⁻¹⁰	0.238	4.31
653	79.3	119.8	15.77	4.55 × 10 ⁻¹⁰	0.179	5.21
654	79.3	140.8	16.56	3.44 × 10 ⁻¹⁰	0.135	6.12
655	78.6	161.6	17.34	3.00 × 10 ⁻¹⁰	0.118	7.03
656	78.6	181.4	17.98	2.68 × 10 ⁻¹⁰	0.105	7.89
657	78.3	198.6	18.34	2.45 × 10 ⁻¹⁰	0.0963	8.63

(Minus time lag of 11.0 min.)

LITERATURE CITED

1. H. S. Taylor, Proc. Roy. Soc. A108, 105 (1925).
2. H. S. Taylor, J. Phys. Chem. 30, 145 (1926).
3. G. A. Somorjai and F. J. Szalkowski, J. Chem. Phys. 54, 389 (1971).
4. G. A. Somorjai and H. H. Farrell, Advan. Chem. Phys. 20, 215 (1971).
5. J. W. May, Advances in Catalysis 21, 151 (1970).
6. C. C. Chang, Surface Science 25, 53 (1971).
7. G. A. Somorjai and F. J. Szalkowski, Advan. in High. Temp. Chem. 4, 137 (1971).
8. B. Lang, R. W. Joyner, and G. A. Somorjai, Surface Science 30, 440 (1972).
9. B. Lang, R. W. Joyner, and G. A. Somorjai, Surface Science 30, 454 (1972).
10. R. W. Joyner, B. Lang, and G. A. Somorjai, J. Catalysis 27, 405 (1972).
11. K. Baron, D. W. Blakely, and G. A. Somorjai, Surface Science (to be published).
12. S. L. Bernasek, W. J. Siekhaus, and G. A. Somorjai, Phys. Rev. Letters 30, 1202 (1973).
13. G. A. Somorjai, "Principles of Surface Chemistry," Prentice-Hall, 1972.
14. J. H. Sinfelt, Catalysis Reviews 3, 175 (1969).
15. A. D. O. Cinneide and J. K. A. Clarke, Catalysis Reviews 7, 213 (1972).
16. T. E. Whyte, Jr., Catalysis Reviews 8, 117 (1973).
17. M. Boudart, Advances in Catalysis 20, 153 (1969).

18. R. Van Hardeveld and A. Van Montfoort, *Surface Science* 4, 396 (1966).
19. O. M. Poltorak and V. S. Boronin, *Russ. J. Phys. Chem.* 40, 1436 (1966).
20. O. M. Poltorak, V. S. Boronin, and A. N. Mitrofanovia, *Fourth Int'l Congr. Catal., Moscow, 1968, Preprint 68.*
21. G. C. Bond, *Fourth Int'l Congr. Catal., Moscow, 1968, Preprint 67.*
22. T. A. Dorling and R. L. Moss, *J. Catalysis* 5, 111 (1966).
23. M. Boudart, A. Aldag, J. E. Benson, N. A. Dougharty, and C. G. Harkins, *J. Catalysis* 6, 92 (1966).
24. T. A. Dorling, M. J. Eastlake, and R. L. Moss, *J. Catalysis* 14, 23 (1969).
25. J. C. Carter, J. A. Cusumano, and J. H. Sinfelt, *J. Phys. Chem.* 70, 2257 (1966).
26. D. J. C. Yates and J. H. Sinfelt, *J. Catalysis* 8, 348 (1967).
27. M. Boudart, A. W. Aldag, L. D. Ptak, and J. E. Benson, *J. Catalysis* 11, 35 (1968).
28. C. Corolleur, F. G. Gault, D. Juttard, G. Maire, and J. M. Muller, *J. Catalysis* 27, 466 (1972).
29. R. G. Oliver and P. B. Wells, *Fifth Int'l Congr. Catal., Amsterdam, 1972, Preprint 45.*
30. J. W. E. Coenen, R. Z. C. Van Meerten, and H. Th. Rijnten, *Fifth Int'l Congr. Catal., Amsterdam, 1972, Preprint 46.*
31. D. R. Kahn, Ph.D. Thesis, Department of Chemical Engineering, University of California, Berkeley, 1973.
32. Materials Research Corporation, Orangeburg, N.Y.
33. J. Perdereau and G. E. Rhead, *Surface Science* 24, 555 (1971).

34. D. Blakely, private communication.
35. R. W. Joyner, J. L. Gland, and G. A. Somorjai, U. S. Atomic Energy Comm., Report LBL-414 (1971).
36. G. A. Somorjai, Catalysis Reviews 7, 87 (1972).
37. Y. Ebusuzaki, W. J. Kass, and M. O'Keefe, J. Chem. Phys. 49, 3329 (1968).
38. J. E. Purcell and L. S. Ettre, J. Gas Chrom. 3, 69 (1965).
39. G. C. Bond and J. Sheridan, Trans. Faraday Soc. 48, 713 (1952).
40. G. C. Bond and J. Turkevich, Trans. Faraday Soc. 50, 1335 (1954).
41. J. Addy and G. C. Bond, Trans. Faraday Soc. 53, 368, 377, 383, 388 (1957).
42. G. C. Bond and J. Newham, Trans. Faraday Soc. 56, 1501 (1960).
43. J. Newham, Chem. Rev. 63, 123 (1963).
44. D. W. McKee, J. Phys. Chem. 67, 1336 (1963).
45. N. A. Dougharty, Ph.D. Thesis, Department of Chemical Engineering, University of California, Berkeley, 1964.
46. J. H. Sinfelt, D. J. C. Yates, and W. F. Taylor, J. Phys. Chem. 69, 1877 (1965).
47. J. R. Anderson and N. R. Avery, J. Catalysis 8, 48 (1967).
48. J. R. Balder, Ph.D. Thesis, Department of Chemical Engineering, University of California, Berkeley, 1967.
49. R. A. Dalla Betta, J. A. Cusumano, and J. H. Sinfelt, J. Catalysis 19, 343 (1970).
50. L. L. Hegedus, Ph.D. Thesis, Department of Chemical Engineering, University of California, Berkeley, 1972.
51. L. L. Hegedus and E. E. Petersen, J. Catalysis 28, 150 (1973).

52. K. H. Yang and O. A. Hougen, Chem. Eng. Progr. 46, 146 (1950).
53. G. C. Bond, "Catalysis by Metals," Academic Press Inc., 1962.
54. O. M. Poltorak and V. S. Boronin, Russ. J. Phys. Chem. (English Transl.) 39, 1329 (1965).
55. O. M. Poltorak and V. S. Boronin, Zh. Fiz. Khim. 40, 2671 (1966).
56. J. L. Gland, private communication.
57. S. J. Thomson and J. L. Wishlade, Trans. Faraday Soc. 58, 1170 (1962).
58. R. D. Clay, Ph.D. Thesis, Department of Chemical Engineering, University of California, Berkeley, 1967.
59. J. L. Hahn, Master's Thesis, Department of Chemical Engineering, University of California, Berkeley, 1968.
60. E. E. Petersen, "Chemical Reaction Analysis," Prentice-Hall, 1965.
61. A. S. Foust, L. A. Wenzel, C. W. Clump, L. Maus, and L. B. Andersen, "Principles of Unit Operations," John Wiley and Sons, 1962.
62. T. A. Massarro, Ph.D. Thesis, Department of Chemical Engineering, University of California, Berkeley, 1970.
63. G. Stoll, private communication.
64. Y. Berthier, M. Perdereau, and J. Oudar, Surface Science 36, 225 (1973).
65. K. Baron, private communication.

LEGAL NOTICE

This report was prepared as an account of work sponsored by the United States Government. Neither the United States nor the United States Atomic Energy Commission, nor any of their employees, nor any of their contractors, subcontractors, or their employees, makes any warranty, express or implied, or assumes any legal liability or responsibility for the accuracy, completeness or usefulness of any information, apparatus, product or process disclosed, or represents that its use would not infringe privately owned rights.

TECHNICAL INFORMATION DIVISION
LAWRENCE BERKELEY LABORATORY
UNIVERSITY OF CALIFORNIA
BERKELEY, CALIFORNIA 94720